AD-758 461

FEASIBILITY INVESTIGATION FOR DETERMINING
ARMY HELICOPTER GAS TURBINE ENGINE MAXI-
MUM POWER AVAILABLE

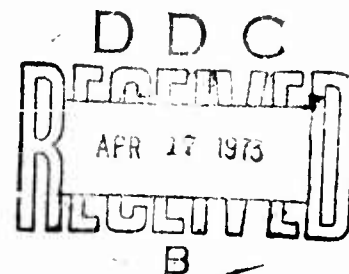Joseph M. Kos, et al

Hamilton Standard

AD 758461

AD

USAAMRDL TECHNICAL REPORT 72-58

FEASIBILITY INVESTIGATION FOR DETERMINING ARMY HELICOPTER GAS TURBINE ENGINE MAXIMUM POWER AVAILABLE

By

Joseph M. Kos
Anthony J. Martin
Peter D. Miller
John Saunders
Roy W. Schneider
Louis A. Urban
Frank C. Zuliani

February 1973

D D C
RECEIVED
APR 17 1973
B

EUSTIS DIRECTORATE
U. S. ARMY AIR MOBILITY RESEARCH AND DEVELOPMENT LABORATORY
FORT EUSTIS, VIRGINIA

CONTRACT DAAJ02-72-C-0003
HAMILTON STANDARD
DIVISION OF UNITED AIRCRAFT CORPORATION
WINDSOR LOCKS, CONNECTICUT

Approved for public release;
distribution unlimited.

129

DISCLAIMERS

The findings in this report are not to be construed as an official Department of the Army position unless so designated by other authorized documents.

When Government drawings, specifications, or other data are used for any purpose other than in connection with a definitely related Government procurement operation, the United States Government thereby incurs no responsibility nor any obligation whatsoever; and the fact that the Government may have formulated, furnished, or in any way supplied the said drawings, specifications, or other data is not to be regarded by implication or otherwise as in any manner licensing the holder or any other person or corporation, or conveying any rights or permission, to manufacture, use, or sell any patented invention that may in any way be related thereto.

Trade names cited in this report do not constitute an official endorsement or approval of the use of such commercial hardware or software.

DISPOSITION INSTRUCTIONS

Destroy this report when no longer needed. Do not return it to the originator.

This report was prepared by the Hamilton Standard Division of United Aircraft Corporation under Contract DAAJ02-72-C-0003. The basic objective of the effort was to determine the feasibility of developing a method to predict the maximum power available (MPA) from a helicopter gas turbine engine at full-power conditions. The MPA prediction was to be made with an accuracy goal of at least ±1% using information obtained from the engine while the engine was operated at a partial-power condition of no more than 30% of normal rated power.

The report consists of a discussion of the various algorithms that could be considered in determining maximum power available, and the algorithm that provides the most accurate method for predicting maximum power available is selected.

The results of the investigation show that development of a method to predict the MPA of an Army helicopter gas turbine engine prior to lift-off is feasible; however, before an MPA prediction system with an accuracy of ±1% can be developed, more accurate sensors must be developed. The accuracy of such a system can also be enhanced by acquiring the necessary parametric information while operating the engine at partial-power conditions higher than 30% of normal rated power.

The conclusion and recommendations are generally concurred in by this Directorate; however, before an MPA prediction system is fabricated, it is felt that an intermediate effort should be conducted to determine the accuracy of and optimize a system that uses parametric information obtained from an engine operated at a power condition higher than 30% of normal rated power.

The technical monitor for this contract was Mr. G. William Hogg, Military Operations Technology Division.

DOCUMENT CONTROL DATA - R & D

(Security classification of title, body of abstract and indexing annotation must be entered when the overall report is classified)

1 ORIGINATING ACTIVITY *(Corporate author)*	2a. REPORT SECURITY CLASSIFICATION
Hamilton Standard Division of United Aircraft Corporation Windsor Locks, Connecticut	Unclassified
	2b. GROUP

3 REPORT TITLE

FEASIBILITY INVESTIGATION FOR DETERMINING ARMY HELICOPTER GAS TURBINE ENGINE MAXIMUM POWER AVAILABLE

4 DESCRIPTIVE NOTES *(Type of report and inclusive dates)*

Final

5 AUTHOR(S) *(First name, middle initial, last name)*

Joseph M. Kos	John Saunders	Frank C. Zuliani
Anthony J. Martin	Roy W. Schneider	
Peter D. Miller	Louis A. Urban	

6 REPORT DATE	7a. TOTAL NO. OF PAGES	7b. NO. OF REFS
February 1973	118	

8a. CONTRACT OR GRANT NO DAAJ02-72-C-0003	9a. ORIGINATOR'S REPORT NUMBER(S)
b. PROJECT NO	USAAMRDL Technical Report 72-58
c. Task 1F162203A43405	9b. OTHER REPORT NO(S) *(Any other numbers that may be assigned this report)*
d.	

10 DISTRIBUTION STATEMENT

Approved for public release; distribution unlimited.

11 SUPPLEMENTARY NOTES	12. SPONSORING MILITARY ACTIVITY
	Eustis Directorate U.S. Army Air Mobility R&D Laboratory Fort Eustis, Virginia

13 ABSTRACT

The purpose of this investigation was to determine the feasibility of developing a method to predict, with an accuracy of better than ±1%, the maximum power which can be produced by a helicopter gas turbine engine at full-power conditions. The prediction was to be made using information obtained from the engine while the engine was operated prior to lift-off at a partial-power condition of no more than 30% of normal rated power. The prediction method was to be capable of identifying the changes in maximum engine power available due to all possible types of engine deterioration and all ambient conditions. The study was based on a Lycoming T53-L13 gas turbine engine currently being used in the Army UH-1 helicopter. The feasibility study was first based on the use of information available from existing sensors normally installed on the engine. It was determined, however, that the use of these sensors did not permit the desired ±1% accuracy to be obtained, and for this reason the feasibility study was expanded to include the use of additional and/or more accurate sensors. In addition, it was assumed that input information was available which provided atmospheric density data with an accuracy of ±.75%.

DD FORM **1473** REPLACES DD FORM 1473, 1 JAN 64, WHICH IS
NOV 66 OBSOLETE FOR ARMY USE.

14. KEY WORDS	LINK A		LINK B		LINK C	
	ROLE	WT	ROLE	WT	ROLE	WT
Gas Turbine Engine						
Maximum Power Available (MPA)						
Full Power Conditions						
Engine Deterioration						
Low Power Conditions						
Normal Rated Power						

SUMMARY

An investigation was conducted by Hamilton Standard Division of UAC, Windsor Locks, Connecticut, to determine the feasibility of developing a method to predict the maximum power available (MPA) from a helicopter gas turbine engine at full-power conditions. The MPA prediction was to be made with an accuracy goal of at least ±1% using information obtained from the engine while the engine was operated at a partial-power condition of no more than 30% normal rated power. The MPA prediction was to take into account the effects of all ambient conditions and all internal modes of engine deterioration.

The Lycoming T53-L13 engine, a gas turbine engine presently in use on the Army UH-1 helicopter, was selected for the investigation. A mathematical model of the T53-L13 engine and an MPA prediction system was developed based on Hamilton Standard's prior experience and knowledge of engine control and diagnostic systems. This model was analyzed to determine the best attainable MPA prediction accuracy assuming perfect sensors, inaccuracies, and effects on predicted MPA due to all input parameters, the effect of power condition on MPA prediction, and possible alternate MPA prediction methods using various sets of parametric sensors and making various assumptions regarding the relative values of independent engine parameters. The model was further evaluated by the use of actual engine operational test data taken by Hamilton Standard as a part of the U. S. Army UH-1 AIDAPS feasibility study. Hardware implementation of an MPA prediction system was also investigated.

Development of an MPA prediction system is feasible. An initial system accuracy of ±3.5% can be achieved using an aircraft-mounted digital computer and the most accurate, aircraft type parametric sensors available today.

Attainment of the ±1% accuracy goal is not feasible under the ground rules for this study. Further studies are required to determine if ±1% accuracy is attainable when the MPA prediction is made at power levels higher than 30%, on multi-engine helicopters for example, and when the baseline engine data, stored in the computer, is updated during flight to reduce errors due to ambient variations and engine degradation.

TABLE OF CONTENTS

Preceding page blank

LIST OF ILLUSTRATIONS

LIST OF TABLES

ix

LIST OF SYMBOLS

A_N	Power turbine inlet nozzle effective area, in.[2]
A_5	Gas generator turbine inlet nozzle effective area, in.[2]
$B_{(bij)}$	Matrix relating relative variations in engine airflow pumping capacity, component efficiencies, and geometries to measured relative variations in engine parameters sensed at low power at a constant value of P_3/δ_1.
$C_{(Cij)}$	Matrix relating the relative variations in maximum power at each control limit to the computed relative variations in engine pumping capacity, component efficiencies and geometries.
CF	Nonoptimal N_2 correction factor
DAN	Computed relative change in A_N
DA5	Computed relative change in A_5
δ_1	Relative compressor inlet absolute pressure (= $P_1/14.7$)
DETAC	Computed relative change in η_c
DETAPT	Computed relative change in η_{pt}
DETAT	Computed relative change in η_t
DN1	Measured relative change in $N_1/\sqrt{\theta_1}$ at constant P_3/δ_1
DP7	Measured relative change in P_7/δ_1 at constant P_3/δ_1
DSHP	Measured relative change in $SHP/\delta_1\sqrt{\theta_1}$ at constant P_3/δ_1
DT3	Measured relative change in T_3/θ_1 at constant P_3/δ_1
DT7	Measured relative change in T_7/θ_1 at constant P_3/δ_1
DT9	Measured relative change in T_9/θ_1 at constant P_3/δ_1
DWA	Computed relative change in $W_a\sqrt{\theta_1}/\delta_1$ (engine pumping capacity)

DWF	Measured relative change in $W_f/\delta_1\theta_1^{.8}$ at constant P_3/δ_1
η_c	Compressor efficiency
η_{pt}	Power turbine efficiency
η_t	Gas generator turbine efficiency
f_N	Ambient temperature correction factor in computing maximum horsepower at N_1 limit
f_T	Ambient temperature correction factor in computing maximum horsepower at T_7 limit
f_W	Ambient temperature correction factor in computing maximum horsepower at W_f limit
MPA	Maximum power available, hp
N_1	Gas generator turbine rotational speed, rpm
N_2	Free power turbine rotational speed, rpm
P_{AM}	Ambient pressure, psia
P_1	Compressor inlet total pressure, psia
P_3	Compressor discharge pressure, psia
P_7	Power turbine inlet pressure, psia
SHP	Power turbine shaft horsepower, hp
SHP_{CO}	Optimal power turbine horsepower referred to sea-level standard-day conditions, hp
SHPON	Predicted maximum power at N_1 limit, hp
SHPOT	Predicted maximum power at T_7 limit, hp
SHPOW	Predicted maximum power at W_f limit, hp

SHP_{REF}	Sea-level standard-day value of horsepower at each control limit, hp
SPE/W_a	Shaft power extraction/(lb/sec of compressor airflow), hp/(lb/sec)
T_{AM}	Ambient temperature, °R
T_1	Compressor inlet total temperature, °R
T_3	Compressor discharge total temperature, °R
T_7	Power turbine inlet total temperature, °R
T_9	Power turbine discharge total temperature, °R
τ_1	Relative compressor inlet absolute temperature ($= T_1/518.7$)
W_{BL}	Compressor discharge bleed air as a percentage of total compressor airflow
W_f	Engine fuel flow, pph

SUBSCRIPT

B	Designates corrected base-line values
C	Designates quantities referred to sea-level standard-day conditions

INTRODUCTION

The purpose of this investigation was to determine the feasibility of developing a method to predict, with an accuracy of better than ±1%, the maximum power which can be produced by a helicopter gas turbine engine at full-power conditions. The prediction was to be made using information obtained from the engine while the engine was operated prior to lift-off at a partial-power condition of no more than 30% of normal rated power. The prediction method was to be capable of identifying the changes in maximum engine power available due to all possible types cf engine deterioration and all ambient conditions. The study was based on a Lycoming T53-L13 gas turbine engine currently being used in the Army UH-1 helicopter. The feasibility study was first based on the use of information available from existing sensors normally installed on the engine. It was determined, however, that the use of these sensors did not permit the desired ±1% accuracy to be obtained, and for this reason the feasibility study was expanded to include the use of additional and/or more accurate sensors. In addition, it was assumed that input information was available which provided atmospheric density data with an accuracy of ±.75%.

The following tasks were undertaken:

PHASE I - ESTABLISHMENT AND DEFINITION OF METHOD

1. A mathematical model of a method to predict MPA was constructed.

2. An estimated attainable MPA prediction accuracy was derived. Inaccuracies due to input information were identified.

3. Effects of power condition on MPA prediction accuracy were determined.

4. The hardware and components required to implement the method were described.

PHASE II - EVALUATION OF METHOD

1. An evaluation of the MPA prediction method was made using actual engine operational test data, in the following manner.

    a. Input parameters were taken from engine operational test data at the recommended low-power condition.

1

b. Using MPA prediction methods and the input parameters above, the MPA was computed.

c. The actual maximum power, as taken from the engine test data used in (a) above, was then compared to the computed value determined in (b) above.

2. The above procedure was used to evaluate the ability of the prediction method to determine the maximum power available when the engine deteriorated in performance because of either internal deterioration or changes in atmospheric conditions.

a. In considering engine performance deterioration due to internal deterioration, the evaluation procedure used engine test data taken from engines known to be internally deteriorated, or from engines where internal deterioration was simulated.

b. In considering engine performance deterioration due to changes in atmospheric conditions, the evaluation procedure used data from at least three different engine test runs which included at least 29°F variation in ambient temperature, and from at least three different engine test runs which included at least 8,000 feet variation in altitude.

PHASE III – RECOMMENDATIONS

As a result of the feasibility investigation, recommendations were made in the areas of further sensor development, hardware implementation, system growth, and continued alternate MPA prediction system studies.

DISCUSSION

THE MATHEMATICAL SYSTEM MODEL

A mathematical system model was constructed that included the basic power prediction concept plus additional features for computing the errors in power prediction. A prerequisite for constructing this prediction model involved a detailed knowledge of the engine characteristics on which the maximum power was to be predicted.

A mathematical model of a "typical" Lycoming T53-L13 engine was evolved on an IBM 370 computer, based on engine modeling concepts developed by Hamilton Standard. The so-called "typical" T53-L13 engine was actually the average characteristics of test-cell data from 75 engines. This test data provided the steady-state values for N_1, T_3, P_3, T_9, SHP, and W_f at standard-day conditions from idle to maximum power. The independent variables (such as component efficiencies and geometries) of the generic engine model were selected to duplicate the steady-state test data from the "typical" engine. The resulting computer model of the T53-L13 engine was then used to provide all required interrelationships. For example, changes in engine speed, temperature, pressure, or power resulting from changes in engine geometry, component efficiency, or air pumping capacity were computed. The engine model was used to compute the partial derivatives or influence of any engine parameter on any engine variable, called influence coefficients in this report.

The basic maximum power prediction concept is an extension of the engine diagnostic techniques previously developed by Hamilton Standard. This prediction concept is described as follows. The prediction computer contains three types of predetermined stored engine characteristics.

1. Base-line characteristics, consisting of steady-state locus of values for measured engine variables over the range of engine operation at which prediction can be performed.

2. A matrix of influence coefficients relating changes in the engine base-line variables to changes in such engine parameters as component efficiencies and geometries, called the "B-matrix" in this report.

3. A matrix of influence coefficients relating changes in engine parameters to changes in the engine power limit, called the "C-matrix" in this report.

3

Figure 1 shows a schematic diagram of a single-spool free-power turbine engine and identifies the various engine station numbers for future reference.

Measurements of engine variables and environmental conditions are obtained at low power. After measurement filtering and determination that the engine is in steady state, the measurement data is corrected to standard-day conditions. The percentage of point variations between the measurement data and stored base lines is determined. A gas-path analysis is then used to determine changes in engine characteristics (efficiencies, airflow, and geometries) from the values that existed when the stored base lines were determined. The percentage of point variations in engine characteristics, as determined at low power, is also assumed to exist at high power. Maximum power is determined by computing the fractional change in environment resulting from each change in engine characteristics and each change in environment from standard-day conditions. The complete computation of maximum power is performed for each control limit influencing maximum power, specifically a gas generator speed limit, a turbine discharge temperature limit, and a metered fuel limit. The lowest of the three computed values for maximum power is selected as the maximum available horsepower.

The gas-path analysis, performed on measurements obtained at low power, consists of a stored data matrix relating the increment between measurement and base-line data to variations in engine characteristics. This data matrix is determined in advance based on the engine thermodynamic relations. Numerical values of this matrix are stored at several low-power conditions, allowing a power prediction computation over a range of engine power. Similarly, the computation of the fractional change in maximum power is determined by a stored data matrix relating the variation of each engine characteristic and environment to the fractional change in maximum horsepower. This stored matrix is determined in advance based on engine thermodynamic relations at the standard-day maximum-power condition.

The basic tool in developing the power prediction algorithm is a technique developed by Hamilton Standard which quantitatively defines how the various engine performance parameters change with respect to each other or with changes in the environment or the engine fuel control. From a steady-state operating condition, a set of "influence coefficients" interrelating all the various engine performance parameters is determined. From this set of influence coefficients, the steady-state characteristics as well as the influence coefficients at any other power condition can be determined. The influence coefficients computed will ultimately be used in the power prediction scheme. Since the accuracy to which power can be predicted is affected by the accuracy of the influence coefficients, it is necessary that these coefficients be computed as precisely as possible.

4
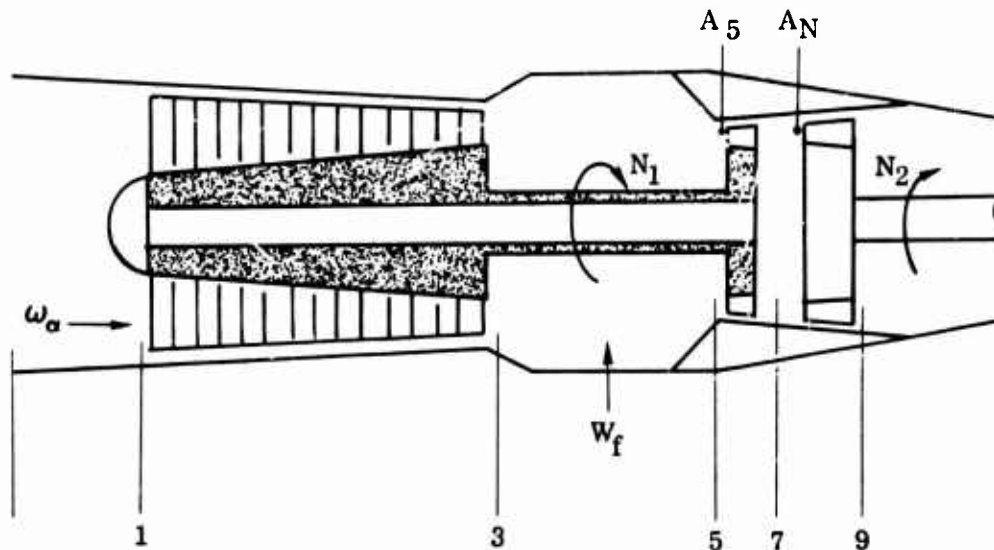
Symbol	Definition
A_5	Gas Generator Turbine Inlet Nozzle Effective Area
A_N	Power Turbine Inlet Nozzle Effective Area
N_1	Gas Generator Turbine Rotational Speed
N_2	Free-Power Turbine Rotational Speed
W_f	Engine Fuel Flow Rate
η_c	Compressor Efficiency
η_t	Gas Generator Turbine Efficiency
η_{pt}	Power Turbine Efficiency
W_a	Airflow Rate
WBL	Compressor Discharge Bleed Airflow
SPE	Compressor Shaft Power Extraction

Figure 1. Schematic Diagram of a Single-Spool
Free-Power Turbine Engine.

The accuracy of the influence coefficients is judged by determining if the computed steady-state characteristics correspond to actual steady-state characteristics of the engine obtained from tests. By varying compressor efficiency, gas generator turbine efficiency, and power turbine efficiency, the computed steady-state characteristics can be tailored to match actual steady-state characteristics for the particular engine.

Because of the large amount of test data available, the power prediction concept was specifically developed for the Lycoming T53-L13 engine. However, the general concepts are applicable to any free-turbine engine. A modern fuel control mode similar to the Hamilton Standard JFC 80 (used on the Lycoming LTC-4V-1 engine) was used for this program. In particular, it was assumed that maximum power is limited by a gas generator speed limit, a gas generator turbine discharge temperature limit, and a metered fuel flow limit. For component efficiencies as defined in Figure 2 through 4, the base-line steady-state characteristics as a function of corrected compressor discharge pressure are shown in Figures 5 through 10. Note that all engine characteristics are plotted as corrected quantities. Actual base-line data obtained by averaging test data of 75 T53-L13 engines are also shown in Figures 5 through 10.

Depending on the number and kind of sensor measurements made at low power, various specific cases of the basic power prediction concept were determined. (Selection of the specific cases most likely to yield the best power prediction was guided in part by the results of the engine diagnostic studies in the Army UH-1 AIDAPS Feasibility Program.) In this study, four such specific cases were evaluated. The four cases are defined by the following sets of low-power sensor measurements:

Set I $\quad$ $(T_1, \; P_1, \; N_1, \; N_2, \; P_3, \; T_3, \; W_f, \; P_7, \; SHP, \; T_7)$

Set II $\quad$ $(T_1, \; P_1, \; N_1, \; N_2, \; P_3, \; T_3, \; W_f, \; SHP, \; T_9)$
$\quad\quad\quad$ and assume $\partial A_N / A_N = \partial \eta_{pt} / \eta_{pt}$

Set III $\quad$ $(T_1, \; P_1, \; N_1, \; N_2, \; P_3, \; T_3, \; W_f, \; P_7, \; T_9, \; T_7)$

Set IV $\quad$ $(T_1, \; P_1, \; N_1, \; N_2, \; P_3, \; T_3, \; W_f, \; SHP, \; T_7)$
$\quad\quad\quad$ and assume $\partial A_N / A_N = \partial \eta_{pt} / \eta_{pt}$

For the first set of sensors, the power prediction algorithm can be outlined in detail as follows:
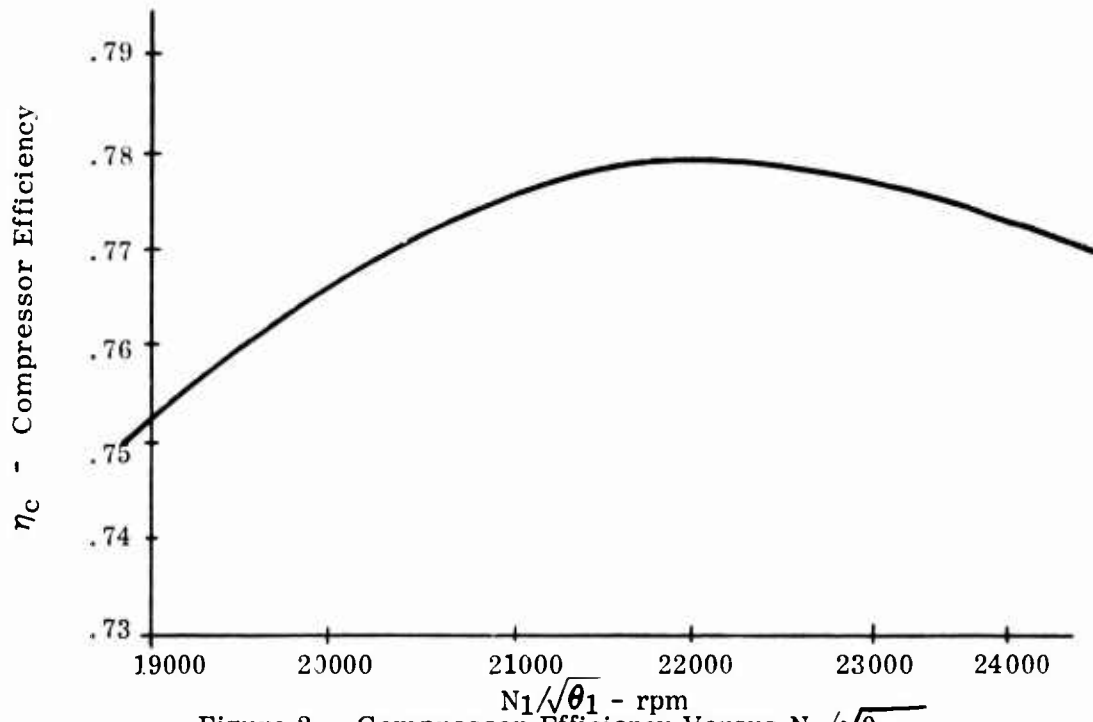
Figure 2. Compressor Efficiency Versus $N_1/\sqrt{\theta_1}$.
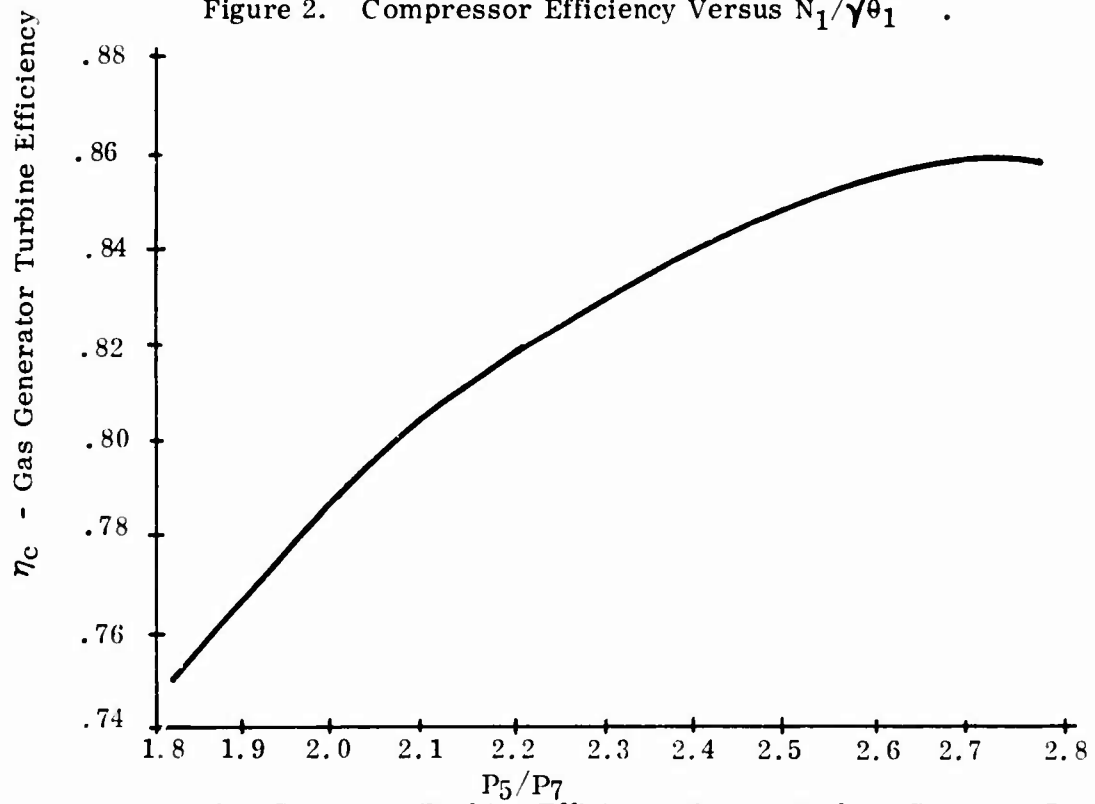
Figure 3. Gas Generator Turbine Efficiency Versus Turbine Pressure Ratio.

7
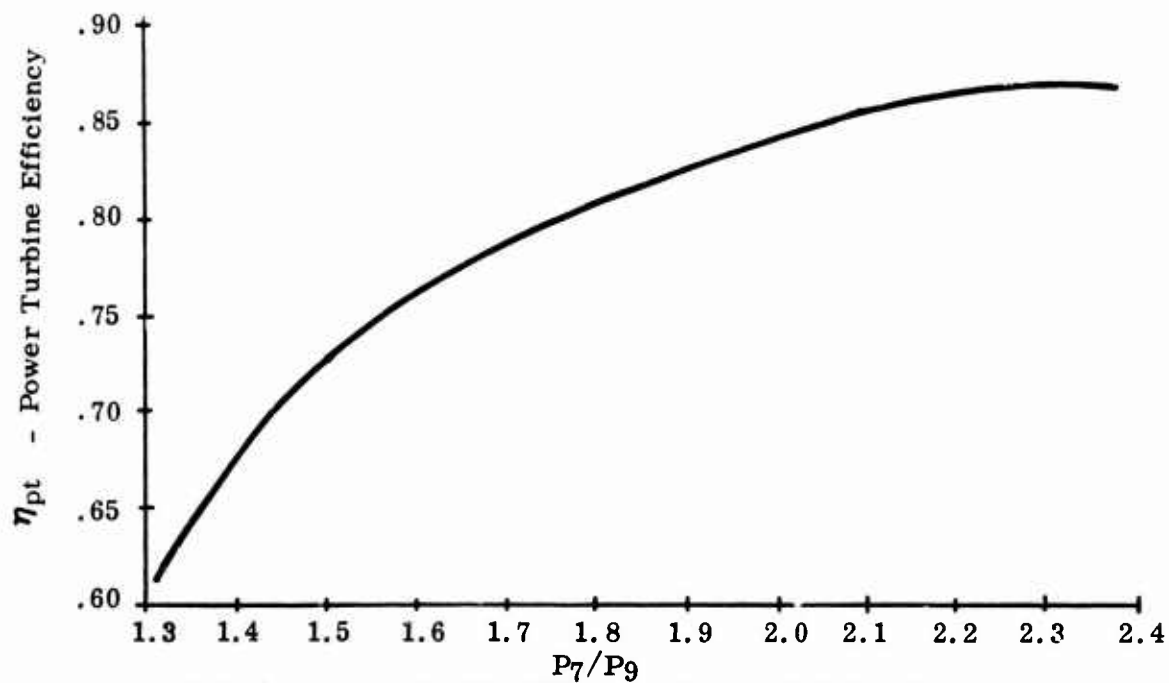
Figure 4. Power Turbine Efficiency Versus Turbine Pressure Ratio.
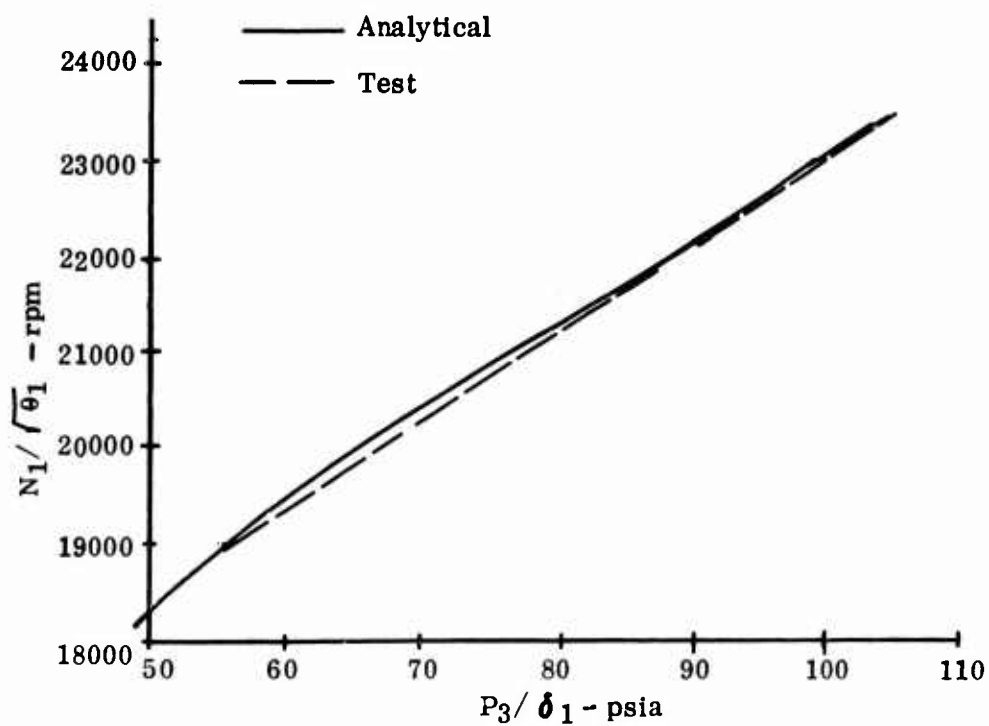
Figure 5. Corrected Gas Generator Speed Versus Corrected Compressor Discharge Pressure.
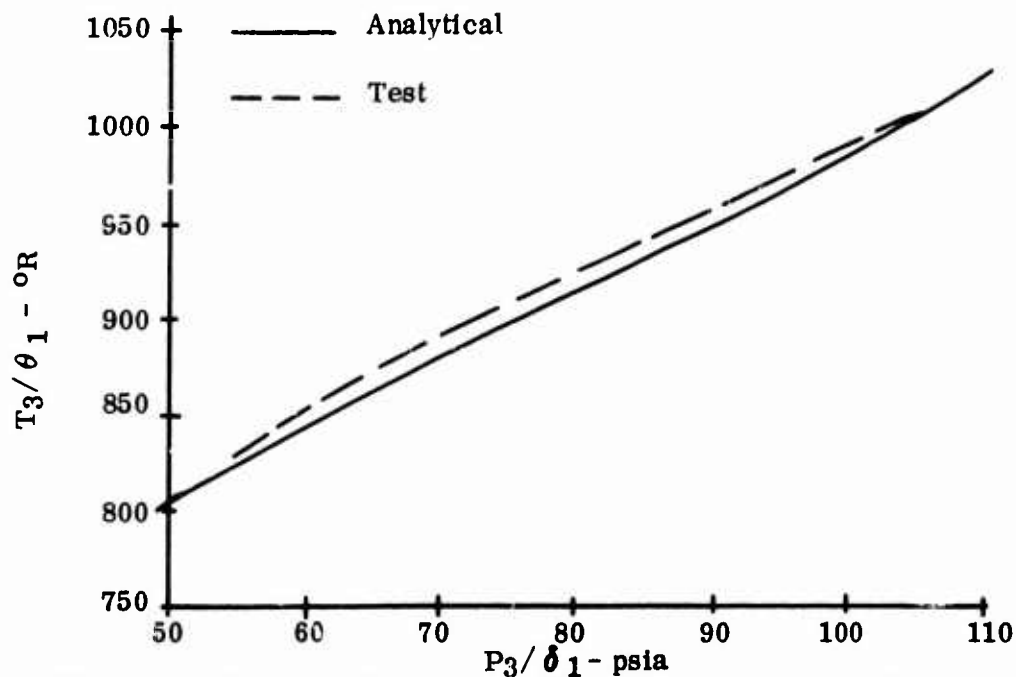
Figure 6. Corrected Compressor Discharge Temperature Versus Corrected Compressor Discharge Pressure.
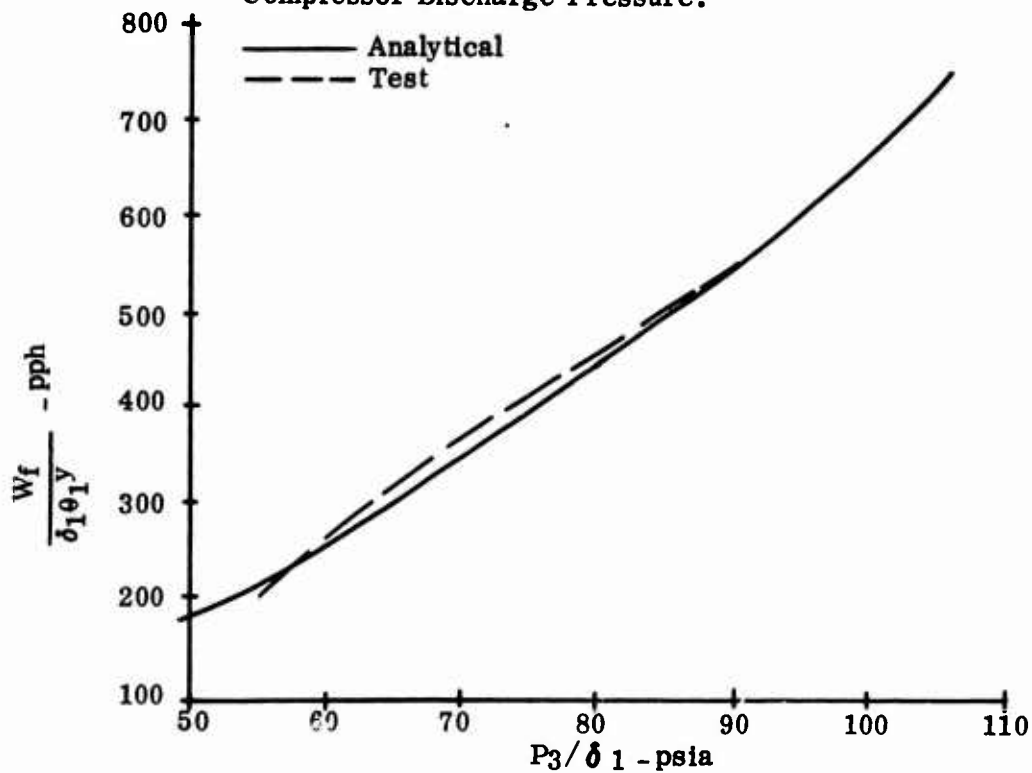
Figure 7. Corrected Fuel Flow Versus Corrected Compressor Discharge Pressure.

9
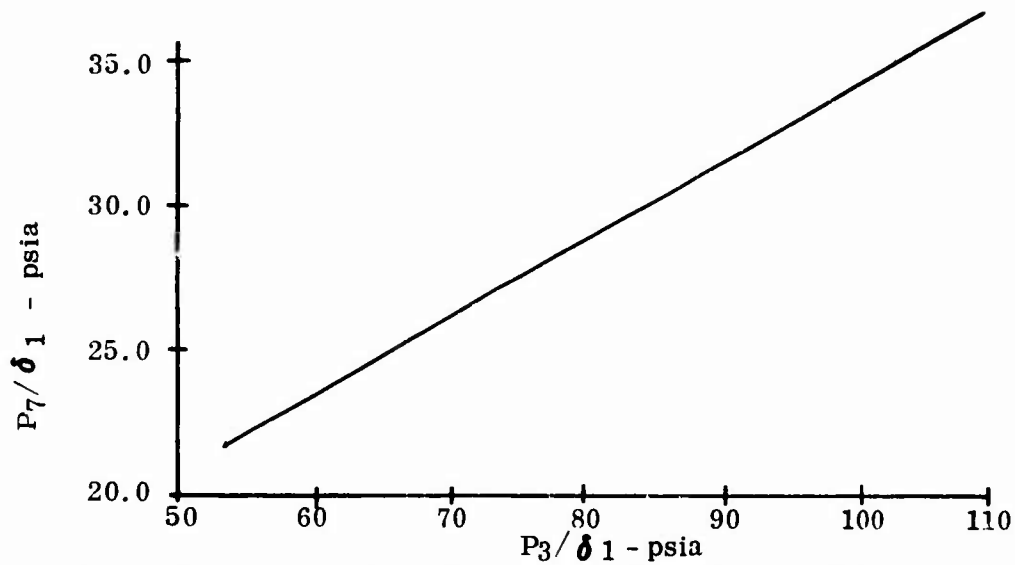
Figure 8. Corrected Gas Generator Turbine Discharge Pressure Versus
Corrected Compressor Discharge Pressure.
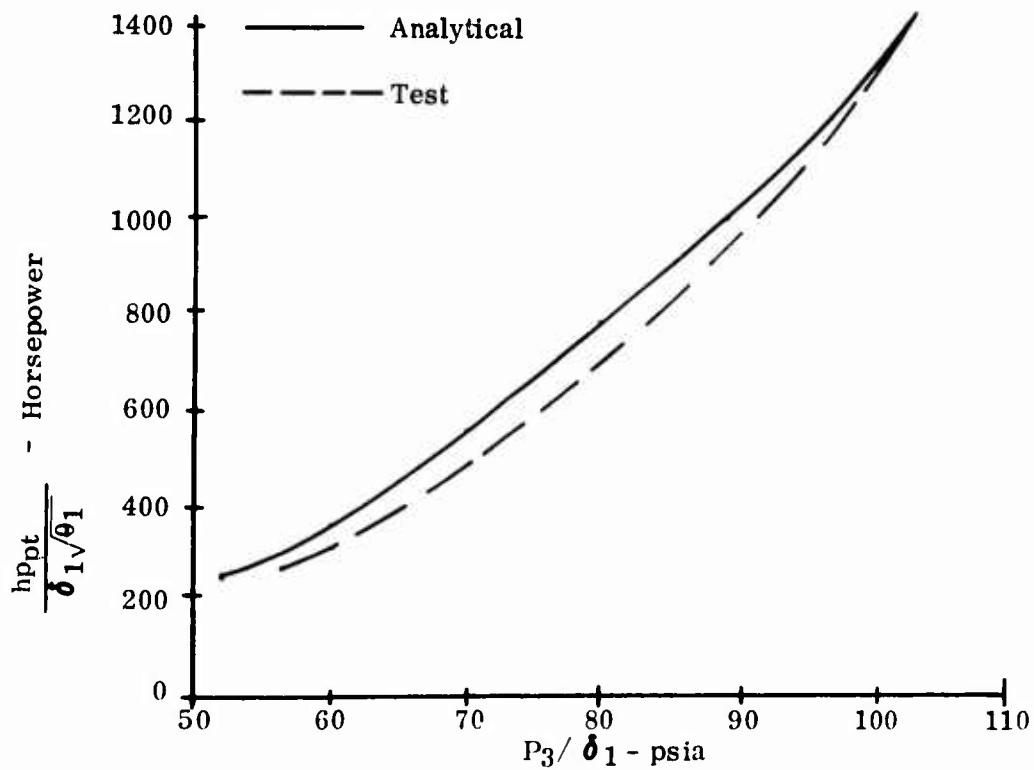
Figure 9. Corrected Power Turbine Horsepower Versus Corrected
Compressor Discharge Pressure.

10
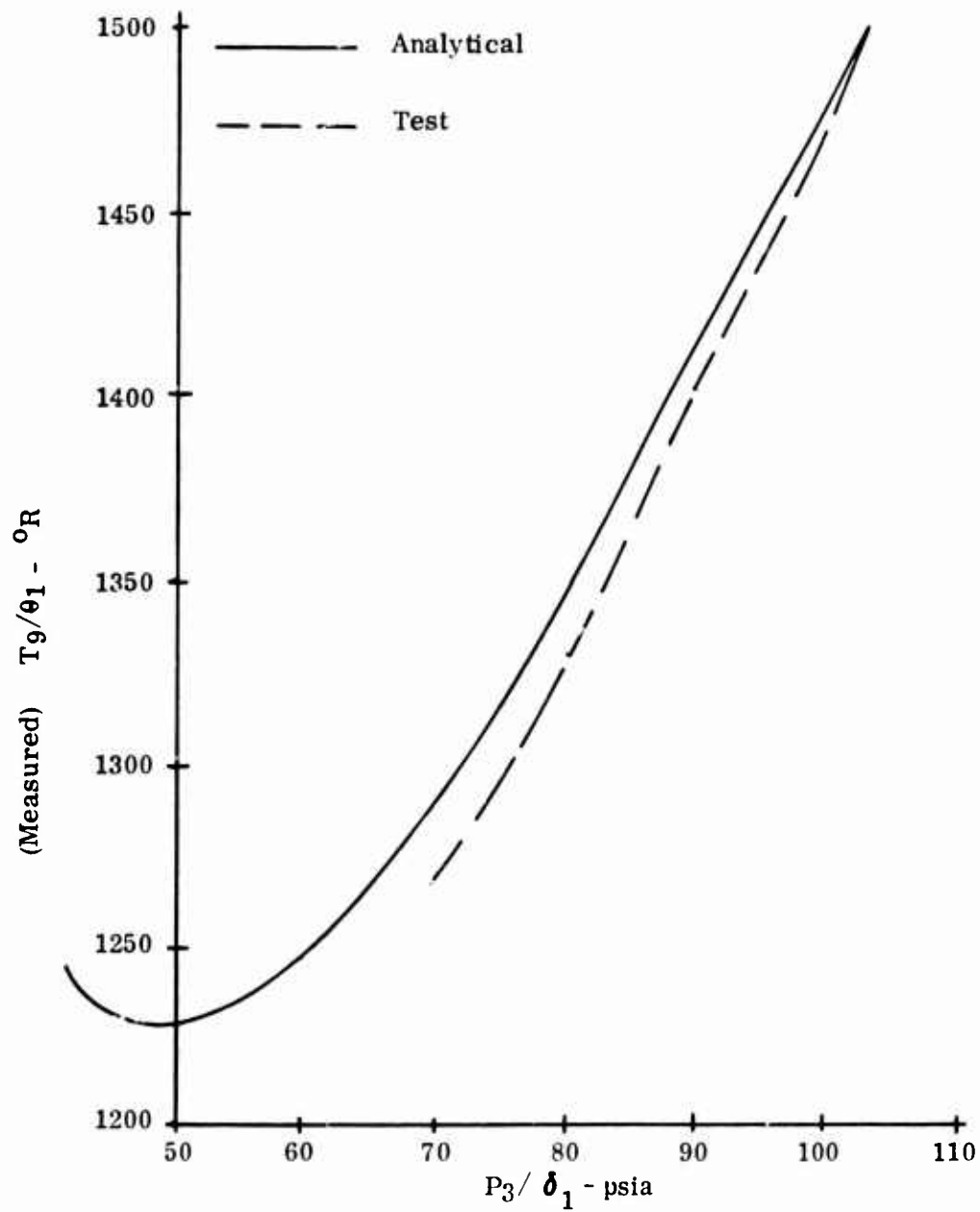
Figure 10. Corrected Power Turbine Discharge Temperature Versus Corrected Compressor Discharge Pressure.

I. Refer low-power sensor readings to standard-day conditions.

$$\theta_1 = T_1/518.7$$

$$\delta_1 = P_1/14.7$$

$$N_{1C} = N_1/\sqrt{\theta_1}$$

$$N_{2C} = N_2/\sqrt{\theta_1}$$

$$P_{3C} = P_3/\delta_1$$

$$T_{3C} = T_3/\theta_1 \qquad (1)$$

$$W_{fC} = W_f/\delta_1\theta_1^{\ Y}$$

$$SHP_C = SHP/\delta_1\sqrt{\theta_1}$$

$$P_{7C} = P_7/\delta_1$$

$$T_{7C} = T_7/\delta_1$$

II. Determine base-line values from stored hardware at the same P_{3C} value as in I.

$$N_{1CB} = f_1(P_{3C})$$

$$N_{2CB} = f_2(P_{3C})$$

$$T_{3CB} = f_3(P_{3C})$$

$$W_{fCB} = f_4(P_{3C}) \qquad (2)$$

$$SHP_{CB} = f_5(P_{3C})$$

$$P_{7CB} = f_6(P_{3C})$$

$$T_{7CB} = f_7(P_{3C})$$

III. Compute optimal corrected SHP from corrected SHP.

$$\text{Correction Factor (CF)} = \left[(N_{2C} - N_{2CB})/N_{2CB}\right]^2 \qquad (3)$$

$$SHP_{CO} = SHP_C/(1 - CF) \qquad (4)$$

IV. Compute the relative deviation of the measurement data from the stored base-line data.

$$DN1 = (N_{1C} - N_{1CB})/N_{1CB}$$

$$DT5 = (T_{3C} - T_{3CB})/T_{3CB}$$

$$DWF = (W_{f\,C} - W_{f\,CB})/W_{f\,CB}$$

$$DSHP = (SHP_{CO} - SHP_{CB})/SHP_{CB} \qquad (5)$$

$$DT7 = (T_{7C} - T_{7CB})/T_{7CB}$$

$$DP7 = (P_{7C} - P_{7CB})/P_{7CB}$$

V. Compute the variations in airflow pumping capacity, efficiencies, and geometries from the following matrix equation.

$$
\begin{bmatrix}
DWA \\
DETAC \\
DETAT \\
DETAPT \\
DAS \\
DAN
\end{bmatrix}
=
\left\{
\begin{array}{c}
\left[(W_{aC} - W_{aCB})/W_{aCB}\right] PC \\
(\eta_C - \eta_{CB})/\eta_{CB} \\
(\eta_t - \eta_{tB})/\eta_{tB} \\
(\eta_{pt} - \eta_{ptB})/\eta_{ptB} \\
(A_5 - A_{5B})/A_{5B} \\
(A_N - A_{NB})/A_{NB}
\end{array}
\right\}
= B
\begin{bmatrix}
DN1 \\
DT3 \\
DWF \\
DNPPT \\
DT7 \\
DP7
\end{bmatrix}
\qquad (6)
$$

The B-matrix in Equation 6 is computed from the influence coefficients and is a function of the set of engine parameters measured at low power. A different set of low-power sensors would require a different B-matrix.

Since the value of P3C at which the low-power measurements are determined is not known in advance, the "B"-matrix has been determined and stored at several values of P3C, and linear interpolation on P3C is used to obtain the actual "B"-matrix to be used in Equation 6. In the sensitivity studies to be discussed later, an augmented "B"-matrix was used to take into account the effects of uncertainty in compressor discharge air bleed and shaft power extraction at low power on predicted power.

VI. Compute maximum power at each of the control limits from the following equation.

On the T_7 temperature limit

$$SHPOT = (SHP_{REF})\ \delta_1\ (1 + DWA)^{C11}\ (1 + DETAC)^{C12}\ (1 + \Gamma ETAT)^{C13}$$

$$(1 + DETAPT)^{C14}\ (1 + DA5)^{C15}\ (1 + DAN)^{C16}\ f_T\ (T_{AM}) \quad (7)$$

On N_1 speed limit

$$SHPON = (SHP_{REF})\ \delta_1{}^{C27}\ (1 + DWA)^{C21}\ (1 + DETAC)^{C22}\ (1 + DETAT)^{C23}$$

$$(1 + DETAPT)^{C24}\ (1 + DA5)^{C25}\ (1 + DAN)^{C26}\ f_N\ (T_{AM}) \quad (8)$$

On W_f limit

$$SHPOW = (SHP_{REF})\ \delta_1{}^{C37}\ (1 + DWA)^{C31}\ (1 + DETAC)^{C32}\ (1 + DETAT)^{C33}$$

$$(1 + DETAPT)^{C24}\ (1 + DA5)^{C25}\ (1 + DAN)^{C26}\ f_W\ (T_{AM}) \quad (9)$$

In Equations 7 through 9 it has tacitly been assumed that the changes in component efficiencies, airflow, and geometries computed at low power also apply at high power. This assumption is a source of power prediction error which is taken into account in the error analysis. In the sensitivity studies to be discussed later, Equations 7 through 9 were expanded to take into account the effects of control and sensor inaccuracy at high power on predicted power as were the effects of uncertainty in compressor discharge air bleed and shaft power extraction and high power on predicted power. These factors are important in evaluating the overall accuracy of the model; however, they do not enter into the actual power prediction algorithm.

14

From the horsepowers computed at the three control limits, the minimum is chosen as the maximum power available; that is,

$$MPA = MIN \text{ (SHPOT, SHPON, SHPOW)} \qquad (10)$$

For any other set of low-power measurements, the procedure for determining the maximum power available is analogous to the procedure described above except that a different B-matrix is used. The "C" coefficients in Equations 7 through 9 do not change unless the engine control mode is changed.

Of the many variables which enter into the power prediction scheme, the one which has the widest range of variation is ambient temperature. The ambient temperature range of -60°F to 120°F represents a -42.3% to +11.8% variation from the standard-day ambient temperature value of 518.7°R ($\approx 59°$F). In the development of the power prediction algorithm, the effect of ambient temperature appeared as a factor in the equation for horsepower of the form $[T_{AM}/(T_{AM})_{REF}]^{CTAM}$. In using this factor, it was found that over the wide ambient temperature range expected, the exponent CTAM varied sufficiently such that using a constant value for CTAM resulted in prohibitively large errors in predicted horsepower.

An alternate procedure was chosen which uses an ambient temperature correction factor to account for ambient temperature variations. At a given ambient temperature, the ambient temperature correction factor is defined to be the ratio of actual horsepower at the specified ambient temperature to the actual horsepower at the standard-day reference temperature of 518.7°F. A separate ambient temperature correction factor is required for each of the three control limits and is shown in Figures 11, 12 and 13 for the base-line engine.

As the engine degrades, the ambient temperature correction factor will shift. The power prediction algorithm does not take into account this shift but uses the ambient temperature correction factors defined in Figures 11, 12 and 13 for all engines. As a result, an error in the predicted power will be introduced for degraded engines for nonstandard-day ambient temperatures.

Engine diagnostic studies in the UH-1 AIDAPS feasibility program have demonstrated the need for determining that the engine is sufficiently near steady state to obtain meaningful steady-state data. This evaluation has not been duplicated in this feasibility study, as the evaluation in the AIDAPS program is applicable to power prediction. Therefore, the technique for determining steady-state
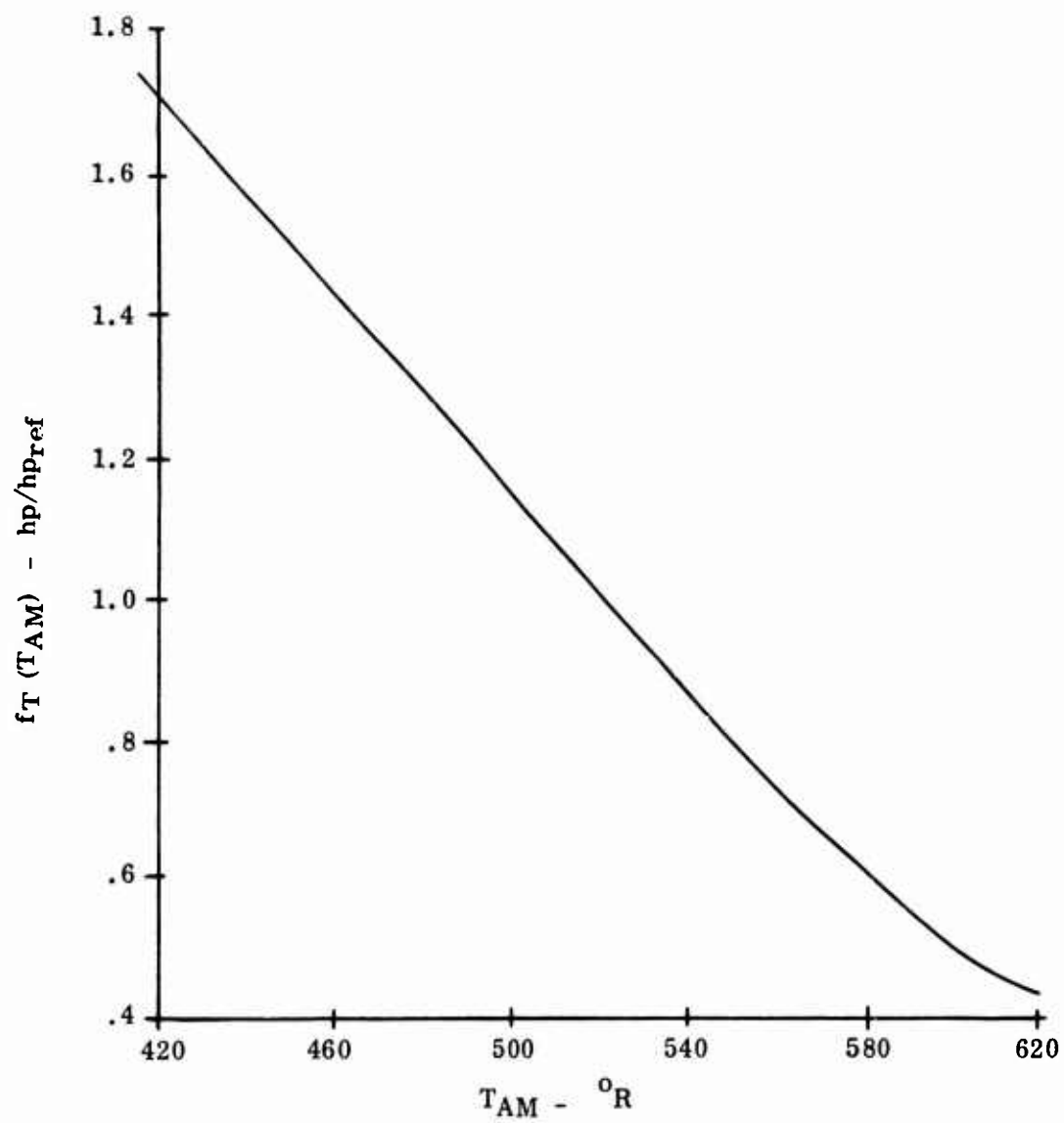
Figure 11. T_7 Limit Mode Ambient Temperature Correction Factor Versus T_{AM}.

16
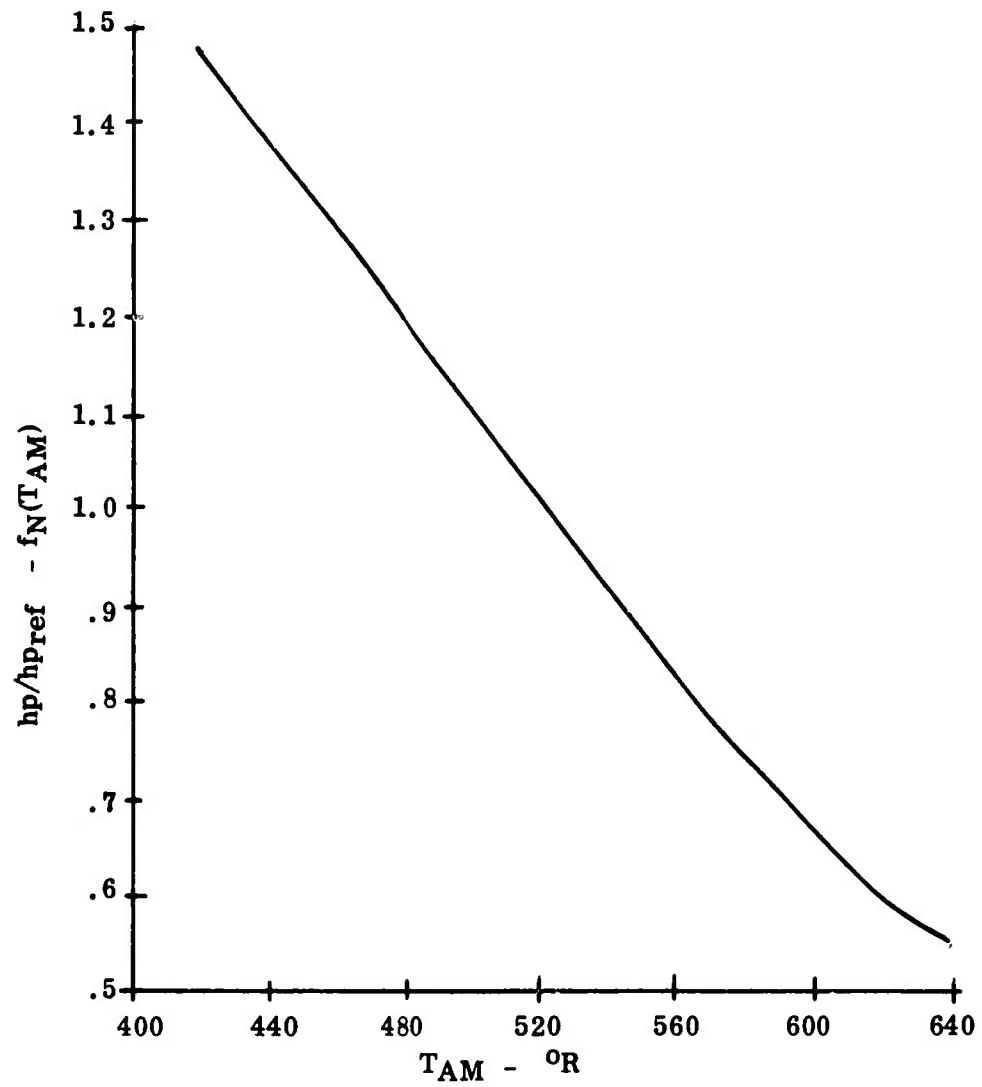
Figure 12. N_1 Limiting Mode Ambient Temperature Correction Factor Versus T_{AM}.

17
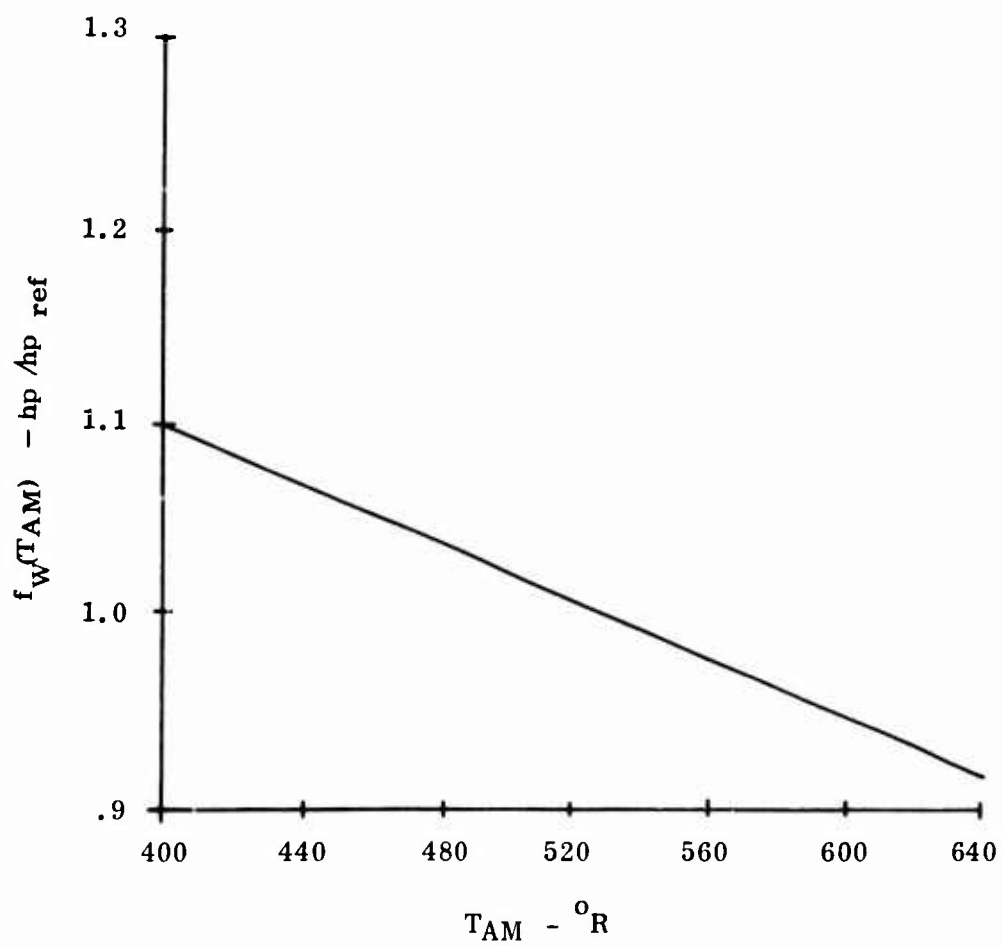
Figure 13. W_f Limit Mode Ambient Temperature Correction Factor Versus T_{AM}.

18

conditions evolved in the UH-1 AIDAPS program will also be used in the power prediction algorithm. Satisfying all three of the following conditions indicates that the engine is sufficiently near steady state to take measurements for prediction.

1. N_1 MAX - N_1 MIN within a frame ≤ 200 rpm

2. $|\Delta N_1 C|$ between frames ≤ 100 rpm

3. T_{T7C} MAX - T_{T7C} MIN $\leq 2.5°F$ for 60 seconds

One frame of data represents two seconds of measurement time. There are four speed measurements and four temperature measurements in one frame.

The power prediction algorithm involves the use of predetermined "B"-matrix, "C"-matrix, and base lines. As noted, the "B"-matrix relates the variations in engine efficiency, geometry, and airflow pumping capacity to measured variations in speed, temperature, pressure, power, and fuel at low power, whereas the "C"-matrix relates the variations in maximum power on each control limit to the computed variations in maximum power on each control limit to the computed variations in engine efficiency, geometry, and airflow pumping capacity. Studies have indicated that neglect of the changes in the "B"-matrix and "C"-matrix resulting from engine degradation causes a relatively minor error in the power prediction algorithm. Therefore, the "B"-matrix and "C"-matrix, as computed for the typical engine, may be used in all units; i.e., every prediction computer will contain identical stored "B" and "C" matrices for the same engine model.

However, a review of the actual steady-state data from the 75 engines tested shows relatively large engine-to-engine variations in the base lines. As a result, it appears necessary to measure and store a unique set of base-line values for each engine to avoid significant errors in prediction. This requires an initial steady-state "calibration" for each engine to be loaded into the prediction computer. The power prediction can then accurately predict the effect of any subsequent engine degradation. It should be noted that this initial calibration requirement of the engine base lines is based on observed engine-to-engine variations of the T53-L13 model and may not apply to another engine model.

19

CONFIRMATION OF MODEL ACCURACY

To analytically evaluate the validity of the algorithm for computing MPA, the base-line engine was "degraded" by making a 1% increase in η_C, η_t, η_{pt}, A_5, and A_N. The influence coefficients were used to obtain a set of steady-state engine data for the "degraded" engine. This data served as the source of low-power measurements for the degraded engine. The MPA was calculated using the steady-state characteristics for the degraded engine and using the power prediction algorithm. All computations were made at sea-level standard-day conditions and at optimal N_2 speed.

In order to determine MPA when on N_1 speed limiting for the steady-state characteristics of the degraded engine, it is first necessary to determine the new N_1 limiting speed. It is assumed that the fuel control is a W_f/δ_1 type droop control with a droop slope given by:

$$\left(\frac{\partial W_f/\delta_1}{W_f/\delta_1} \middle/ \frac{\partial N_1/\sqrt{\theta_1}}{N_1/\sqrt{\theta_1}} \right) = -6.5 \tag{11}$$

Droop Line

For sea-level standard-day conditions, Figure 14 shows a plot of W_f/δ_1 vs. $N_1/\sqrt{\theta_1}$ for both the base-line and degraded engines. Also shown in Figure 14 is the control droop line which passes through the base-line point of $N_1/\sqrt{\theta} = 24,700$ rpm and $W_f/\delta_1 = 793$ pph and whose slope is given by Equation 11. The intersection of the "degraded" steady-state line with the droop line defines the N_1 limiting speed for the degraded engine. From Figure 14, the limiting speed for the degraded engine is approximately 24,820 rpm. Figure 15 shows power turbine horsepower as a function of gas producer speed for the base-line and degraded engines. The horsepower at the N_1 limiting speed for the degraded engine is designated by the symbol "SHPON" and is found to be 1383 hp. Figure 16 shows power turbine horsepower as a function of T_7 for the base-line and degraded engines. At the T_7 limit value of $1743°R$, the horsepower for the degraded engine designated by "SHPOT" is found to be 1545 hp. Figure 17 shows power turbine horsepower as a function of fuel flow for the base-line and degraded engines. At the W_f limit value of 793 pph, the horsepower for the degraded engine designated by SHPON is found to be 1440. The above results were analytically determined from the steady-state characteristics of the "degraded" engine. From these results, the MPA is given by:

$$\text{MPA} = \text{MIN (SHPON, SHPOT, SHPOW)} = 1383 \text{ hp} \tag{12}$$
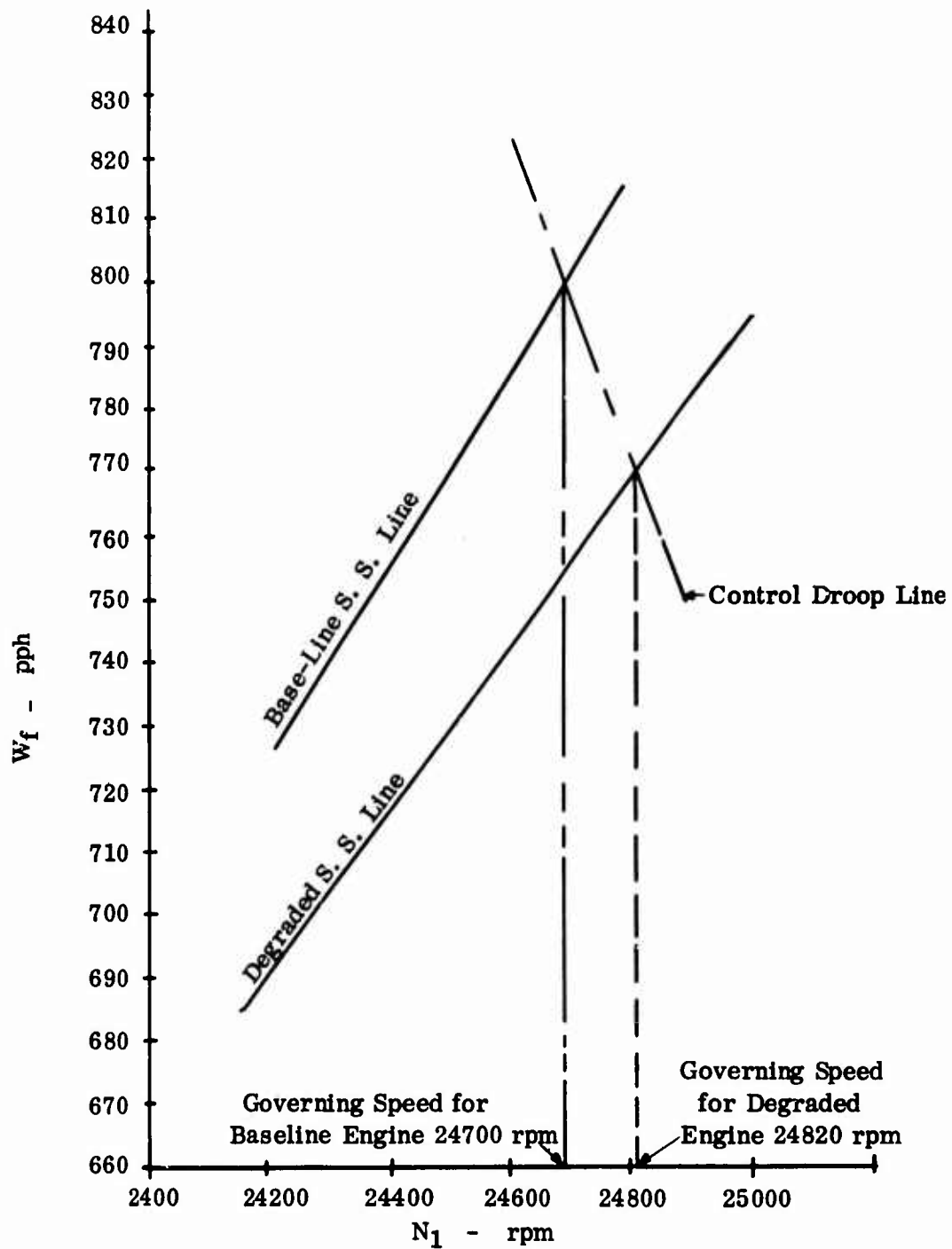
Figure 14.   Wf Versus N_1 for Base-Line Engine and for Base-Line Engine Degraded by 1% Increase in η_c, η_t, η_{pt}, A_5 and A_N.

21
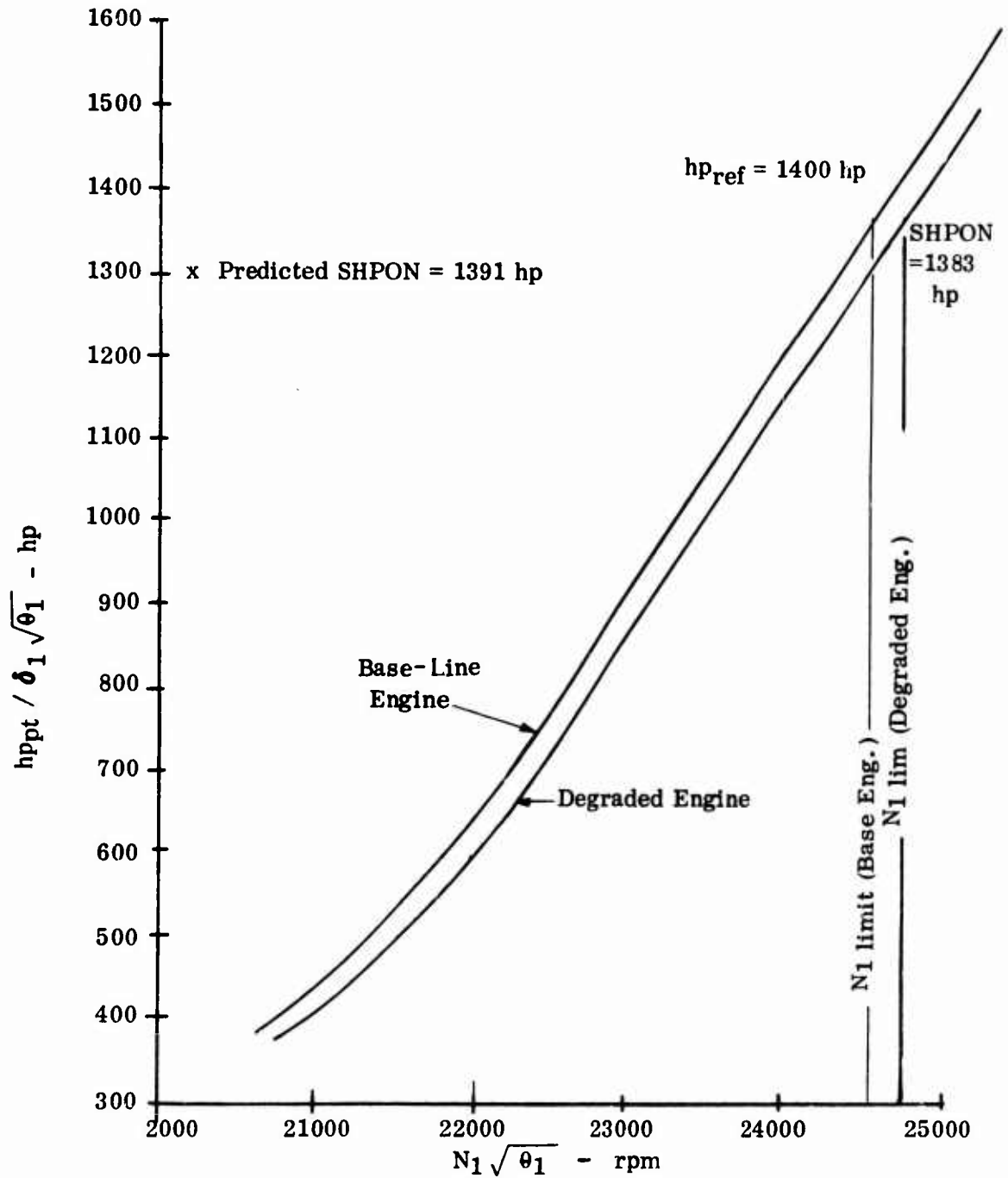
Figure 15. hp_{pt} Versus N_1 for Base-Line Engine and for Base-Line Engine Degraded by 1% Increase in η_c, η_t, η_{pt}, A_5, and A_N.
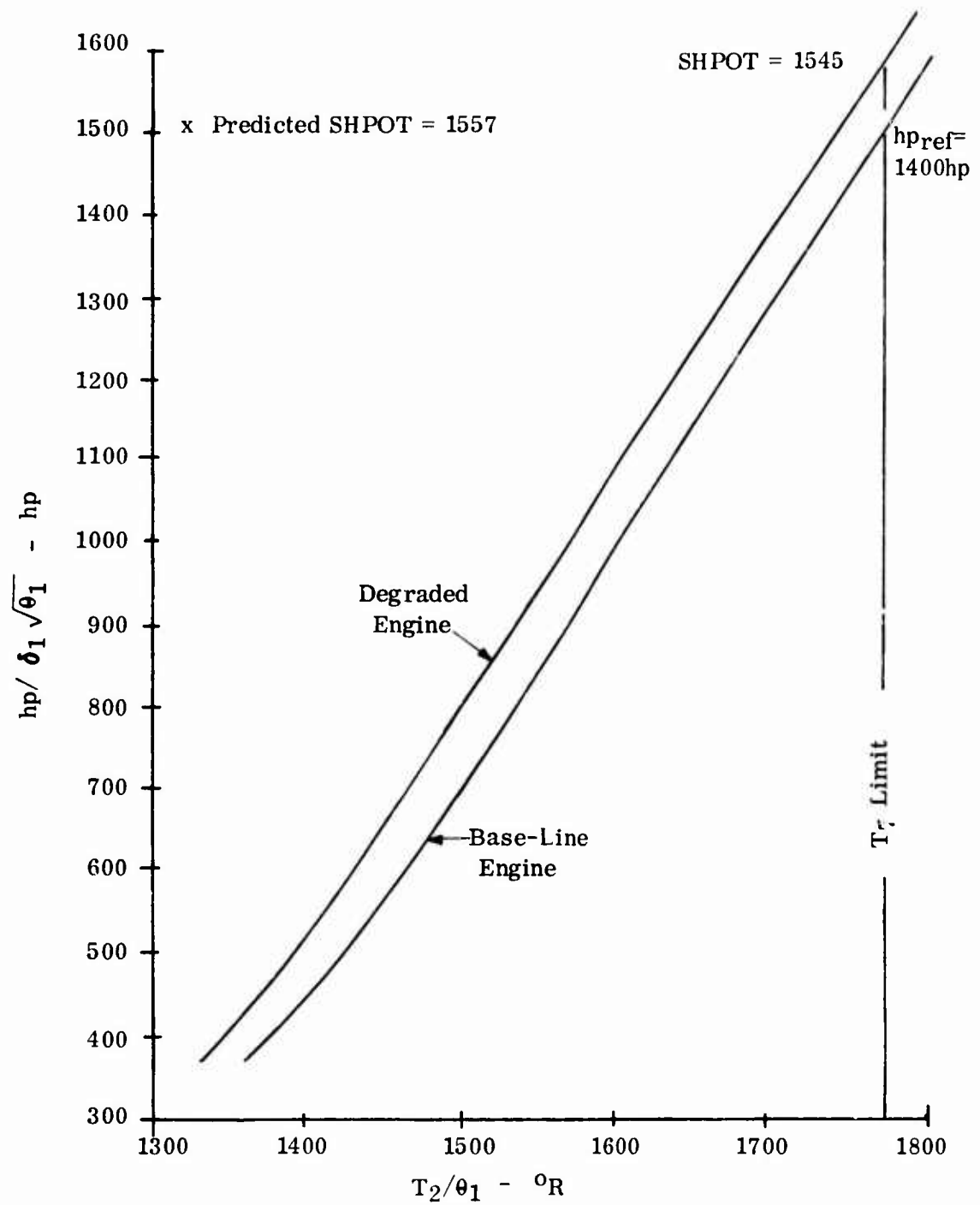
Figure 16. hp_{pt} Versus T_7 for Base-Line Engine and for Base-Line Engine Degraded by 1% Increase in η_c, η_t η_{pt}, A_5 and A_N.
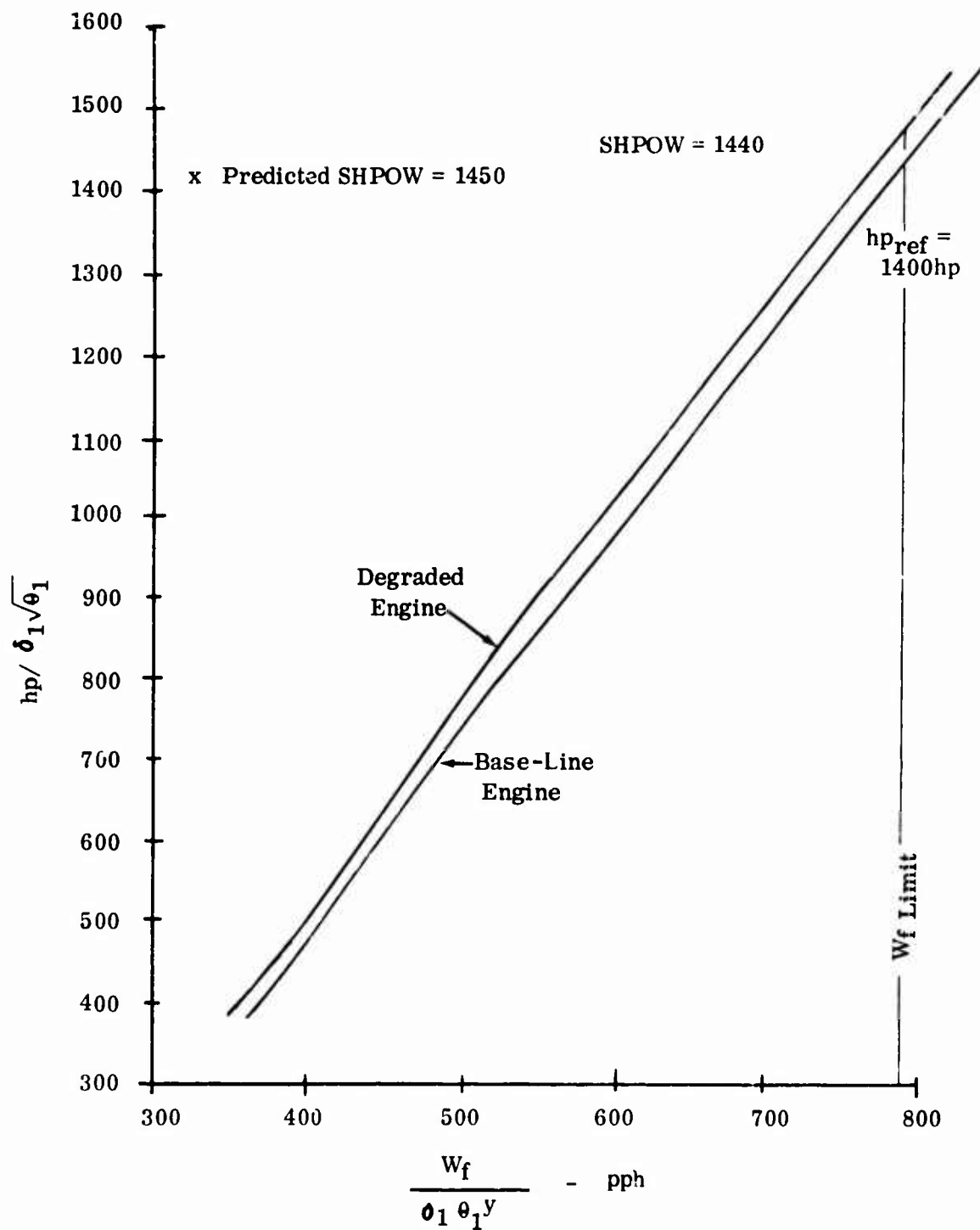
Figure 17. hp_{pt} Versus W_f for Base-Line Engine and for Base-Line Engine Degraded by 1% Increase in η_c, η_t, η_{pt}, A_5, & A_N.

At a relatively low power condition, input data for the power prediction program was obtained from the steady-state characteristics of the degraded engine at a constant P_3/δ_1 value. Table I shows the steady-state values used as measurements in the power prediction program at P_3/δ_1 = 60.3647 psia.

The results from the power prediction program are summarized as follows:

$$SHPON = 1390.9448 \text{ hp} \qquad (N_1 \text{ Limiting})$$

$$SHPOT = 1557.09668 \text{ hp} \qquad (T_7 \text{ Limiting})$$

$$SHPOW = 1449.7737 \text{ hp} \qquad (W_f \text{ Limiting})$$

These predicted values are also shown in Figures 15, 16, and 17. From the power prediction program, the MPA is given by

$$MPA = MIN (SHPON, SHPOT, SHPOW) = 1377.877 \text{ hp}$$

The results from the power prediction program are within 1% of the analytical results based on the steady-state characteristics. The small errors are due in part to errors in precisely determining the steady-state characteristics of the degraded engine, errors in predicting power at each control limit, and computer round-off errors. The results, however, do show that the power prediction algorithm is conceptually correct.

PARAMETRIC SENSITIVITY STUDIES AND ERROR ANALYSES

The following conditions were assumed for the parametric sensitivity studies and error analyses:

1. The pilot-selected N_2 speed and collective pitch result in 100% rotor speed at the maximum power condition being predicted.

2. The detailed error analysis was performed using the T53-L13 helicopter engine with a modern helicopter engine control similar to the control mode used on the Lycoming LTC-4V-1 engine. Specifically, it is assumed that maximum power is limited by the least of three control limits on N_1, T_7 and W_f.

TABLE I. MEASUREMENTS AT LOW POWER FOR ANALYTICAL CONFIRMATION OF MODEL ACCURACY

$$P_3/\delta_1 = 60.3647 \text{ psia}$$

Parameter	Base-Line Values	Degraded Engine*
$N_1/\sqrt{\theta_1}$	20,700 rpm	20,800 rpm
T_3/θ_1	851.456°R	847.824°R
$W_f/(\delta_1\theta_1^y)$	354.036 pph	343.846 pph
P_7/δ_1	23.7552 psia	23.7057 psia
$(hp_{pt})/(\delta_1\sqrt{\theta_1})$	369.493 hp	363.159 hp
T_7/θ_1	1369.86°R	1333.32°R

* Measurements corresponding to 1% increase in η_C, η_t, η_{pt}, A_5, and A_N.

3. Specific assumptions needed to perform the error analyses were included in Appendix I.

4. The interest in power prediction is limited to lift-off conditions; therefore, effects of flight speed need not be included in the error analysis.

Sensitivity studies were conducted to determine the influence of each pertinent factor on the accuracy of computed maximum power. Sensor errors at low power and at high power are considered separately.

The results of the sensitivity study for Set I sensors are shown in Table II. Table II also gives the error in predicted power due to uncertainty in compressor bleed air (W_{BL}) and compressor shaft power extraction (SPE/W_a) at low power and high power. As an example, Table II shows that an N_1 speed sensor indicating a speed 1% higher than actual speed at low power $(N_1 = 21,900$ rpm, $SHP = 35.2\%$ of maximum power) causes the computed maximum power to be 4.02% less than the actual maximum power if the engine is on the T_7 control limit.

Note that N_2 speed at both low and high power is defined as 100%. The N_2 speed is actually dependent on both pilot-selected N_2 limiting speed and pilot-selected collective pitch. Similarly, it is assumed that N_2 speed is 100%, and collective pitch is selected to cause the engine to encounter a control limit while at high power.

The percent-of-point temperature and pressure sensor errors are percentage of absolute temperature $(°R)$ and absolute pressure $(psia)$, respectively. (W_{BL}) is percentage of compressor airflow. (SPE/W_a) is horsepower per pound per second of compressor airflow.

Table III gives the sensitivity table for Set II sensors. Note that this set of sensors is not sufficient to uniquely determine the six performance parameters. A relationship between the independent variables must be assumed. This assumed relationship (although inexact) is that $\partial A_N/A_N = -\partial \eta_{pt}/\eta_{pt}$ and was demonstrated to be a good approximation in the AIDAPS engine diagnostic program. Note also that this set of measurements at low power was obtained on actual engines in the AIDAPS program.

The total horsepower prediction errors for prediction algorithms using the first two sets of sensors are summarized in Tables IV, V, VI, and VII. Table IV is an error summary when using Set I sensors. Using constant "C" coefficients

TABLE II. SENSITIVITY STUDY - EFFECT OF SENSOR ERRORS AT LOW POWER AND AT HIGH POWER ON POWER REMAINING ACCURACY SET I SENSORS

% Max Power % of Point	Limit Mode	N_1=21,700 hp=35.2%	N_1=21,200 hp=27.%	N_1=20,700 hp=19.7%	N_1=20,200 hp=13.6%	N_1=19,700 hp=8.6%	N_1=24,700 hp=100%
$\dfrac{\partial hp}{\partial N_1}$	N_1	-7.45	-8.50	-10.08	-12.58	-15.14	-3.71
	T_7	-4.02	-5.41	- 7.32	-10.27	-13.23	0.
	W_f	-2.88	-4.08	- 5.83	- 8.69	-11.57	0.
$\dfrac{\partial hp}{\partial T_3}$	N_1	- .14	- .19	- .24	- .29	- .33	0.
	T_7	- .10	- .08	- .05	.00	- .06	0.
	W_f	- .19	- .10	- .10	- .10	- .09	0.
$\dfrac{\partial hp}{\partial W_f}$	N_1	- .59	- .53	- .60	- .60	- .61	+ .56
	T_7	+ .01	+ .02	+ .03	+ .03	+ .04	0.
	W_f	-1.46	-1.46	-1.46	-1.46	-1.46	+1.47
$\partial hp/\partial$ SHP	N_1, T_7, W_f	1.00	1.00	1.00	1.00	1.00	--

TABLE II.   Continued

% Max Power % of Point	Limit Mode	N_1=21,700 hp=35.2%	N_1=21,200 hp=27.%	N_1=20,700 hp=19.7%	N_1=20,200 hp=13.6%	N_1=19,700 hp=8.6%	N_1=24,700 hp=100%
$\frac{\partial hp}{\partial T_7}$	N_1	-.20	-.25	-.30	-.34	.37	0.
	T_7	-4.40	-4.46	-4.52	-4.58	-4.64	-4.31
	W_f	-.03	-.05	-0.7	-.10	-.13	0.
$\frac{\partial hp}{\partial P_7}$	N_1	-.39	-.49	-.59	-.67	-.75	0.
	T_7	-.71	-.98	-1.23	-2.30	-1.98	0.
	W_f	-.52	-.69	-.85	-1.06	-1.25	0.
$\partial hp/\partial N_2$	$N_1\ T_7, W_f$	+1.03	+1.44	+2.10	+3.25	+5.37	--
$\frac{\partial hp}{\partial T_1}$	N_1	+3.68	+4.20	+4.97	+6.20	+7.03	.76
	T_7	+5.36	+5.95	+6.77	+8.08	+8.98	0.
	W_f	+1.79	+2.29	+3.02	+4.29	+5.15	0.
$\frac{\partial hp}{\partial P_1}$	N_1	-.45	-.41	-.38	-.32	-.25	0.
	T_7	-.60	-.40	-.06	+.30	+.77	0.
	W_f	+.84	+.94	+1.12	+1.32	+1.57	-.37

TABLE II. Continued

% Max Power % of Point	Limit Mode	N_1=21,700 hp=35.2%	N_1=21,200 hp=27.%	N_1=20,700 hp=19.7%	N_1=20,200 hp=13.6%	N_1=19,700 hp=8.6%	N_1=24,700 hp=100%
$\dfrac{\partial hp}{\partial P_3}$	N_1	+ .21	+ .18	+ .21	+ .22	+ .23	0.
	T_7	+ .14	+ .09	+ .09	+ .04	+ .03	0.
	W_f	+ .08	+ .05	+ .06	+ .04	+ .01	0.
$\partial hp/\partial N_1$ Set	N_1	0.	0.	0.	0.	0.	+3.71
$\partial hp/\partial T_7$ Set	T_7	0.	0.	0.	0.	0.	+4.31
$\dfrac{\partial hp}{\partial WBL}$	N_1	+ .70	+ .68	+ .66	+ .90	+1.11	+ .78
	T_7	+3.24	+3.25	+3.26	+2.78	+2.35	+3.?9
	W_f	+1.46	+1.38	+1.37	+1.19	+1.04	+1.43
$\left[\dfrac{\partial hp}{\partial\left(\dfrac{SPE}{WA}\right)}\right]^{*}$	N_1	- .39	- .43	- .48	- .53	- .58	+ .22
	T_7	+2.26	+2.44	+2.60	+2.82	+3.02	-1.57
	W_f	+ .95	+1.02	+1.07	+1.14	+1.21	- .68

Notes   *Units are % Max Power/(hp/rps of Airflow)

N_2 = 100%

Standard Day Conditions

TABLE III.   SENSITIVITY STUDY - EFFECT OF SENSOR ERRORS AT LOW POWER AND AT HIGH POWER ON POWER REMAINING ACCURACY SET II SENSORS

% Max Power of Point	Limit Mode	N_1=22,800 hp=57.5%	N_1=21,700 hp=35.2%	N_1=21,200 hp=27%	N_1=20,700 hp=19.7%	N_1=20,200 hp=13.6%	N_1=19,700 hp=8.6%	N_1=24,700 hp=100%
$\frac{\partial hp}{\partial N_1}$	N_1	5.55	7.08	-7.86	-9.03	-10.85	-12.63	-3.71
	T_7	-1.74	-3.14	3.82	-4.57	5.39	- 5.71	0.0
	W_f	-1.14	-2.44	-3.31	-4.54	6.48	- 8.32	0.0
$\frac{\partial hp}{\partial T_3}$	N_1	- .05	- .12	- .16	- .20	- .24	- .28	0.0
	T_7	- .05	- .01	+ .04	+ .08	+ .16	+ .23	0.0
	W_f	- .06	- .06	- .05	- .04	- .02	+ 0.00	0.0
$\frac{\partial hp}{\partial W_f}$	N_1	- .59	- .60	- .60	- .60	- .61	.61	+ .56
	T_7	+ .68	+ .54	+ .42	+ .36	+ .36	+ .32	0.0
	W_f	-1.48	-1.49	1.49	-1.49	- 1.50	- 1.50	+1.47
$\frac{\partial hp}{\partial SHP}$	N_1	+ .92	+ .86	+ .82	+ .81	+ .80	+ .80	--
	T_7	+ .18	+ .23	+ .25	+ .23	+ .21	+ .17	--
	W_f	+ .92	+ .86	+ .78	+ .72	+ .67	.63	--

31

TABLE III. Continued

% Max Power of Point	Limit Mode	N_1=22,800 hp=57.5%	N_1=21,700 hp=35.2%	N_1=21,200 hp=27%	N_1=20,700 hp=19.7%	N_1=20,200 hp=13.6%	N_1=19,700 hp=8.6%	N_1=24,700 hp=100%
$\dfrac{\partial hp}{\partial T_9}$	N_1	- .04	- .06	- .08	- .10	- .13	.15	0.0
	T_7	-4.56	-4.52	-4.48	-4.46	-4.40	-4.36	-4.31
	W_f	+ .09	+ .17	+ .20	+ .23	+ .26	+ .28	0.0
$\dfrac{\partial hp}{\partial N_2}$	N_1	+ .40	+ .88	+1.22	+1.75	+2.71	+4.48	--
	T_7	+ .38	+ .73	+ .92	+1.14	+1.41	+1.78	--
	W_f	+ .38	+ .84	+1.14	+1.61	+2.41	+3.87	--
$\dfrac{\partial hp}{\partial T_1}$	N_1	+2.75	+3.52	+3.94	+4.56	+5.59	+6.28	- .76
	T_7	+4.64	+5.15	+5.35	+5.58	+5.72	+5.42	0.0
	W_f	+1.02	+1.46	+1.79	+2.30	+3.16	+3.70	0.0
$\dfrac{\partial hp}{\partial P_1}$	N_1	- .81	- .68	- .70	- .76	- .76	- .78	0.0
	T_7	-1.05	- .91	- .86	- .78	- .71	- .60	0.0
	W_f	+ .38	+ .51	+ .52	+ .54	+ .60	+ .65	- .37
$\dfrac{\partial hp}{\partial P_3}$	N_1	+ .33	+ .22	+ .20	+ .22	+ .24	+ .24	0.0
	T_7	+ .16	+ .10	+ .06	+ .05	+ .03	+ .02	0.0
	W_f	+ .23	+ .08	+ .07	+ .07	+ .06	+ .03	0.0

TABLE III.   Continued

% Max Power % of Point	Limit Mode	N_1=22,800 hp=57.5%	N_1=21,700 hp=35.2%	N_1=21,200 hp=27%	N_1=20,700 hp=19.7%	N_1=20,200 hp=13.6%	N_1=19,700 hp=8.6%	N_1=24,700 hp=100%
$\partial hp/\partial N_1$ SET	N_1	0.	0.	0.	0.	0.	0.	+3.71
$\partial hp/\partial T_7$ SET	T_7	0.	0.	0.	0.	0.	0.	+4.31
$\dfrac{\partial hp}{\partial W_{BL}}$	N_1	+ .74	+ .72	+ .70	+ .69	+ .67	+ .65	- .78
	T_7	+3.07	+3.16	+3.21	+3.26	+3.32	+3.37	-3.29
	W_f	+1.44	+1.43	+1.46	+1.42	+1.41	+1.41	-1.43
$\left[\dfrac{\partial hp}{\partial\left(\frac{SPE}{W_a}\right)}\right]$ *	N_1	- .315	- .390	- .425	- .463	- .514	- .560	+ .22
	T_7	+1.79	+2.13	+2.33	+2.52	+2.76	+2.98	-1.57
	W_f	+0.84	+ .969	+1.04	+1.10	+1.18	+1.25	- .68

Notes: * $\dfrac{\text{Units are \% Max Power}}{\text{(hp/pps of airflow)}}$

N_2 = 100%
Standard Day Conditions

33

TABLE IV. ERROR SUMMARY SHEET - PREDICTION AT 35.2% HORSEPOWER AT N_2 = 100% USING CONSTANT "C" IN PREDICTION ALGORITHM SET I SENSORS

Error Source	N_1 Limit % Power	T_7 Limit % Power	W_f Limit % Power	Detailed Error List Table No.	Applicable Notes (Appendix I)
Linearization of nonlinear differential equations	0.50	1.23	0.35	VIII	1.
Nonstandard day	0.31	4.98	3.61	IX, X	2,3
Use of base engine "C" for degraded engine	0.03	0.50	0.03	XI	4,5
High-power degradation being different from low-power degradation	0.22	0.68	0.22	XII	6
Change in actual power due to uncertainty in WBL and SPE at high power	1.17	4.96	2.15	XIII, II	7
Uncertainty in WBL and SPE low power	0.37	1.76	0.78	XIV	8
Sensor errors at low power	2.61	3.60	2.33	XV, XVI, II	9
Control limit and sensor errors at high power	0.52	1.55	0.74	XV, XVI, II	9
Total Error:	3.00	8.37	4.94		

34

TABLE V. ERROR SUMMARY SHEET - PREDICTION AT 35.2% HORSEPOWER
AT N_2 = 100% USING INTERPOLATED "C" IN PREDICTION
ALGORITHM SET I SENSORS

Error Source	N_1 Limit % Power	T_7 Limit % Power	W_f Limit % Power	Detailed Error List Table No.	Applicable Notes (Appendix I)
Linearization of nonlinear differential equations	0.50	1.25	0.35	VIII	1
Nonstandard day	0.10	0.23	0.21		2,3
Use of base engine "C" for degraded engine	0.03	0.50	0.03	XI	4,5
High-power degradation being different from low-power degradation	0.22	0.68	0.22	XII	6
Change in actual power due to uncertainty in W_{BL} and SPE at high power	1.17	4.96	2.15	XIII, II	7
Uncertainty in W_{BL} and SPE at low power	0.37	1.76	0.78	XIV	8
Sensor errors at low power	2.61	3.60	2.33	XV, XVI, II	9
Control limit and sensor errors at high power	0.52	1.55	0.74	XV, XVI, II	9
(RSS) Total Error	2.98	6.73	3.38		

TABLE V – CONTINUED

Error Source	N1 Limit % Power	T$_7$ Limit % Power	W$_f$ Limit % Power	Detailed Error List Table No.	Applicable Notes (Appendix I)
Standard Sensors:					
Sensor Errors at low power	6.5	7.02	6.46	XV, XVII, II	10
Control limit and sensor errors at high power	0.52	1.55	0.99	XV, XVII, II	10
(RSS) Total Error	7.15	9.03	6.53		

36

TABLE VI. ERROR SUMMARY SHEET - PREDICTION AT 19.7% POWER AT N2 = 100% USING INTERPOLATED "C" IN PREDICTION ALGORITHM SET I SENSORS

Error Source	N_1 Limit % Power	T_7 Limit % Power	W_f Limit % Power	Detailed Error List Table No.	Applicable Notes (Appendix I)
Linearization of nonlinear differential equations	0.50	1.23	0.35	VIII	1
Nonstandard day	0.10	0.23	0.21		2,3
Use of base engine "C" for degraded engine	0.03	0.50	0.03	XI	4,5
High-power degradation being different from low-power degradation	0.22	0.68	0.22	XII	6
Change in actual power due to uncertainty in W_{BL} and SPE at high power	1.17	4.96	2.15	XIII, II	7
Uncertainty in W_{BL} and SPE at low power	0.36	1.77	0.76	XIV	8
Sensor errors at low power	4.20	5.06	3.93	XV, XVIII, II	9
Control limit and sensor errors at high power	0.52	1.55	0.74	XV, XVIII, II	9
(RSS) Total Error	4.44	7.62	4.63		

TABLE VII. ERROR SUMMARY SHEET - PREDICTION AT 35.2% HORSEPOWER AT N_2 = 100% USING INTERPOLATED "C" IN PREDICTION ALGORITHM SET II SENSORS

Error Source	N_1 Limit % Power	T_7 Limit % Power	W_f Limit % Power	Detailed Error List Table No.	Applicable Notes (Appendix I)
Linearization of nonlinear differential equations	0.50	1.23	0.35	VIII	1
$\partial A_N/A_N$ not equal to $-\partial \eta_{pt}/\eta_{pt}$	0.30	0.54	0.40		11
Nonstandard day	0.10	0.23	0.21		2,3
Use of base engine "C" for degraded engine	0.03	0.50	0.30	XI	4,5
High-power degradation being different from low-power degradation	0.22	0.68	0.22	XII	6
Change in actual power due to uncertainty in W_{BL} and SPE at high power	1.17	4.96	2.15	XIII, III	7
Uncertainty in W_{BL} and SPE at low power	0.38	1.70	0.78	XIV	8
Sensor Errors at low power	2.34	3.17	2.02	XV, XIX	8

TABLE VII.   Continued

Error Source	N_1 Lim % Power	T_7 Lim % Power	W_f Lim % Power	Detailed Error List Table No.	Applicable Notes (Appendix I)
Control Limit and sensor errors at high power	0.52	1.55	0.74	XV, XIX, III	9
Total Error	2.77	6.52	3.20		
Standard Sensors:					
Sensor errors at low power	5.66	3.65	5.49	XV, XX, III	10
Control limit and sensor errors at high power	0.52	.55	0.29	XV, XX, III	10
Total Error	5.85	6.77	6.07		

(computed at maximum power on a standard day) results in a significant prediction error at nonstandard-day conditions. Table V is an error summary having the same conditions as Table IV except that all "C" are interpolated values. Details about interpolation of "C" are described later. Table VI is an error summary using the same algorithm as in Table V, but predicting maximum power at a lower horsepower (19.7%). Table VII is an error summary when using Set II measurements at low power.

Tables IV through VII summarize the root sum squared (RSS) prediction error for each of the three control limits (N_1, T_7, and W_f). Tables VIII through XX contain a detailed error list. Also, Appendix I provides additional information and the conditions assumed when performing the error analysis. Tables V and VII also contain an error summary when using so-called "standard sensors". In particular, the pressure sensors and shaft horsepower sensors are not the "best available." Errors in the assumption that $\partial A_N/A_N = -\partial\eta_{pt}/\eta_{pt}$ are a source of power prediction error and are included in the error summary sheet.

The range of ambient conditions where each control limit influences maximum power is defined in Figure 18. This figure shows the combinations of P_1 and T_1 where the N_1 limit, T_7 limit, and W_f limit determine the maximum power. For example, horsepower is limited by W_f at high P_1 and limited by N_1 at low P_1 in the temperature range of $-12°F$ to $59°F$ for the base engine. All three limits occur simultaneously at standard-day conditions ($P_1 = 14.7$ psia and $T_1 = 518.7°R = 59°F$). The range of thermodynamic conditions where a W_f limit, T_7 limit, or N_1 limit can occur is smaller than the complete range of ambient conditions. Hence, the desired changes in the influence of horsepower on coefficients "C" are correspondingly smaller and are listed in Table IX. The effect of nonstandard day on "C" in the range where each limit can be encountered is shown in Table X.

It is noted in Table IV that a dominant error is caused by the use of a constant "C" (computed at standard day) for nonstandard-day conditions. Studies indicate that most of this error can be eliminated by storing two values of each "C" (instead of one) and then interpolating as a function of the existing P_1 and T_1. The specific conditions where "C" is computed (and stored) and the method of interpolation for each limit are defined below:

TABLE VIII. DETAILED ERROR LIST – LINEARIZATION OF NONLINEAR DIFFERENTIAL EQUATIONS

Variable	Maximum Variation %	Base Engine "C" N₁ Limit	T₇ Limit	Wf Limit	hp Error at ±5% "C" N₁ Limit % Power	T₇ Limit % Power	Wf Limit % Power
η_c	-3.5	-.7620	3.3798	.8269	.133	.59	.145
η_t	-2.5	-.9790	4.3485	1.1859	.122	.544	.148
η_{pt}	-2.5	1.0044	1.0061	1.0051	.176	.126	.126
A_5	+2.2	.7930	-1.5644	-.6320	.089	.176	.070
AN	+2.2	-1.6937	2.4311	-.034	.186	.267	.004
W_a	-2.0	1.2929	-.0597	-.1159	.129	.006	.016
				RSS Error	.35	.87	.25
η_c	-3.5	-.7620	3.3798	.8269	.133	.59	.145
η_t	-2.5	-.9790	4.3485	1.1859	.122	.544	.148
η_{pt}	-2.5	1.0044	1.0061	1.0051	.176	.126	.126
A_5	+2.2	.7930	-1.5644	-.6320	.087	.172	.070
AN	+2.2	-1.6937	2.4311	-.034	.186	.267	.004
W_a	-2.0	1.2929	-.0597	-.1159	.129	.006	.016
				RSS Error	.35 (hp Error at ±5% "B")	.87	.25
				RSS Error due to ±5% error in "C" and ±5% error in "B".	.50	1.28	.35

41

TABLE IX. DETAILED ERROR LIST – EFFECT OF NONSTANDARD DAY ON THE VALUE OF "C" BASE ENGINE

	N_1 Limit		
	$T_1 = 59°F$ $N_{1C} = 24,700$	$T_1 = -12°F$ $N_{1C} = 26,600$	
Variable	"C"	" C "	Δ"C"
η_c	- .7620	- .7950	+ .0330
η_t	- .9790	-1.0583	+ .0793
η_{pt}	1.0044	1.0061	- .0017
A_N	-1.6937	-1.6377	- .0560
W_a	1.2929	1.3710	- .0781
A_5	.7930	.7579	+ .0351

	T_7 Limit		
	$T_1 = 59°F$ $N_{1C} = 24,700$	$T_1 = 120°F$ $N_{1C} = 22,900$	
Variable	"C "	" C "	Δ"C"
η_c	3.3798	4.3462	- .9664
η_t	4.3485	5.5683	-1.2198
η_{pt}	1.0061	1.0052	+ .0009
A_N	2.4311	3.1649	- .7338
W_a	- .0597	- .3484	+ .2887
A_5	-1.5644	-2.0589.	+ .4945

TABLE IX - Continued

W$_f$ Limit

Variable	"C" $T_1 = 59°F$, $N_1C = 24,700$, $P_1 = 14.7$ psia	"C" $T_1 = -60°F$, $N_1C = 26,900$, $P_1 = 11$	"C" $T_1 = 72°F$, $N_1C = 24,340$, $P_1 = 16$	"C" (Col. 1 - Col. 2)	"C" (Col. 1 - Col. 3)
P_1/P_{1Ref}	-.8409	-.6377	-.8835	-.2032	.0426
η_c	.8269	.6351	.8758	.1918	-.0489
η_t	1.1859	.9046	1.2533	.2813	-.0674
η_{PT}	1.0051	1.0071	1.0047	-.0020	+.0004
AN	-.0340	-.1105	.0058	+.0765	-.0398
W_a	-.0281	+.0727	-.0479	-.1008	+.0198
A_5	-.4873	-.3507	-.5209	-.1366	+.0336

43

TABLE X. DETAILED ERROR LIST – PREDICTION ERROR AT NONSTANDARD DAY CAUSED BY USING CONSTANT "C" ("C" COMPUTED AT STANDARD DAY)

PREDICTION AT COLDEST DAY

Variable	Maximum Δ From Nominal	Speed Limit ($T_1 = -12°F$) Δ "C"	hp Error	Fuel Limit ($T_1 = -60°F$) Δ "C"	hp Error
P_1/P_{1REF}	17%			-.2032	3.454
η_c	3.5%	+.0330	+.116	.1918	.671
η_t	2.5%	+.0793	.198	.2813	.703
η_{pt}	2.5%	-.0017	.004	-.0020	.005
A_N	2.2%	-.0560	.123	+.0765	.168
W_a	2.0%	-.0731	.156	-.1008	.202
A_5	2.2%	+.0351	.077	-.1366	.301
			.313% RSS Error		3.61% RSS Error

PREDICTION AT HOTTEST DAY

Variable	Maximum Δ From Nominal	Temp. Limit ($T_1 = 120°F$) Δ "C"	hp Error	Fuel Limit ($T_1 = 72°F$) Δ "C"	hp Error
P_1/P_{1REF}	17%			.0426	.724
η_c	3.5%	-.9664	3.382	-.0489	.171
η_t	2.5%	-1.2198	3.049	-.0674	.169
η_{pt}	2.5%	+.0009	.002	.0004	.001
A_N	2.2%	-.7338	1.614	-.0398	.088
W_a	2.0%	.2887	.577	.0198	.040
A_5	2.2%	.4945	1.088	.0336	.074
			4.98% RSS Error		.772% RSS Error

TABLE XI. DETAILED ERROR LIST – USE OF BASE ENGINE "C" FOR DEGRADED ENGINE

Limit	Variable	Defined Degradation %	Base Engine "C"	Degraded Engine "C"	Average Value of "C"	Error in "C"	Horsepower Error % Power
N_1	η_c	-1.	-.7620	-.7555	-.7583	-.0033	.0033
	η_t	-1.	-.9790	-.9564	-.9677	-.0113	.0113
	η_{pt}	-1.	1.0044	1.0038	1.0041	.0003	.0003
	A_5	+1.	.7930	.8019	.7975	-.0045	.0045
	A_N	+1.	-1.6937	-1.7164	-1.7051	.0114	.0114
						RSS ERROR	0.017
T_2	η_c	-1.	3.3798	3.6521	3.5160	-.1362	.1362
	η_t	-1.	4.3485	4.6728	4.5106	-.1621	.1621
	η_{pt}	-1.	1.0061	1.0055	1.0058	.0003	.0003
	A_5	+1.	-1.5644	-1.7113	-1.6379	.0735	.0735
	A_N	+1.	2.4311	2.6632	2.5471	-.1160	.1160
						RSS ERROR	0.25
W_f	η_c	-1.	8.269	.8454	.8361	-.0092	.0092
	η_t	-1.	1.1859	1.2045	1.1952	-.0093	.0093
	η_{pt}	-1.	1.0051	1.0047	1.0049	.0002	.0002
	A_5	+1.	-.4873	-.5007	-.4940	.0067	.0067
	A_N	+1.	-.0340	-.0323	-.0331	-.0009	.0009
						RSS ERROR	0.015

NOTES:

Consider a "Severe Degradation" to be twice the above "Defined Degradation". The estimated horsepower error is as follows:

N_1 Limit Error = 0.034% T_7 Limit Error = 0.50%

W_f Limit Error = 0.30%

TABLE XII. DETAILED ERROR LIST - HIGH POWER DEGRADATION BEING DIFFERENT FROM LOW POWER DEGRADATION

Limit	Variable	Base Engine "C"	Estimate Difference Between Low and High Power Degradation (% of Point)	Horsepower Error
N_1	η_c	- .7620	± 0.15	.1143
	η_t	- .9790	± 0.10	.0979
	η_{pt}	1.0044	± 0.10	.1004
	W_a	1.2929	± 0.10	.1293
	A_5	.7930	0.	0.
	A_n	-1.6937	0.	0.
			RSS Error	0.22%
T_7	η_c	3.3798	± 0.15	.5070
	η_t	4.3485	± 0.15	.4349
	η_{pt}	1.0061	± 0.10	.1006
	W_a	- .0597	± 0.10	.0060
	A_5	-1.5644	0.	0.
	A_n	2.4311	0.	0.
			RSS Error	0.68%
W_f	η_c	.8269	± 0.15	.1240
	η_t	1.1859	± 0.10	.1186
	η_{pt}	1.0051	± 0.10	.1005
	W_a	- .0281	± 0.10	.0028
	A_5	- .6320	0.	0.
	A_n	- .034	0.	0.
			RSS Error	0.20%

TABLE XIII. DETAILED ERROR LIST – UNCERTAINTY IN COMPRESSOR WBL AND SPE AT MAXIMUM POWER WHEN PREDICTING AT LOW POWER

Variable	Uncertainty	N_1 Limit "C"	T_7 Limit "C"	W_f Limit "C"	Actual Horsepower Variation		
					N_1 Limit % Power	T_7 Limit % Power	W_f Limit % Power
WBL	±1.5% of max. W_a	.78	3.29	1.43	1.17	4.935	2.145
SPE	±.30 hp/pps of W_a	.22	-1.57	-.68	.07	.47	.204
			RSS Error		1.17%	4.96%	2.15%

TABLE XIV. DETAILED ERROR LIST - UNCERTAINTY IN COMPRESSOR W_{BL} AND SPE AT LOW POWER

Sensors & Power per Table	Variable	Uncertainty	Sensitivity			hp Prediction Error		
			N_1 Limit	T_7 Limit	W_f Limit	N_1 Limit	T_7 Limit	W_f Limit
I or II	W_{BL}	±5%	.71	3.24	1.46	.35	1.62	.73
	SPE	±.3 hp/pps	-.39	2.26	.95	.12	.68	.28
				RSS Error		.37%	1.76%	.78%
III	W_{BL}	±5%	.66	3.26	1.37	.33	1.63	.685
	SPE	±.3 hp/pps	-.48	2.60	1.07	.144	.78	.32
				RSS Error		.36%	1.77%	.76%
IV	W_{BL}	±5%	.72	3.16	1.43	.36	1.58	.72
	SPE	±.3 hp/pps	-.390	2.13	.969	.12	.64	.29
				RSS Error		.38%	1.70%	.78%

48

TABLE XV. STEADY-STATE SENSOR AND CONTROL ACCURACY ESTIMATES

Sensor	Range Min.	Range Max.	Sensor Type	Best Available Error Including Sensor Conversion	Standard Sensors Error Including Sensor Conversion
N_1	20K rpm	25K rpm	Tachometer	±2.5 rpm	±2.5 rpm
N_2	13K rpm	22K rpm	Tachometer	±2.5 rpm	±2.5 rpm
T_1	400°R	600°R	Platinum Resistance	±2.2°R	±2.2°R
T_3	670°R	1050°R	Chromel-Alumel (Thermocouple)	±6.3°R	±6.3°R
T_7	1100°R	1800°R	Chromel-Alumel	±6.3°R	±6.3°R
T_9	1000°R	1500°R	Chromel-Alumel	±6.3°R	±6.3°R
P_1	11 psia	16 psia	Strain Gage		$\pm.19$ psi
P_3	50 psia	110 psia	Strain Gage		±1.05 psi
P_7	20 psia	30 psia	Strain Gage		$\pm.36$ psi
P_1	11 psia	16 psia	Vibrating Cylinder	$\pm.02$ psi	
P_3	50 psia	110 psia	Vibrating Cylinder	$\pm.10$ psi	
P_7	20 psia	30 psia	Vibrating Cylinder	$\pm.05$ psi	
W_f	350 pph	800 pph		±2 pph at 400 pph / ±4 pph at 800 pph	±2 pph at 400 pph / ±4 pph at 800 pph
SHP	300 hp	1500 hp		±10 hp	±30 hp
	300 hp	500 hp			

Control

		Best Available	Standard Sensors
N_1 SET	$= 2.2\ (\ N_1\text{SET}/\ T_1\ )$	21 rpm	21 rpm
T_7 SET		0	0
W_f SET	$= .19\ (\ W_f\text{SET}/\ P_1\ )$		
	$= .02\ (\ W_f\text{SET}/\ P_1\ )$	$\pm.27$ pph	±2.55 pph

TABLE XVI. DETAILED ERROR LIST - SENSOR ERRORS AT 35.2% HORSEPOWER AND AT MAXIMUM HORSEPOWER USING SENSORS AT LOW POWER AS TABULATED BEST AVAILABLE SENSORS

Sensor	Error	Error in % of Point	Sensitivity			hp Prediction Error		
			N_1 Limit	T_7 Limit	W_f Limit	N_1 Limit	T_7 Limit	W_f Limit
Low Power:								
N_1	±2.5 rpm	±.012	-7.45	-4.02	-2.88	.0894	.0482	.0346
T_3	±6.3°R	±.71	-.14	-.10	-.19	.0994	.071	.1349
W_f	±2 pph	±.46	-.56	+.01	-1.46	.2714	.0046	.6716
SHP	±10 hp	±2.08	1.0	1.0	1.0	2.08	2.08	2.08
T_7	±6.3°R	±.43	-.20	-4.4	-.03	.0860	1.872	.0129
P_7	±.05 psi	±.19	-.39	-.71	-.52	.074	.1349	.0988
N_2	±2.5 rpm	±.013	1.03	1.03	1.03	.0134	.0134	.0134
T_1	±2.2°R	±.42	3.68	5.36	1.79	1.545	2.251	.7518
P_1	±.02 psi	±.135	-.45	-.60	.84	.0608	.081	.1134
P_3	±.10 psi	±.143	.21	.14	.08	.0300	.0200	.0114
				RSS Error		2.61	3.60	2.33
Maximum Power:								
N_1	±2.5 rpm	±.01	-3.71	0	0	.04	0	0
W_f	±4 pph	±.50	.56	0	1.47	.28	0	.735
T_7	±6.3°R	±.36	0	-4.31	0	0	1.552	0
T_1	±2.2°R	±.42	-.76	0	0	.319	0	0
P_1	±.02 psi	±.143	-.37	0	0	.0529	0	0
N_1 SET	±21 rpm	±.08	3.71	0	0	.2968	0	0
T_7 SET	0	0	0	4.31	0	0	0	0
W_f SET	±.27 pph	±.034	0	0	-1.47	0	0	.0500
				RSS Error		.52%	1.55%	.74%

TABLE XVII.   DETAILED ERROR LIST – SENSOR ERRORS AT 35.2% HORSEPOWER AND AT MAXIMUM POWER USING SENSORS AT LOW POWER AS TABULATED STANDARD SENSOR ACCURACY

Sensor	Error	Error in % of Point	Sensitivity			hp Prediction Error		
			N_1 Limit	T_7 Limit	Wf Limit	N_1 Limit	T_7 Limit	Wf Limit
Low Power:								
N_1	±2.5 rpm	±.012	-7.45	-4.02	-2.88	.0894	.0482	.0346
T_3	±6.3°R	±.71	-.14	-.10	-.19	.0994	.071	.1349
W_f	±2 pph	±.46	-.59	+.01	-1.46	.2714	.0046	.6716
SHP	±30 hp	±6.25	1.00	1.00	1.00	6.25	6.25	6.25
T_7	±6.3°R	±.43	-.20	-4.4	-.03	.0860	1.872	.0129
P_7	±.36 psi	±1.36	-.39	-.71	-.52	.5304	.9656	.7072
N_2	±2.5 rpm	±.013	1.03	1.03	1.03	.0134	.0134	.0134
T_1	±2.2°R	±.42	3.68	5.36	1.79	1.545	2.251	.7518
P_1	±.19 psi	±1.29	-.45	-.60	.84	.5405	.774	1.0836
P_3	±1.05 psi	±1.50	.21	.14	.08	.315	.21	.12
			RSS Error			6.50%	7.02%	6.46%
Maximum Power:								
N_1	±2.5 rpm	±.01	-3.71	0	0	.04	0	0
W_f	±4 pph	±.50	.56	0	1.47	.28	0	.735
T_7	±6.3°R	±.36	0	-4.31	0	0	1.552	0
T_1	±2.2°R	±.42	-.76	0	0	.319	0	0
P_1	±.19 psi	±1.29	0	0	-.37	0	0	.4773
N_1 SET	±21 rpm	±.08	3.71	0	0	.2968	0	0
T_7 SET	0	0	0	4.31	0	0	0	0
W_f SET	±2.55 pph	±.32	0	0	-1.47	0	0	.4704
			RSS Error			.52%	1.55%	.99%

51

TABLE XVIII.   DETAILED ERROR LIST - SENSOR ERRORS AT 19.7% HORSEPOWER USING SENSORS AT LOW POWER AS TABULATED BEST AVAILABLE SENSORS

Sensor	Error	Error in % of Point	Sensitivity			hp Prediction Error		
			N_1 Limit	T_7 Limit	W_f Limit	N_1 Limit	T_7 Limit	W_f Limit
Low Power:								
N_1	±2.5 rpm	±.012	10.08	7.32	5.83	.1210	.0878	.0700
T_3	±6.3°R	±.74	.24	.05	.10	.1776	.0370	.0740
W_f	±2 pph	±.56	.60	.03	1.46	.336	.0168	.817
SHP	-10 hp	±3.62	1.00	1.00	1.00	3.62	3.62	3.62
T_7	±6.3°R	±.46	.30	4.52	.07	.138	2.079	.032
P_7	±.05 psi	±.21	.59	1.23	.85	.1239	.2583	.1785
N_2	±2.5 rpm	±.013	2.10	2.10	2.10	.0273	.0273	.0273
T_1	±2.2°R	±.42	4.97	6.77	3.02	2.087	2.843	1.268
P_1	±.02 psi	±.135	.38	.06	1.12	.0513	.0081	.1512
P_3	±.10 psi	±.17	.21	.09	.06	.02295	.0122	.0081
RSS Error						4.20	5.06	3.93

52

TABLE XIX. DETAILED ERROR LIST - SENSOR ERRORS AT 35.2% POWER AND AT MAXIMUM POWER USING SENSORS AT LOW POWER AS TABULATED BEST AVAILABLE SENSORS

Sensor	Error	Error in % of Point	Sensitivity N1 Limit	Sensitivity T7 Limit	Sensitivity Wf Limit	hp Prediction Error N1 Limit	hp Prediction Error T7 Limit	hp Prediction Error Wf Limit
Low Power:								
N1	±2.5 rpm	±.012	-7.08	-3.14	-2.44	.0849	.0377	.0293
T3	±6.3°R	±.71	-.12	-.01	-.06	.0852	.0071	.0426
Wf	±2 pph	±.46	-.60	+.54	-1.49	.276	.2484	.685
SHP	±10 hp	±2.08	.86	.23	.86	1.79	.48	1.79
T7	±6.3°R	±.50	-.06	-4.52	.17	.03	2.26	.09
N2	±2.5 rpm	±.013	.88	.73	.84	.0114	.0095	.0109
T1	±2.2°R	±.42	3.52	5.15	1.46	1.478	2.16	.613
P1	±.02 psi	±.135	-.68	-.91	+.51	.0918	.1229	.0689
P3	±.10 psi	±.143	.22	.10	.08	.0315	.0143	.0114
				RSS Error		2.34	3.17	2.02
Maximum Power:								
N1	±2.5 rpm	±.01	-3.71	0	0	.04	0	0
Wf	±4 pph	±.50	.56	0	1.47	.28	0	.735
T7	±6.3°R	±.36	0	-4.31	0	0	1.552	0
T1	±2.2°R	±.42	-.76	0	0	.319	0	0
P1	±.02 psi	±.143	0	0	-.37	0	0	.0529
N1 SET	±21 rpm	±.08	3.71	0	0	.2968	0	0
T7 SET	0	0	4.31	0	0	0	0	0
Wf SET	±.27 pph	±.034	0	0	-1.47	0	0	.50
				RSS Error		.52	1.55	.74

53

TABLE XX. DETAILED ERROR LIST - SENSOR ERRORS AT 35.2% HORSEPOWER AND AT MAXIMUM HORSEPOWER USING SENSORS AT LOW POWER AS TABULATED STANDARD SENSOR ACCURACY

Sensor	Error	Error in % of Point	Sensitivity N₁ Limit	Sensitivity T₇ Limit	Sensitivity Wf Limit	hp Prediction Error N₁ Limit	hp Prediction Error T₇ Limit	hp Prediction Error Wf Limit
Low Power:								
N_1	±2.5 rpm	±.012	-7.08	-3.14	-2.24	.0849	.0377	.0293
T_3	±6.3°R	±.71	-.12	-.01	-.06	.0852	.0071	.0426
W_f	±2 pph	±.46	-.60	.54	-1.49	.276	.2484	.6854
SHP	±30 hp	±6.25	.86	.23	.86	5.375	1.438	5.375
T_7	±6.3°R	±.50	-.06	-4.52	.17	.03	2.26	.09
N_2	±2.5 rpm	±.013	.88	.73	.84	.0114	.0095	.0709
T_1	±2.2°R	±.42	3.52	5.15	1.46	1.478	2.163	.613
P_1	±.19 psi	±1.29	-.68	-.9?	+.51	.877	1.174	.658
P_3	±1.05 psi	±1.50	.22	.10	.08	.33	.15	.12
				RSS Error		5.66	3.65	5.49
Maximum Power:								
N_1	±2.5 rpm	±.01	-3.71	0	0	.04	0	0
W_f	±4 rpm	±.50	.56	0	1.47	.28	0	.735
T_7	±6.3°R	±.36	0	-4.31	0	0	1.552	0
T_1	±2.2°R	±.42	-.76	0	0	.319	0	0
P_1	±.19 psi	±1.29	0	0	-.37	0	0	.477
N_1 SET	±21 rpm	±.08	3.71	0	0	.2968	0	0
T_7 SET	0	0	4.31	0	0	0	0	0
W_f SET	±2.55	±.32	0	0	-1.47	0	0	.4704
				RSS Error		.52	1.55	.99
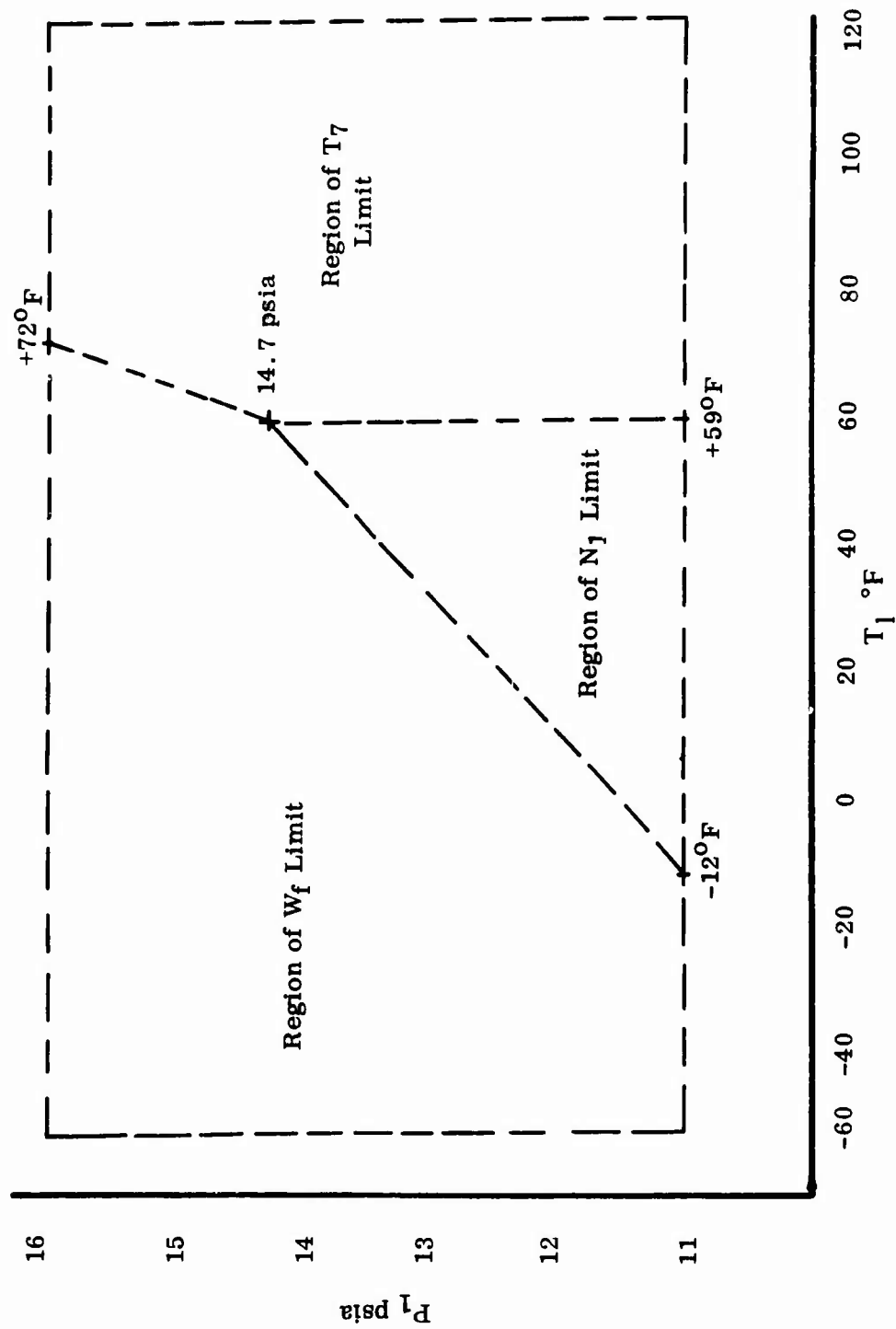
Figure 18.   Ambient Conditions Where Each Control Limit Determines Maximum Power of Base Engine.

Control Limit	Corrected Speed at Which "C" Is Computed (rpm)	Variable Used in the Linear Interpolation	Resulting Max. Error in "C"
N_1	24,700 and 26,600	$\sqrt{T_1}$ or $\sqrt{\theta_1}$	Less than ±.01
T_7	22,900 and 24,700	T_1 or θ_1	Less than ±.02
W_f	24,340 and 26,900	$P_1\sqrt{T_1}$ or $\delta_1\sqrt{\theta_1}$	Less than ±.01

A particularly large prediction error can result from uncertainty in compressor bleed air (W_{BL}). Variations in bleed air at maximum power cause variations in actual maximum power, causing a prediction error. Tables XIII and XIV contain a detailed list of errors caused by W_{BL} and compressor shaft power extraction (SPE).

Sensor characteristics are listed in Table XV. The sensor range and sensor type assumed in this study are identified in addition to the sensor error. Tables XVI through XX contain detailed lists of power prediction errors resulting from sensor errors.

Review of the error summary sheets (Tables V, VI, and VII) indicates that the total RSS error in power prediction is in excess of the ±1% goal. However, several improvements in power prediction accuracy are feasible as noted below and summarized in Table XXI:

1. The error caused by linearization of nonlinear differential equations can be eliminated by a more sophisticated analytical effort to derive "B" and "C" coefficients to be stored in the power prediction computer.

2. The change in actual power can be reduced due to uncertainty in compressor bleed air (W_{BL}) or compressor shaft power extraction (SPE) by providing more nearly constant demands on both W_{BL} and SPE. Assume that all uncertainties in W_{BL} and SPE are eliminated.

3. The W_{BL} and SPE are either controlled or measured in such a manner at the low-power prediction condition that there is no uncertainty in W_{BL} or SPE.

Table XXI is an error summary sheet for these improved conditions. Note that sensor errors are now the dominant error. A review of the sensor detailed error list (Table XVI) indicates that the dominant errors are caused by T_1, T_7, and

Error Source	N₁ Limit % Power	T₇ Limit % Power	W_f Limit % Power
Nonstandard day	.10	.23	.21
Use of base engine "C" for degraded engine	.03	.50	.02
High-power degradation being different from low-power degradation	.22	.68	.22
Change in actual power due to uncertainty in W_{BL} and SPE at high power	0	0	0
Uncertainty in W_{BL} and SPE at low power	0	0	0
Sensor errors at low power	2.61	3.60	2.33
Control limit and sensor errors at high power	.52	1.55	.74
TOTAL RSS ERROR	2.67	4.02	2.46
Errors in T_1, T_7 and SHP sensors at low and high power	2.63	3.92	2.23
All prediction errors excluding errors in T_1, T_7 and SHP sensors	.49	.89	1.02
TOTAL RSS ERROR	2.67	4.02	2.46

Table title:

TABLE XXI. ERROR SUMMARY SHEET – PREDICTION AT 35.2% HORSE-POWER AT N_2 = 100% WITH FEASIBLE IMPROVEMENTS IN POWER PREDICTION USING CURRENT "BEST AVAILABLE" SENSORS SET I LOW-POWER SENSORS

SHP sensor errors. The prediction errors caused by these three sensors are listed separately, and all other prediction errors are lumped together (also tabulated in Table XXI). The prediction error caused by er̃ine degradation, ambient conditions, control errors, and sensor errors is about ±1% or less when the T_1, T_7 and SHP errors are excluded. The power prediction errors caused by T_1, T_7 and SHP sensor errors are much more significant than the combination of all other errors.

In summary, the dominant errors in power prediction are caused by the errors in currently available T_1, T_7, and SHP sensors and uncertainty in W_{BL} and SPE. If it is possible to eliminate the uncertainty in W_{BL} and SPE by some operational procedure, then the dominant errors in power prediction are caused by sensing T_1, T_7, and SPE.

A sensitivity and error analysis was made for Set III sensors to try to reduce the prediction error due to sensor errors at low power. This set is identical to the original set except that the shaft horsepower measurement is replaced by T_9. The sensitivity table for this set of sensors is shown in Table XXII. Table XXIII is a detailed list of the errors due to low-power sensor inaccuracies and uncertainty in W_{BL} and SPE at low power. Table XXIV summarizes the error for the power prediction system using this set of low-power sensors. Instead of reducing the power prediction error, this set of sensors results in a significant increase in the error due to low-power sensor inaccuracy. For this reason, this set of sensors is abandoned as a possible candidate for the final power prediction model.

Set IV, which uses one less sensor than any set previously considered, is identical to Set I but, instead of P_7, assumes the relationship $\partial A_N/A_N = -\partial \eta_{pt}/\eta_{pt}$. This set is also identical to Set II, with T_7 replacing the T_9 measurement at low power. Table XXV is the sensitivity table for this set of sensors. Comparing Table XXV with Table III, it is seen that the sensitivities are not significantly different.

EFFECT OF POWER CONDITION ON MPA PREDICTION

Tables XXVI and XXVII give a detailed listing of the errors due to Set IV sensor inaccuracies at 35.2% and 19.7% power. Generally speaking, as power predictions are made at low power levels, the error in predicted power increases. The increase in error is due primarily to an increase in the sensitivity to sensor errors and also to an increase in the percentage of point sensor errors. Table XXVIII is a summary of all the errors for Set IV sensors when predicting at 35.2% power. Comparing Table XXVIII with Table VII, it is seen that the total error for both sets of sensors is essentially the same.

TABLE XXII. SENSITIVITY STUDY - EFFECT OF SENSOR ERROR AT LOW POWER AND AT HIGH POWER ON POWER REMAINING ACCURACY SET II SENSORS

% Max. Power Limit % of Point	Mode	$N_1 = 21,700$ hp = 35.2%	$N_1 = 21,200$ hp = 27%	$N_1 = 20,700$ hp = 19.7%	$N_1 = 20,200$ hp = 13.6%	$N_1 = 19,700$ hp = 8.6%	$N_1 = 24,700$ hp = 100%
$\frac{\partial hp}{\partial N_1}$	N_1	-6.85	-7.28	-7.55	-7.43	-5.54	-3.71
	T_7	-3.39	-4.15	-4.71	-4.98	-3.40	0
	W_f	-2.24	-2.81	-3.18	-3.31	-1.56	0
$\frac{\partial hp}{\partial T_3}$	N_1	- .05	- .10	- .15	- .20	- .25	0
	T_7	- .01	+ .02	+ .04	+ .09	+ .14	0
	W_f	+ .01	0	- .01	- .01	0	0
$\frac{\partial hp}{\partial W_f}$	N_1	+ .42	+ .41	+ .41	+ .40	+ .40	.56
	T_7	+1.03	+1.03	+1.04	1.04	1.05	0
	W_f	- .46	- .46	- .46	- .46	- .46	1.47
$\frac{\partial hp}{\partial T_7}$	N_1	+7.70	+8.90	+10.02	+11.73	+13.27	0
	T_7	+3.15	+4.30	+5.36	+6.98	+8.43	-4.31
	W_f	+7.88	+9.12	+10.27	+12.00	+13.55	0
$\frac{\partial hp}{\partial T_9}$	N_1	-8.59	-9.94	-11.29	-13.04	-14.75	0
	T_7	-8.59	-9.94	-11.29	-13.05	-14.76	0
	W_f	-8.59	-9.94	-11.29	-13.05	-14.76	0
$\frac{\partial hp}{\partial N_2}$	N_1	+ .93	+1.25	+1.56	+1.93	+2.11	0
	T_7	+ .93	+1.25	+1.56	+1.93	+2.11	0
	W_f	+ .93	+1.25	+1.56	+1.93	+2.11	0

TABLE XXII - Continued

Max. Power Limit	Mode	N₁ = 21,700 hp = 35.2%	N₁ = 21,200 hp = 27%	N₁ = 20,700 hp = 19.7%	N₁ = 20,200 hp = 13.6%	N₁ = 19,700 hp = 8.6%	N₁ = 24,700 hp = 100%
$\frac{\partial hp}{\partial T_1}$	N_1	+7.59	+8.46	+9.19	+9.97	+9.73	- .76
	T_7	+7.11	+8.02	+8.79	+9.63	+9.45	0
	W_f	+5.55	+6.38	+7.07	+7.87	+7.70	0
$\frac{\partial hp}{\partial P_1}$	N_1	-8.29	-9.17	-10.13	-11.67	-13.19	0
	T_7	-4.49	-5.25	-5.97	-7.29	-8.52	0
	W_f	-7.28	-8.14	-9.01	-10.45	-11.85	- .37
$\frac{\partial hp}{\partial P_3}$	N_1	- .99	- .52	+ .03	+ .07	+ .10	0
	T_7	-1.06	- .57	- .06	- .11	- .10	0
	W_f	-1.12	- .61	- .12	- .11	- .12	0
$\frac{\partial hp}{\partial N_1 \text{ SET}}$	N_1	0	0	0	0	0	3.71
$\frac{\partial hp}{\partial T_7 \text{ SET}}$	T_7	0	0	0	0	0	4.31
$\frac{\partial hp}{\partial WBL}$	N_1	+ .32	+ .30	+ .29	.28	.27	- .78
	T_7	+2.95	+2.97	+2.98	3.02	+3.05	-3.29
	W_f	+1.02	+1.01	+1.00	1.00	1.00	-1.43
$\left[\dfrac{\partial hp}{\partial \left(\frac{SPE}{W_a}\right)}\right]$	N_1	- .64	- .71	- .76	- .83	- .88	.22
	T_7	+1.99	+2.15	+2.31	+2.52	+2.70	-1.57
	W_f	+ .69	+ .74	+ .78	+ .83	+ .87	- .68

60

TABLE XXII - Continued

% Max. Power Limit % of Point	Mode	$N_1 = 21,700$ hp = 35.2%	$N_1 = 21,200$ hp = 27%	$N_1 = 20,700$ hp = 19.7%	$N_1 = 20,200$ hp = 13.6%	$N_1 = 19,700$ hp = 8.6%	$N_1 = 24,700$ hp = 100%
$\dfrac{\partial hp}{\partial P_7}$	N_1	+1.09	+ .22	- .59	- .67	- .75	0
	T_7	+ .77	- .27	-1.23	-1.62	-1.98	0
	W_f	+ .96	+ .02	- .85	-1.06	-1.25	0

NOTES: N_2 = 100% standard-day conditions.

61

TABLE XXIII. DETAILED ERROR LIST – SENSOR ERRORS AT 35.2% HORSEPOWER USING SENSORS AT LOW POWER AS TABULATED BEST AVAILABLE SENSORS

Sensor	Error	Error in % of Point	Sensitivity			hp Prediction Error		
			N₁ Limit	T₇ Limit	W_f Limit	N₁ Limit	T₇ Limit	W_f Limit
Low Power:								
N₁	±2.5rpm	±.012	-6.85	-3.39	-2.24	.0822	.04068	.02688
T₃	±6.3°R	±.71	-.05	-.01	+.01	.0355	.0071	.0071
W_f	±2.0pph	±.46	+.42	+1.03	-.46	.1932	.4738	.2116
T₇	±6.3°R	±.43	+7.70	+3.15	+7.88	3.311	1.355	3.388
T₉	±6.3°R	±.50	-8.59	-8.59	-8.59	4.295	4.295	4.295
P₇	±.05psi	±.19	+1.09	+.77	+.96	.2071	.1463	.1824
N₂	±2.5rpm	±.013	+.93	+.93	+.93	.01209	.01209	.01209
T₁	±2.2°R	±.42	+7.59	+7.11	+5.55	3.188	2.986	2.331
P₁	±.02	±.135	-8.29	-4.49	-7.28	1.119	.6062	.9828
P₃	±.10psi	±.143	-.99	-1.06	-1.12	.1416	.1516	.1602
					RSS Error	6.40	5.42	6.24

Uncertainty in compressor discharge air bleed (WBL) and shaft power extraction at low power:

Variable	Uncertainty	Sensitivity			hp Variation		
		N₁ Limit	T₇ Limit	W_f Limit	N₁ Limit	T₇ Limit	W_f Limit
W_BL	±.5%	+.32	+2.95	+1.02	.16	1.475	.51
SPE	±.3hp/pps	-.64	+1.99	+1.69	.192	.597	.507
				RSS Error	.25	1.59	.72

TABLE XXV.	ERROR SUMMARY SHEET - PREDICTION AT 35.2% POWER AT N_2 = 100% USING INTERPOLATED "C" IN PREDICTION ALGORITHM SET III SENSORS

Error Source	N_1 Limit % Power	T_7 Limit % Power	W_f Limit % Power
Linearization of nonlinear differential equations	.50	1.23	.35
Nonstandard day	.10	.23	.21
Use of base engine "C" for degraded engine	.03	.50	.03
High-power degradation being different from low-power degradation	.22	.68	.22
Change in actual power due to uncertainty in W_{BL} and SPE at high power	1.17	4.96	2.15
Uncertainty in W_{BL} and SPE at low power	.25	1.59	.72
Sensor errors at low power*	6.40	5.42	6.24
Control limit and sensor errors at high power*	.52	1.55	.74
TOTAL ERROR:	6.56	7.82	6.70

*Based on best available sensors.

TABLE XXV. SENSITIVITY STUDY – EFFECT OF SENSOR ERRORS AT LOW POWER AND AT HIGH POWER ON POWER REMAINING ACCURACY SET IV SENSORS

	Mode	$N_1 = 22,950$ hp = 60.7%	$N_1 = 21,700$ hp = 35.2%	$N_1 = 21,200$ hp = 27%	$N_1 = 20,700$ hp = 19.7%	$N_1 = 20,200$ hp = 13.6%	$N_1 = 19,700$ hp = 8.6%	$N_1 = 24,700$ hp = 100%
Max. Power Limit % of Point								
$\dfrac{\partial hp}{\partial N_1}$	N_1	-5.31	-7.09	-7.89	-9.06	-10.92	-12.75	-3.71
	T7	-1.57	-3.47	-4.41	-5.60	-7.19	-8.54	0
	Wf	-.96	-2.43	-3.29	-4.49	-6.38	-8.14	0
$\dfrac{\partial hp}{\partial T_3}$	N_1	-.05	-.12	-.16	-.20	-.24	-.28	0
	T7	-.12	-.06	-.01	+.04	+.13	+.21	0
	Wf	-.05	-.06	-.05	-.04	-.02	0	0
$\dfrac{\partial hp}{\partial W_f}$	N_1	-.58	-.60	-.60	-.60	-.61	-.62	.56
	T7	-.005	0	+.006	+.01	+.01	+.02	0
	Wf	-1.47	-1.47	-1.47	-1.47	-1.46	-1.46	1.47
$\dfrac{\partial hp}{\partial SHP}$	N_1	+.95	+.87	+.87	+.83	+.83	+.82	0
	T7	+.89	+.77	+.73	+.65	+.59	+.53	0
	Wf	+.91	+.83	+.81	+.76	+.73	+.71	0
$\dfrac{\partial hp}{\partial T_7}$	N_1	-.04	-.06	-.07	-.09	-.12	-.14	0
	T7	-4.19	-4.17	-4.15	-4.13	-4.09	-4.05	-4.31
	Wf	+.08	+.16	+.19	+.22	+.24	+.26	0
$\dfrac{\partial hp}{\partial N_2}$	N_1	+.36	+.88	+1.22	+1.75	+2.72	+4.52	0
	T7	+.34	+.78	+1.02	+1.36	+1.89	+2.78	0
	Wf	+.55	+.84	+1.14	+1.59	+2.38	+3.80	0

TABLE XXV - Continued

% of Point	Mode	N₁ = 22,950 hp = 60.7%	N₁ = 21,700 hp = 35.2%	N₁ = 21,200 hp = 27%	N₁ = 20,700 hp = 19.7%	N₁ = 20,200 hp = 13.6%	N₁ = 19,700 hp = 8.6%	N₁ = 24,700 hp = 100%
$\frac{\partial hp}{\partial T_1}$	N_1	+2.65	+3.52	+3.94	+4.53	+5.60	+6.29	-.76
	T_7	+4.48	+5.21	+5.54	+6.01	+6.60	+6.83	0
	W_f	+.96	+1.46	+1.78	+2.28	+3.12	+3.62	0
$\frac{\partial hp}{\partial P_1}$	N_1	-.82	-.68	-.70	-.76	-.76	-.88	0
	T_7	-1.26	-1.02	-.98	-.88	-.80	-.54	0
	W_f	+.37	+.52	+.53	+.55	+.60	+.66	-.37
$\frac{\partial hp}{\partial P_3}$	N_1	+.18	+.22	+.20	+.22	+.24	+.24	0
	T_7	+.16	+.15	+.12	+.10	+.07	+.06	0
	W_f	+.10	+.08	+.07	+.07	+.06	+.03	0
$\frac{\partial hp}{\partial N_1 \text{ SET}}$	N_1	0	0	0	0	0	0	3.71
$\frac{\partial hp}{\partial T_7 \text{ SET}}$	T_7	0	0	0	0	0	0	4.31
$\frac{\partial hp}{\partial \text{WBL}}$	N_1	+.75	+.72	+.70	+.69	+.67	+.65	-.78
	T_7	+3.34	+3.38	+3.40	+3.42	+3.45	+3.49	-3.29
	W_f	+1.43	+1.43	+1.42	+1.42	+1.41	+1.41	-1.43
$\left[\frac{\partial hp}{\partial \left(\frac{\text{SPE}}{W_a}\right)}\right]^*$	N_1	-.31	-.38	-.42	-.46	-.51	-.56	.22
	T_7	+1.91	+2.27	+2.46	+2.64	+2.87	+3.08	-1.57
	W_f	+.82	+.96	+1.03	+1.10	+1.17	+1.24	-.68

NOTES: * Units are % max. power/(hp/PPS of airflow).
  N_2 = 100% standard-day conditions.

TABLE XXVI. DETAILED ERROR LIST – SENSOR ERRORS AT 35.2% POWER USING SENSORS AT LOW POWER AS TABULATED BEST AVAILABLE SENSORS

Sensor	Error	Error in % of Point	Sensitivity			hp Prediction Error		
			N₁ Limit	T₇ Limit	Wf Limit	N₁ Limit	T₇ Limit	Wf Limit
Low Power:								
N_1	± 2.5 rpm	$\pm .012$	-7.09	-3.47	-2.43	.0851	.0416	.0292
T_3	$\pm 6.3°R$	$\pm .71$	- .12	- .06	- .06	.0852	.0426	.0426
W_f	± 2.0 pph	$\pm .46$	- .60	0	-1.47	.2760	0	.6762
SHP	± 10 hp	± 2.08	+ .87	+ .77	+ .83	1.810	1.602	1.726
T_7	$\pm 6.3°R$	$\pm .43$	- .06	-4.17	+ .16	.0258	1.793	.0688
N_2	± 2.5 rpm	$\pm .013$	+ .88	+ .78	+ .84	.0114	.0101	.0109
T_1	$\pm 2.2°R$	$\pm .42$	+3.52	+5.21	+1.46	1.478	2.188	.6132
P_1	$\pm .02$ psi	$\pm .135$	- .68	-1.02	+ .52	.0918	.1377	.0702
P_3	$\pm .10$ psi	$\pm .143$	+ .22	+ .15	-1.08	.0315	.0215	.0114
				RSS Error		2.34	3.25	1.96

Uncertainty in compressor discharge air bleed (W_{BL}) and shaft power extraction at low power:

Variable	Uncertainty	Sensitivity			hp Variation		
		N₁ Limit	T₇ Limit	Wf Limit	N₁ Limit	T₇ Limit	Wf Limit
W_{BL}	$\pm 5\%$	+ .72	+3.38	+1.43	.36	1.69	.715
SPE	$\pm .3$ hp/pps	- .38	+2.27	+ .96	.114	.681	.288
			RSS Error		.38	1.82	.77

66

TABLE XXVII. DETAILED ERROR LIST - SENSOR ERRORS AT 19.7% HORSEPOWER USING LOW-POWER SENSORS AS TABULATED BEST AVAILABLE SENSORS

Sensor	Error	Error in % of Point	Sensitivity N_1 Limit	T_7 Limit	W_f Limit	hp Prediction Error N_1 Limit	T_7 Limit	W_f Limit
N_1	$\pm$2.5rpm	$\pm$.012	-9.06	-5.60	-4.49	.1087	.0072	.0549
T_3	$\pm$6.3°R	$\pm$.74	-.20	+.04	-.04	.1480	.0296	.0296
W_f	$\pm$2.0pph	$\pm$.56	-.60	+.01	-1.47	.336	.0056	.8232
SHP	$\pm$10hp	$\pm$3.62	+.83	+.65	+.76	3.005	2.353	2.751
T_7	$\pm$6.3°R	$\pm$.46	-.09	-4.13	+.22	.0414	1.900	.1012
N_2	$\pm$2.5rpm	$\pm$.013	+1.75	+1.36	+1.59	.0228	.0177	.0207
T_1	$\pm$2.2°R	$\pm$.42	+4.53	+6.0?	+2.28	1.903	2.524	.9576
P_1	$\pm$.02psi	$\pm$.135	-.76	-.88	+.55	.1026	.1188	.0743
P_3	$\pm$.10psi	$\pm$.17	+.22	+.10	+.07	.0374	.017	.0119
				Total RSS Error		3.58	3.94	3.03

Uncertainty in compressor discharge air bleed (W_{BL}) and shaft power extraction at low power:

Variable	Uncertainty	Sensitivity N_1 Limit	T_7 Limit	W_f Limit	hp Variation N_1 Limit	T_7 Limit	W_f Limit
W_{BL}	$\pm$.5%	+.69	+3.42	+1.42	.345	1.71	.71
SPE	$\pm$.3 hp/pps	-.46	+2.64	+1.10	.138	.792	.33
			RSS Error		.37	1.88	.77

TABLE XXVIII. ERROR SUMMARY SHEET – PREDICTION AT 35.2% POWER AT $N_2 = 10$ USING INTERPOLATED "C" IN PREDICTION ALGORITHM SET IV SENSORS

Error Source	N_1 Limit % Power	T_7 Limit % Power	W_f Limit % Power
Linearization of nonlinear differential equations	.50	1.23	.35
$\partial A_N/A_N$ not equal to $-\partial \eta_{pt}/\eta_{pt}$	.30	.54	.40
Nonstandard day	.10	.23	.21
Use of base engine "C" for degraded engine	.03	.50	.03
High-power degradation being different from low-power degradation	.22	.68	.22
Change in actual power due to uncertainty in W_{BL} and SPE at high power	1.17	4.96	2.15
Uncertainty in W_{BL} and SPE at low power	.38	1.82	.77
Sensor errors at low power	2.34	3.25	1.96
Control limit and sensor errors at high power	.52	1.55	.74
TOTAL ERROR	2.77	6.59	3.16

Since accuracy improves when the predictions are made at higher power levels, errors due to sensor inaccuracies at approximately 60% power were calculated for the system using Set II and Set IV low-power sensors; i.e., T_9 or T_7 without P_7 and the approximation $\partial A_N/A_N = -\partial \eta_{pt}/\eta_{pt}$. For single-engine applications, prediction at 60% power would not be feasible since it is desired to make the prediction while still on the ground (30% or less of maximum rotor power). In twin-engine installations, however, one engine could be operating at 60% power while the other engine is essentially at 0% power. Table III also includes sensitivities at 57.5% power. Tables XXIX and XXX list the errors due to sensor inaccuracies at approximately 60% power for Set II and Set IV sensors, respectively. There is no significant difference in the error between the two sets of sensors. Comparing Table XIX to Table XXIX and Table XXVI to Table XXX, there is a moderate improvement in the power prediction accuracy due to low-power sensor errors.

ALTERNATE MPA SYSTEM STUDIES

The power prediction model described below is presented as a possible alternative approach to predicting maximum power available. This alternate model is significantly less complex than the primary model since it does not involve the rather elaborate gas-path analysis used in the primary model. The prediction concept is based on the assumption that the engine performance remains unchanged after the power prediction calibration. A major disadvantage of this simpler approach is that changes in maximum power caused by degradation in the engine (since power prediction calibration) directly result in a power prediction error.

The alternate power prediction scheme can be divided into two major operations: a simple one-point calibration, and the actual power prediction operation. The calibration operation is done once and thereafter is repeated only when it is ascertained that the engine health has deteriorated from the time the previous calibration was made.

A detailed outline of the alternate power prediction model is given below. The first step establishes a low-power reference value for (P_3/δ_1), (T_7/θ_1), and $(W_f/\delta_1 \theta_1 \cdot^{743})$ at a corrected speed of 21,500 rpm; the 21,500-rpm point corresponds approximately to 30% power. The first time that the first step is executed, the values for the above three corrected parameters are stored for future power prediction.

The second step establishes the optimum horsepower corrected to standard-day sea-level conditions at each of the control limits. These values are also stored for future power prediction.

TABLE XXIX.   DETAILED ERROR LIST - SENSOR ERRORS AT 57.5% HORSEPOWER USING LOW-POWER SENSORS AS TABULATED BEST AVAILABLE SENSORS

Sensor	Nom. Value	Error in % of Point	Sensitivity			hp Prediction Error		
			N_1 Limit	T_7 Limit	W_f Limit	N_1 Limit	T_7 Limit	W_f Limit
N_1	22,800	±.011	-5.55	-1.74	-1.14	.06105	.01914	.01254
T_3	936.5	±.67	-.05	-.05	-.06	.0335	.0335	.0402
W_f	554.4	±.36	-.59	+.68	-1.48	.2124	.2448	.5328
SHP	804.8	±1.24	+.92	+.181	+.92	1.1408	.22444	1.1408
T_9	1,342.5	±.47	-.04	-4.56	+.09	.0188	2.14	.0423
N_2	19,518	±.013	+.40	+.38	+.39	.0052	.00494	.00507
T_1	5i8.7	±.42	+2.75	+4.64	+1.02	1.155	1.949	.4284
P_1	14.7	±.135	-.81	-1.05	+.38	.10935	.14175	.0513
P_3	81.76	±.122	+.33	+.16	+.23	.04026	.01952	.02806
				RSS Error		1.64%	2.92%	1.33%

TABLE XXX. DETAILED ERROR LIST - SENSOR ERRORS AT 60.7% HORSEPOWER USING LOW-POWER SENSORS AS TABULATED BEST AVAILABLE SENSORS

Sensor	Error	Error in % of Point	Sensitivity N_1 Limit	Sensitivity T_7 Limit	Sensitivity W_f Limit	hp Prediction Error N_1 Limit	hp Prediction Error T_7 Limit	hp Prediction Error W_f Limit
N_1	$\pm$2.5rpm	$\pm$.011	-5.31	-1.57	-.96	.0584	.0173	.0106
T_3	$\pm$6.3°R	$\pm$.67	-.05	-.12	-.05	.0335	.0804	.0335
W_f	$\pm$2.0pph	$\pm$.35	-.58	-.005	-1.47	.203	.0018	.5145
SHP	$\pm$10hp	$\pm$1.18	+.93	+.89	+.91	1.0974	1.0502	1.0738
T_7	$\pm$6.3°R	$\pm$.40	-.04	-4.19	+.08	.0160	1.676	.0320
N_2	$\pm$2.5rpm	$\pm$.013	+.36	+.34	+.35	.0047	.0044	.0046
T_1	$\pm$2.2°R	$\pm$.42	+2.65	+4.48	+.96	1.113	1.882	.4032
P_1	$\pm$.02psi	$\pm$.136	-.82	-1.26	+.37	.1115	.1714	.0503
P_3	$\pm$.10psi	$\pm$.12	+.18	+.16	+.10	.0216	.0192	.0120
					RSS Error	1.58%	2.74%	1.26%

Uncertainty in compressor discharge air bleed (W_{BL}) and shaft power extraction at low power:

Variable	Uncertainty	Sensitivity N_1 Limit	Sensitivity T_7 Limit	Sensitivity W_f Limit	hp Variation N_1 Limit	hp Variation T_7 Limit	hp Variation W_f Limit
W_{BL}	$\pm$5%	+.75	+3.34	+1.43	.375	1.67	.715
SPE	$\pm$.3 hp/pps	-.31	+1.91	+.82	.093	.573	.246
			RSS Error		.386	1.81	.77

The third step in the outline describes the actual power prediction operation. Each time a power prediction is to be made, the values of (P_3/δ_1), (T_7/θ_1), and $(W_f/\delta_1\theta_1 \cdot^{743})$ are obtained at a corrected speed of 21, 500 rpm as described under the first step of the outline. The present computed values are then compared to the original stored values. If the corresponding values agree to within specified tolerances, then the predicted power obtained under the third step is credible; otherwise it is not. The above tolerances have not been established but would be strongly influenced by sensor inaccuracy and also by anticipated engine degradation.

The constants required in the several equations given for the alternate system are obtained from the steady-state engine characteristics for the base engine. The values of the constants are given in Table XXXI.

I. Establish Low Power Reference Values for (P_3/δ_1), (T_7/θ_1), and $(W_f/\delta_1\theta_1 \cdot^{743})$ at $N_1/\sqrt{\theta_1} = 21, 500$ ($\approx 30\%$ power).

   A. Measure T_1

   B. Compute $\theta_1 = T_1/518.7$

   C. Compute N_1 set $= 21, 500\sqrt{\theta_1}$

   D. Pilot sets actual N_1 speed to a value equal to N_1 SET± 200 rpm.

   E. Allow engine to achieve steady state and measure N_1, P_3, T_7, and W_f.

   F. Compute:

$$\left.\begin{array}{rcl} \delta_1 &=& P_1/14.7 \\[1.2em] N_{1C} &=& N_1/\sqrt{\theta_1} \\[1.2em] P_{3C} &=& P_3/\delta_1 \\[1.2em] T_{7C} &=& T_7/\theta_1 \\[1.2em] W_{fC} &=& (W_f/\delta_1\theta_1 \cdot^{743}) \end{array}\right\} \quad \text{Corrected Quantities}$$

Note: Step I-F is repeated periodically to correct for engine deterioration.

72

C. Extrapolate corrected measurements to $N_1/\sqrt{\theta_1} = 21,500$ thus:

$$(P_3/\delta_1)\bigg|_{(N_1\sqrt{\theta_1})\ =\ 21,500} = P_{3C}\,(21,500/N_{1C})^{CPNPL}$$

$$(T_7/\theta_1)\bigg|_{(N_1/\sqrt{\theta_1})\ =\ 21,500} = T_{7C}\,(21,500/N_{1C})^{CTNPL}$$

$$(W_f/\delta_1\theta_1{}^{.743})\bigg|_{(N_1/\sqrt{\theta_1})\ =\ 21,500} = W_{fC}\,(21,500/N_{1C})^{CWNLP}$$

H. When calibrating, the values obtained under (G) are stored for future power prediction.

II. Establish optimum horsepower corrected to standard-day sea-level conditions at each control limit.

A. At or near max. power, measure the following T_1, P_1, N_1, N_2, W_f, T_7, SHP, and P_1/P_{AM}.

B. Compute corrected quantities

$$\theta_1 = T_1/518.7$$

$$\delta_1 = P_1/14.7$$

$$N_{1C} = N_1/\sqrt{\theta_1}$$

$$N_{2C} = N_2/\sqrt{\theta_1}$$

$$SHP_C = SHP/\delta_1\sqrt{\theta_1}$$

$$W_{fC} = (W_f/\delta_1\theta_1{}^{.674})$$

C. Apply correction factor to SHP_C for nonoptimal N_2

$$(N_{2C})_{OPT} = f(N_{1C}) \quad \text{(curve lookup)}$$

$$CF = \left\{ \left[N_{2C} - (N_{2C})_{OPT} \right] / (N_{2C})_{OPT} \right\}^2$$

$$SHP_{CO} = SHP_C / (1 - CF)$$

where OPT is optimal.

D. Predict N_1 limit (actual rpm)

$$N_{1\,Lim} = 24,700 \left[(793/W_{fC}) \right]^{.09322} (N_{1C}/24,700)^{.3941}$$

E. Compute optimal horsepower at $N_{1\,Lim}$, T_{7Lim}, and W_{fLim}.

$$hp_{CNREF} = SHP_{CO} (N_{1\,Lim}/N_{1C})^{CHN} (P_1/P_{AM})^{-C1}$$

$$hp_{CTREF} = SHP_{CO} (T_{7Lim}/T_{7C})^{CHT} (P_1/P_{AM})^{-C2}$$

$$hp_{CWREF} = SHP_{CO} (W_{fLim}/W_{fC})^{CHW}$$

F. Store $N_{1\,Lim}$, hp_{CNREF}, hp_{CTREF}, and hp_{CWREF} for future power prediction.

Note: Step II is repeated periodically to correct for engine deterioration.

III. Predict Maximum Power Available (MPA).

At some future time after the calibration procedure outlined under steps I and II have been completed, the following procedure is used to predict maximum available horsepower:

A. Repeat I-A through I-G.

B. Compare present computed values of (P_3/δ_1), (T_7/θ_1), and $(N_F/\delta_1 \theta_1^{.743})$ at $N_1/\sqrt{\theta_1} = 21,500$ to the stored values. If the values agree within specified tolerances (to be established), then the following power prediction is credible; otherwise, it is not.

On N_1 limit:

$$SHPON = (hp_{CNREF})(\delta_1)(f_N)(P_1/P_{AM})^{C1}$$

On T_7 limit:

$$SHPOT = (hp_{CTREF})(\delta_1)(f_T)(P_1/P_{AM})^{C2}$$

On W_f limit:

$$SHPOW = (hp_{CWREF})(\delta_1^{C3})(f_W)$$

f_N, f_T, and f_W are defined by Figures 11, 12, and 13, respectively.

$$MPA = MIN (SHPON, SHPOT, SHPOW)$$

Error Analysis (Alternate Model)

Table XXXII summarizes the error for the alternate power prediction model.
Details regarding the error calculations can be found in Tables XXXIII and XXXIV.

In addition to having large errors in predicting maximum power, this model has
the severe disadvantage of not being able to compute changes in maximum power
due to engine degradation (since calibration). For these reasons, this model is
judged to be unacceptable for a power prediction system.

FINAL SYSTEM SELECTION

Based on accuracy considerations and the number of sensors required, the power
prediction model selected is the basic power prediction concept with sensor
Set IV. The final selected system is described as follows.

At a relatively low power condition not to exceed 30% of the nominal sea-level
standard-day value of maximum power turbine horsepower for single-engine
applications, the following steady-state engine and environmental parameters
are measured.

TABLE XXXI.	ALTERNATE POWER PREDICTION MODEL DEFINITION OF CONSTANTS	
	Symbol	Value*
	CPNPL	3.1423
	CTNPL	1.235
	CWNLP	4.5782
	CHN	5.5394
	C_1	1.139
	C_{HT}	3.8169
	C_2	1.1078
	C_{HW}	1.319
	C_3	-.8406

*Numerical values were obtained from the analytic.l base-line engine characteristics.

TABLE XXXII. SUMMARY OF ERRORS FOR THE ALTERNATE PREDICTION SYSTEM

Error Source	N_1 Limit % Power	T_7 Limit % Power	W_f Limit % Power	Detailed Error List Table No.	Notes
Control limit and sensor errors at high power	2.35	2.95	2.30	XXXII	
Not being at the limit when establishing reference horsepower values	-.462	-.600	-.294		1
Nonstandard day	-4.52	-6.50	-3.33		2
Sensor errors at low power	-.477	1.51	.21	XXXII	3
Degradation since last calibration	.29	.73	.20	XXXIII	
Uncertainty in shaft power and bleed air at high power	.20	.91	.40	XXXIII	
RSS Error	5.15	7.41	4.09		

NOTES

1. The error resulting from not being at the limit when establishing reference horsepower values was obtained by assuming that the high-power measurements can be made as much as 500 rpm N_1 below the N_1 limit.

2. Errors due to nonstandard-day conditions were computed for the base engine as follows:

   a. On N_1 limiting, the horsepower ref. corresponding to a -12°F ambient temperature was computed. This is the lowest temperature that can exist and still be on the N_1 limit.

   b. On T_7 limiting, the horsepower ref. corresponding to a 120°F day was computed.

   c. On W_f limiting, the horsepower ref. corresponding to a -60°F day and $P_1 = 11.3$ psia was computed.

3. At low power, the only sensors which affect power prediction are P_1 and T_7.

TABLE XXXIII. DETAILED ERROR LIST FOR THE ALTERNATE PREDICTION SYSTEM CONTROL LIMIT AND SENSOR ERRORS AT HIGH POWER AND LOW POWER

High-Power Sensor	Error in % of Point	Sensitivity			hp Prediction Error		
		N_1 Limit	T_7 Limit	W_f Limit	N_1 Limit	T_7 Limit	W_f Limit
T_1	$\pm.42$	1.527	3.317	.389	.641	1.393	.163
P_1	$\pm.143$	$-.484$	-1	.319	.069	.143	.046
N_1	$\pm.01$	-3.36	0	0	.0336	0	0
W_f	$\pm.50$	$-.516$	0	-1.319	.258	0	.66
T_7	$\pm.36$	0	-3.82	0	0	1.38	0
hp	±2.0	1.1	1.1	1.1	2.2	2.2	2.2
N_1 SET	$\pm.08$	5.539	0	0	.443	0	0
T_7 SET	±0	0	3.82	0	0	0	0
W_f SET	$\pm.034$	0	0	1.319	0	0	.045
			RSS Error		2.35%	2.95%	2.3%

Low-Power Sensor	Error in % of Point	Sensitivity			hp Prediction Error		
		N_1 Limit	T_7 Limit	W_f Limit	N_1 Limit	T_7 Limit	W_f Limit
P_1	$\pm.136$	1	1	$-.8406$	.136	.136	.114
T_1	$\pm.423$	-1.081	-3.55	$-.425$	.457	1.5	.18
			RSS Error		.477	1.51	.21

TABLE XXXIV. DETAILED ERROR LIST FOR THE ALTERNATE PREDICTION SYSTEM ERRORS DUE TO DEGRADATION SINCE LAST CALIBRATION AND ERRORS DUE TO UNCERTAINTY IN SPE AND W_{BL}

Variable	Assumed Degradation	hp N_1 Limit "C"	Error	hp T_7 Limit "C"	Error	hp W_f Limit "C"	Error
η_c	.15%	- .762	.1143	3.3798	.5070	.8269	.1240
η_t	1%	- .979	.0979	4.3485	.4349	1.1859	.1186
η_{pt}	1%	1.0044	.1004	1.0061	.1006	1.007	.1007
A_N	1%	-1.6937	.1694	2.4311	.2431	- .1105	.0111
W_a	1%	1.2929	.1293	- .0597	.0060	.0727	.0073
A_5	1%	.793	.0793	-1.5644	.1564	- .3507	.0351
RSS Error			.029%		.73%		.20%

Variable	Error*	"C" Exponent N_1 Limit	T_7 Limit	W_f Limit	Predicted Horsepower Error N_1 Limit	T_7 Limit	W_f Limit
SPE	$\pm$.25	.0024029	- .01554	.006748	.06	.39	.17
W_{BL}	$\pm$.25	.775	3.29	1.43	.19	.82	.36
RSS Error					.20%	.91%	.40%

*The errors given represent the assumed maximum differences between the values of SPE and W_{BL} at the time of calibration and the values at the time of prediction.

For shaft power extraction (SPE), units are hp of airflow.

For bleed air (W_{BL}), units are percentage of max. airflow.

79

Low-power sensor set (T_1, P_1, P_3, T_3, N_1, N_2, W_f, SHP, and T_7). The engine will be considered to be operating in steady state if the following three conditions are satisfied:

1. N_1 max. $- N_1$ min. within a frame ≤ 200 rpm.

2. $\left| \Delta N_{1C} \right|$ between frames ≤ 100 rpm.

3. T_{7C} max. $- T_{7C}$ min. $\leq 2.5°F$ for 60 seconds.

In the above conditions, a frame of data represents four speed and four temperature measurements in two seconds of measurement time.

From the low-power sensor set defined above, the following set of corrected qualities is computed:

Corrected Sensor Set (P_3/δ_1), $(N_1/\sqrt{\theta_1})$, (T_3/θ_1), $(W_f/\delta_1 \theta_1 \cdot {}^Y)$, $(SHP/\delta_1\sqrt{\theta_1})$, (T_7/θ_1), $(N_2/\sqrt{\theta_1})$

where

$$\delta_1 = (P_1/14.69) \text{ and } \theta_1 = (T_1/518.7)$$

From stored base lines, the base-line values of the corrected parameters are computed at the same corrected sensor value of P_3/δ_1. The stored base lines define the nominal steady-state characteristics as a function of P_3/δ_1 using linear interpolation. Test data from the AIDAPS program showed a significant engine-to-engine variability in the base lines. It is therefore necessary to store a unique base line for each engine rather than a universal base line for a particular model engine to minimize prediction error. At the same corrected P_3/δ_1 value, a base-line set of corrected engine parameters is obtained. Base Set (N_{1CB}, T_{3CB}, W_{fCB}, SHP_{CB}, T_{7CB}). The corrected shaft horsepower measurement is then corrected to optimal shaft horsepower due to operation at nonoptimal N_2 speed.

$$CF = \left[(N_{2C} - N_{2CB})/N_{2CB} \right]^2$$

$$SHP_{CO} = SHP_C/(1 - CF)$$

Relative deviations of the corrected measurements from the base-line data are computed as follows:

$$DN1 = (N_{1C} - N_{1CB})/N_{1CB}$$

$$DT3 = (T_{3C} - T_{3CB})/T_{3CB}$$

$$DWF = (W_{fC} - W_{fCB})/W_{fCB}$$

$$DSHP = (SHP_{CO} - SHP_{CB})/SHP_{CB}$$

$$DT7 = (T_{7C} - T_{7CB})/T_{7CB}$$

Relative deviations in airflow pumping capacity, component efficiencies, and gas generator inlet nozzle effective area are computed from the matrix equation:

$$
\begin{bmatrix}
DNA \\
DETAC \\
DETAT \\
DETAFT \\
DA5
\end{bmatrix}
= B
\begin{bmatrix}
DN1 \\
DT3 \\
DWF \\
DSHP \\
DT7
\end{bmatrix}
$$

The elements of the "B"-matrix are actually the influence coefficients developed and include the approximation that $(\partial A_N/A_N) = (-\partial \eta_{pt}/\eta_{pt})$. A universal "B"-matrix is used for all engines of the same model number. Since the value of P_3/δ_1 at which the low-power sensor readings are taken is not known in advance, several values of the B-matrix sufficient to cover the expected range of P_3/δ_1 will be stored, and linear interpolation with respect to P_3/δ_1 will be made to arrive at the proper B-matrix.

The low-power sensor measurements are not sufficient to compute variations in all six performance parameters. The relative variation in power turbine inlet nozzle effective area is obtained from the approximate relationship

$$DAN = -DETAPT$$

Maximum power of each of the control limits is computed from the following equations:

On the T_7 limit:

$$\text{SHPOT} = (\text{SHP}_{REF})\,(\delta_1)\,(1 + DWA)^{C11}\,(1 + DETAC)^{C12}\,(1 + DETAT)^{C13}$$

$$(1 + DETAPT)^{C14}\,(1 + DAS)^{C15}\,(1 + DAN)^{C16}\,f_T$$

On the N_1 limit:

$$\text{SHPON} = (\text{SHP}_{REF})\,(\delta_1{}^{C27})\,(1 + DWA)^{C21}\,(1 + DETAC)^{C22}\,(1 + DETAT)^{C23}$$

$$(1 + DETAPT)^{C24}\,(1 + DAS)^{C25}\,(1 + DAN)^{C26}\,f_N$$

On the W_f limit:

$$\text{SHPON} = (\text{SHP}_{REF})\,(\delta_1{}^{C37})\,(1 + DWA)^{C31}\,(1 + DETAC)^{C32}\,(1 + DETAT)^{C33}$$

$$(1 + DETAPT)^{C34}\,(1 + DAS)^{C35}\,(1 + DAN)^{C36}\,f_W$$

f_T, f_N and f_W represent the ambient temperature correction factor and are stored as univariate functions of ambient temperature. These are universal curves valid for any engine of a given model number. The "C" coefficients are also unique for a particular model engine. An analytical technique developed by Hamilton Standard is used to compute the elements of the "C"-matrix. For each of the "C" coefficients, two values are stored, and linear interpolation as defined below is used to obtain the actual "C" coefficient.

Control Limit	Variable Used in the Linear Interpolation
N_1	$\sqrt{T_1}$ or $\sqrt{\theta_1}$
T_7	T_1 or θ_1
W_f	$P_1\sqrt{T_1}$ or $\delta_1\sqrt{\theta_1}$

From the horsepower computed at the three limits, the minimum is chosen as the maximum power available, that is,

$$MPA = MIN (SHPOT, SHPON, SHPOW)$$

From an accuracy consideration alone, the Set II sensors (T_9 without P_7) have the smallest total error in predicted maximum power (see Table VII). The selected model has only a slightly higher total error; however, it offers a major advantage over Set II sensors in that it requires one less sensor. With Set II sensors, a T_9 sensor is required at low power and a T_7 sensor at high power; with Set IV, the T_7 sensor is used at both low and high power.

In the event that engine diagnostics are desired in addition to maximum power prediction, then with the selected system only one additional sensor would be required (P_7) to achieve one of the best-known engine diagnostic algorithms. Conversely, if engine diagnostics are already present, then maximum power prediction system can make use of the available sensors and not require any additional sensors.

For the selected system, the expected accuracy in predicted power at the three power levels considered using the best available sensors is:

Total RSS Error in Predicted Power Including Uncertainty in W_{BL} and SPE

Power Level	N_1 Limiting	T_7 Limiting	Wf Limiting
20% power	±3.87%	±6.97%	±3.91%
35% power	±2.77%	±6.59%	±3.16%
60% power	±2.17%	±6.35%	±2.78%

The T_7, T_1, and horsepower sensors at low power alone result in an error in predicted power of nearly 2%. To achieve the best accuracy, it is necessary to eliminate uncertainty in compressor bleed air and shaft horsepower extraction and to make the prediction at the highest practical power level. On single-engine installations, this level would be approximately 30% power. On twin-engine installations, the level would be substantially higher if all engines were operated at zero power except the engine on which maximum power was being predicted.

As mentioned previously, a major contribution to the total inaccuracy in predicted power is the uncertainty in compressor bleed air and shaft power extraction. It may be possible through procedural techniques to significantly reduce and essentially eliminate the error due to these two error sources. If these errors are eliminated, then the expected accuracy of the selected power prediction system at the three power levels considered using the best available sensors is:

Expected RSS Error in Predicted Power at No Uncertainty in W_{BL} and SPE

Power Level	N_1 Limiting	T_7 Limiting	W_f Limiting
20% power	±3.67%	±4.52%	±3.17%
35% power	±2.48%	±3.94%	±2.18%
60% power	±1.79%	±3.53%	±1.59%

T_1 accuracy may be improved by selecting platinum resistance sensors to have more nearly uniform characteristics and by computer compensation of errors due to nonlinearity. This selective process will increase sensor cost and computer complexity. However, the T_1 sensor plus interface error under these conditions can be reduced from ±2.2°R to ±1.1°R. Then the prediction error caused by sensor errors at maximum power (shown in Table XVI) is reduced from .52% to .44% when on the N_1 limit. Also, prediction errors caused by the T_1 sensor errors at 35.2% power (Table XXVI) are reduced from 1.478, 2.188, .6132 to .739, 1.094, .307 when on the N_1, T_7, W_f limits, respectively. The total expected RSS error in maximum power when predicted from 35% power is summarized below:

Expected RSS Error in Predicted Power at No Uncertainty in W_{BL} and SPE

Also With T_1 Probes Selected for More Uniform Characteristics

Power Level	N_1 Limiting	T_7 Limiting	W_f Limiting
35% power	±2.11%	±3.46%	±2.12%

A comparison of the prediction errors caused by the various sensor errors (Table XXVI at low power and Table XVI at maximum power) with T_1 sensor

errors reduced by selective matching of probes shows that the dominant errors are now caused by the SHP and T7 sensors.

If in addition to selecting T_1 probes for more uniform characteristics the SHP and T7 sensor error could be reduced by a factor of say 4, then the total expected RSS error when predicted from 35% power would be:

Expected RSS Error in Predicted Power at No Uncertainty in W_{BL} and SPE

Also With T_1 Probes Selected for More Uniform Characteristics and SHP and T_7

Sensor Errors Reduced by a Factor of 4

Power Level	N_1 Limiting	T_7 Limiting	W_f Limiting
35% power	±1.18%	±2.07%	±1.30%

If sensor inaccuracies could be eliminated altogether, the total expected RSS error in maximum power predicted would be significantly improved. When predicted at a 35% power level, the total RSS error in predicted power, assuming no uncertainty in W_{BL} and SPE and perfect sensors at low and high power would be:

Expected RSS Error in Predicted Power at No Uncertainty in W_{BL} and SPE

Also No Sensor Errors at Low and High Powers

Power Level	N_1 Limiting	T_7 Limiting	W_f Limiting
35% power	±.70%	±1.60%	±.78%

These remaining errors result from a) linearization of the complex nonlinear differential equations base engine (modeling errors), b) using incremental variations from the base engine model for nonstandard-day conditions, c) using incremental variations from the base engine model for engine degradation, and d) high power degradation characteristics at prediction power. It can be concluded from the above analysis that within the ground rules of the present study, a prediction accuracy of at least ±1% is not attainable, even with error free sensors. However, significant improvement in accuracy may be achieved on multi-engine helicopters where the MPA prediction can be made at high power levels, and if the single-point ground computation concept is expanded into a "continuous update system" as described in Appendix I paragraph A of this

report. In a continuous update system, the data stored in the MPA computer would be continuously and automatically modified as the engines are operated through their power range under random ambient and flight conditions.

In this manner, the errors due to ambient variations and engine degradation can be virtually eliminated. The pilot could even run individual engines to their power limit during flight to ensure the best possible MPA reading prior to the next take off.

In light of further possible accuracy improvement under slightly different study ground rules, it is recommended (see Recommendations) that further analytical studies be conducted to determine the feasibility of predicting MPA within ±1% accuracy at higher power levels using a continuous update type of prediction system.

SYSTEM MODEL EVALUATION USING AIDAPS FLIGHT TEST DATA

The actual engine test data obtained from the UH-1 AIDAPS program was prepared for evaluation of the maximum power available (MPA) algorithm. The AIDAPS data reduction program was modified to extract the engine data of interest from the raw flight test data. AIDAPS data was selected based on its operating range (horsepower, altitude, ambient temperature). This data was then subjected to the following steady-state test constraints:

1. N_1 max. $- N_1$ min. within a frame ≤ 200 rpm

2. $\left| \Delta N_{1C} \right|$ between frames $\leq \pm 100$ rpm

3. T_{T9C} max. $- T_{T9C}$ min. $\leq 2.5°F$ for 60 seconds

One frame of data represented 2 seconds of flight.

Data from 27 flight test runs passed these test constraints. Of these 27 flights, the 3 test flights having the greatest ambient temperature variations were selected, being $\Delta T_{Amb} = 31°F$, $30°F$ and $29°F$. In addition, 4 flights having the greatest change in altitude were selected, being about 11,200 ft, 9700 ft, 8000 ft, and 8000 ft.

It is noted that the set of three flights having the largest ambient temperature variations is included in the set of four flights having the largest altitude variation. This is to be expected, because the ambient temperature typically

86

decreases about 3.5°F to 4.0°F per 1000-ft increase in altitude. Therefore, the flights to the highest altitude are most likely to also have the largest temperature variation.

Several flights were made with altitude variations greater than 10,000 ft. However, only the flights referenced above passed the steady-state test constraints. Test pilots were reluctant to fly above 10,000 ft for safety reasons. (The probability of completing a safe autorotation landing during a power climb to high altitudes or while hovering at high altitude is greatly diminished.) For these reasons, no flights were made to 13,000 ft, or above, which would have resulted in a $\Delta T_{AM} = 51°F$. Additional tests of three different engines having degraded engine components were evaluated. These three engines contained a degraded compressor, erroded N_1 nozzles (A5 too large), and a degraded turbine respectively. Safety reasons prevented flight tests with degraded engines at power in excess of 1000 horsepower (about 70% of rated power). Therefore, the MPA algorithm was temporarily modified to correspond to engines and controls having a lower maximum power. This temporary modification permitted studies of the algorithm on degraded engines.

The sensors available in the flight test data were not compatible with the final choice of the MPA algorithm. Specifically, the test data did not contain measurements of gas generator turbine discharge temperature (T_7). Therefore, the test data could not be used to evaluate the MPA in the T_7 limit mode. In addition, a slightly different algorithm must be used (involving the use of T_9 instead of T_7 measurements at the low-power conditions).

Actual engine test data obtained from the AIDAPS program could not be used to check the validity of the power prediction system selected as the best overall system because of the lack of actual T_7 engine data. Instead, the algorithm which uses T_9 without P_7 and assumes that DAN = -DETAPT was evaluated using actual engine test data. Because the test data does not contain measurements of gas generator turbine discharge temperature (T_7), prediction of the horsepower in the T_7 limit mode could not be made.

Eight cases were evaluated: four at sea-level standard-day conditions and four at altitude. Table XXXV summarizes the results of the evaluation study. Before discussing each case separately, several general remarks can be made regarding Table XXXIV:

1. The computed engine deteriorations shown in Table I are not to be interpreted as an accurate indication of engine health. They serve only as an intermediate step in the power prediction scheme.

TABLE XXXV. VERIFICATION OF POWER PREDICTION ALGORITHM USING ACTUAL FLIGHT TEST DATA FROM AIDAPS PROGRAM SENSORS SET II

		Case 1	Case 2	Case 3	Case 4	Case 5	Case 6	Case 7	Case 8
		Brand X	LE2079I Degraded	LE1830I Degraded	LE1?376 Degraded	Brand X	Brand X	LE2079I Base	LE2079I Base
	Alt. (Ft)	0	0	0	0	11000	11000	10000	10000
	TAM (^{O}R)	518.7	518.7	518.7	518.7	479.5	479.5	483.	483.
	PAM(psia)	14.7	14.7	14.7	14.7	9.72	9.72	10.1	10.1
	$\delta 1$	1	1	1	1	0.661	0.661	0.687	0.687
	$\theta 1$	1	1	1	1	0.925	0.925	0.931	0.931
Actual S.S. Engine Data	N_1 CB	20840.	21420	20950	21900.	–	22250.	–	22420.
	T3C	863.	860.	849	896.	–	922.	–	922.5
	T9C	1251.	1283.	1246.	1292.	–	1306.	–	1322.
	WFC	374.	356.	368.	442.5	–	500.	–	500.
	SHP	322.	274.	318.	455.	–	631.	–	630.
Stored S.S. Base-Line Values	N_1CB	20700.	21120.	20460.	21900.	–	22200	–	22200.
	T3 CB	851.456	860.	851.	898	–	911.988	–	911.988
	T9 CB	1246.02	1254.	1258.7	1292.	–	1305.55	–	1305.55
	WFCB	354.036	356.	350.	442.5	–	488.038	–	488.038
	SHPCB	369.493	325.	298.	460.	–	672.840	–	672.84

TABLE XXXV (Continued)

Computed Engine Deterioration	DWA	+5.6%	-7.2%	-3.3%	.27%	0	3.9%	0	-1.6%
	DETAC	-3.5%	-.3%	.15%	.53%	0	-2.5%	0	-2.7%
	DETAT	+0.8%	-6.5%	1.8%	-.62%	0	1.6%	0	-.4%
	DETAPT	-5.5%	-6.3%	-3.5%	-.55%	0	-6.3%	0	-5.4%
	DA5	+8.7%	-1.6%	7.2%	+.11%	0	4.9%	0	3.8%
	DAN	+5.5%	+6.3%	3.5%	+.55%	0	6.3%	0	5.4%
At N1 Limit	SHPON	1412.	806.91	905.6	990.6	1069	1018	1088	1002
	SHPActual	1365.	896.0	853.	948.	1093	1093	1112.	1112.
	% Error	+3.44%	-9.93%	6.2%	4.53%	-2.2%	-6.9%	-2.2	-9.9%
At Wf Limit	SHPOW	1240.	865.5	954.6	990.4%	1826	1715	1761	1662
	SHPActual	1345.	985.	800.	1000.	-	-	-	-
	% Error	-7.8%	-12.13%	19.3%	-1.0%	-	-	-	-
Predicted Actual % Error	MPA	1240.	806.91	905.6	990.4	1069.	1018	1088	1002
	MPA	1345.	896.0	800.	948.	1093.	1093	1112	1112
	% Error	-7.8%	-9.93%	13.2%	4.53%	-2.2	-6.9%	-2.2%	-9.9%

Variable	Units
N1	rpm
T3	°R
T9	°R
SHP	hp
Wf	pph
MPA	hp

2. For all cases, shaft power extraction and compressor bleed air were assumed to be 0.

3. The "B" and "C" coefficients required in the prediction algorithm were obtained from the analytical base engine as described previously.

4. The predicted MPA is the minimum of the predicted horsepower at N_1 limit and the predicted power at the W_f limit. The actual MPA is the minimum of the actual measured horsepower at N_1 limit and the actual horsepower at the W_f limit.

5. For cases 2, 3 and 4, which evaluate the algorithm against degraded engines, the algorithm was modified to correspond to engines and controls having a base-line maximum power of 1000 hp. This was necessary because, for safety reasons, flight tests with degraded engines were not carried out at powers much greater than 1000 hp (approximately 70% of rated power).

Case 1

This case attempts to predict MPA at sea-level standard-day conditions for a nondegraded engine of unknown serial number which is identified as "Brand X". The stored base-line values were obtained at a P_3 value of 60.36 psia. This is the closest point to 30% power for which computed values of the "B" coefficients were available. For this case, the actual maximum horsepower available is 1345 hp and occurs at the W_f limit. The maximum power as predicted by the algorithm is 1240 hp. The error in predicted power is -7.8%.

Cases 2, 3, and 4

These cases attempt to predict MPA at sea-level standard-day conditions for degraded engines. The stored steady-state base-line values prior to degradation as well as the actual steady-state engine data for the degraded engines were obtained from actual flight test data at a P_3 value of 60.34 psia for cases 2 and 3 and at a P_3 value of 69.94 psia for case 4. For each case, the values of N_1 and W_f corresponding to a steady-state base-line horsepower of 1000 hp were found and used to establish the "C" coefficients at high power.

Cases 5 and 6

Cases 5 and 6 evaluate the power prediction algorithm at a standard-day 11,000-ft altitude condition for the "Brand X" engine. Case 5 shows the effect of sensor inaccuracy and uncertainty in bleed air and shaft power extraction at high power. Case 6 shows the effect of comparing actual test data against the analytical base line. For case 6, low power measurements were obtained at a corrected P_3 value of 75.23 psia. This corresponds to approximately 30% power at 11,000-ft standard-day conditions. It should be noted that the predicted power at the W_f limit is so much greater than the predicted power at the N_1 limit that it would never be selected as the minimum. This is as expected since at altitude, fuel flow is not a limiting factor.

Cases 7 and 8

Cases 7 and 8 evaluate the power prediction scheme at a standard-day 10,000-ft-altitude condition for a different engine. The comments for cases 5 and 6 apply for these cases as well.

Results

The AIDAPS flight test data was obtained with normal flight type sensors which were not of the high accuracy required for power prediction. As a result, the accuracy of the prediction algorithm evaluated cannot be established from the flight test data; however, the computed accuracy of the prediction algorithm evaluated is within the limitation of the available data. The available AIDAPS data was also not sufficient to evaluate the power prediction algorithm selected as the overall best prediction scheme.

SYSTEM HARDWARE IMPLEMENTATION

System implementation studies drew heavily upon the accuracy studies previously discussed. The complexity of the prediction system selected for implementation studies requires a digital computer and an indicator unit together with associated sensors.

For the purposes of this study, no dependence upon, or interconnection with, any other system not an essential part of existing Army helicopters was considered. It was also assumed that the MPA system, although useful for single-engine helicopters, will more commonly be used with multiengine helicopters. Therefore, a study was made of separate versus integrated computer installations for multiengine applications.

System Configuration Study

Since one of the prime purposes of the MPA indicating system is improving flight safety, a major consideration of the basic system configuration is that of failure characteristics and possible operational redundancy. No system configuration can be considered single-failure tolerant unless it can provide the MPA of all engines despite a failure of any MPA system part. Information on the MPA of one engine alone on multiengine helicopters is of very little operational use. If redundant MPA systems (a computer and indicator for each engine) were to be true single-failure-tolerant systems, then all computers would require access to all sensors on all engines and all indicators would require access to all computers. Such a system would be more complex and expensive than a single, nonredundant system with only one MPA computer and indicator per helicopter.

Hardware functional built-in-test (BIT) would be used on either type of system to determine if the electronics were functioning properly. BIT would be supplemented in redundant systems by the ability of the pilot to compare the MPA of each engine. Each engine's MPA should not differ from the others by more than a definable amount.

In a single computer installation, BIT must leave negligible chance for a failure producing readings which are not obviously incorrect. A feasible (and typical) method to supplement BIT for greater reliability of single nonredundant systems consists of making a dummy MPA calculation with simulated sensor inputs.

A further safety consideration is sensor isolation where sensors are shared with flight instrumentation. This is important in redundant systems and is critical for a single nonredundant system because a short circuit between sensor inputs which are used for purposes other than MPA calculation could provide incorrect readings for all engines to which they are connected through the MPA system. Such an effect could persist even though the MPA computer power is removed. The necessary isolation can be implemented either externally or internally to the computer. A recommended external method is to design into the flight instrumentation an isolated, conditioned output. This may be a separate retransmitting potentiometer or a semiconductor amplifier. It is also possible to resistively limit faults inside the MPA computer. If this is done, the isolation must be effective for both power-on and power-off conditions, and it must not have any failure modes which cause shorting between inputs from different engines, or be of a nature that gives a nonobvious error. For other sensors

used only for the MPA system, isolation must be sufficient to prevent overloading of sensors or wiring, and preferably to ensure that no computer fault damages the sensor.

It is concluded that since sufficient reliability and safety measures are available, and since significant size, weight, and cost savings can be realized, a single nonredundant MPA system with sensor isolation, BIT, and the capability to perform dummy MPA calculations is the best overall method of implementation.

System Installation

The MPA computer is expected to be too large for installation behind the cockpit instrument panel. Therefore, a separate instrument-type indicator/control unit (I/CU) is recommended for MPA display and for control of the system from the cockpit instrument panel. The computer can be mounted in an electronics bay or other suitable location. A diagram showing the possible appearance of the I/CU and system interconnections is given in Figure 19.

MPA Display

Since, in multiengine helicopters, the engines are run up separately, only one display is required for MPA. This display can be used sequentially to read out the MPA for each engine and/or to indicate the total MPA for all engines combined. A digital display is preferred for its accuracy, ease of reading, small physical size, and compatibility with digital processing. An electronic display is also desirable for reliability reasons. Many types are available. This application permits the use of solid-state, light-emitting diodes, which offer the smallest physical size and high reliability.

A rotary switch can be used for mode control, having positions for standby, MPA for each engine, and total MPA. The individual engine positions can be used for the convenience of the pilot to indicate the condition of each engine. The display will be blank until the MPA calculation is complete. It is anticipated that the computer will be able to determine from engine measurements which engine is being examined and perform the calculation correctly. Thus, the pilot can use the mode switch for check purposes without disturbing the calculations.

A reset push button is provided so that the pilot can cancel a readout and command a second calculation to observe repeatability for checking purposes. A fault indicator light will be connected to fail-safe circuits which continually monitor
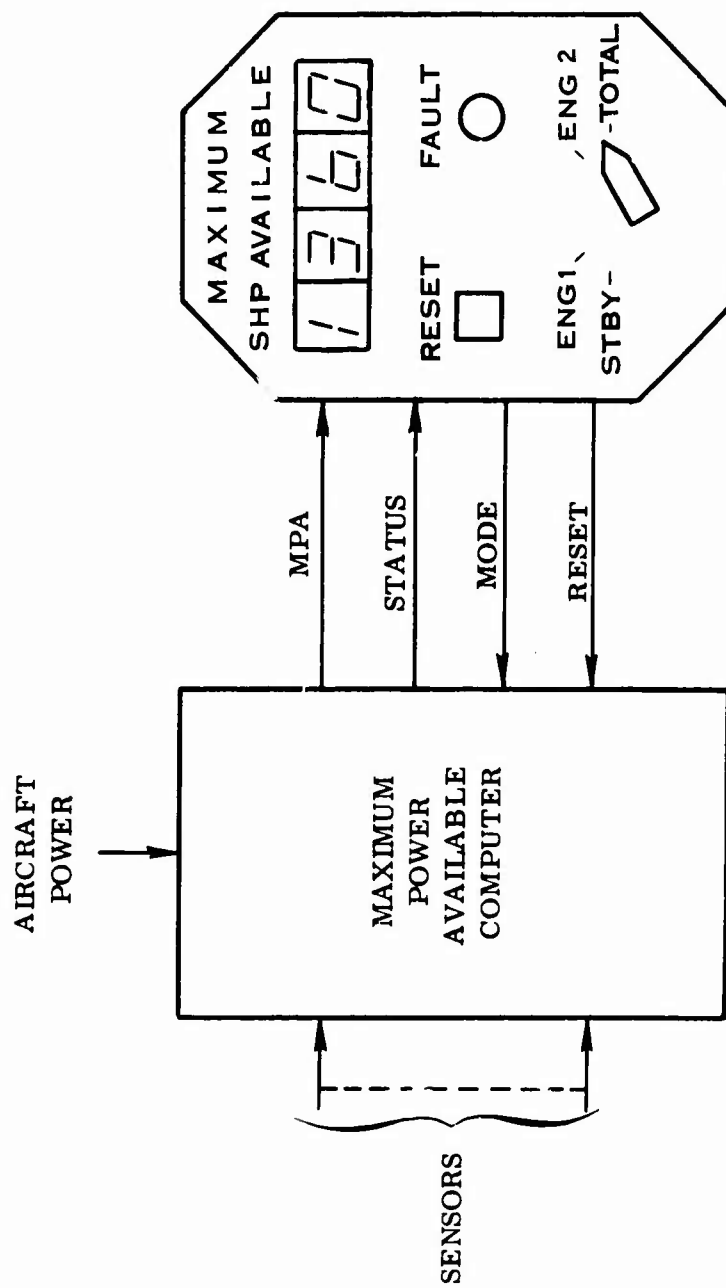
Figure 19. MPA System Configuration.

94

power circuits and processor capability during a calculation. For an exhaustive check, the processor would perform a dummy MPA calculation in the standby mode using simulated sensor inputs. The result could be displayed and should be visually confirmed by the pilot to within allowable tolerance limits. The computer should also briefly command a lamp test of the display when switched into and out of standby to verify visually that all segments are operating (all 8's display). The fault light should also be tested at this time. The recommended means of communication of the MPA data to the indicator is by a serial digital signal, using a two-wire, twisted, shielded pair. Operational status is shown by sending a ground to the computer, causing the display to be lit from a positive power supply inside the indicator unit. Mode commands are implemented by BCD-coded contact closures to ground, and the system is reset by momentary contact closure to ground in the instrument (reset button).

Computer Unit Description

A block diagram of a computer unit is shown in Figure 20. The unit is shown for a twin-engine helicopter. However, this system could easily be expanded into a three-engine capability. The essential sections are a frequency (pulse rate) input interface, an analog input interface, an input interface control, the processor, memory, output interface, and power supply.

Frequency Input Interface

This section converts frequencies into digital signals. By counting the number of cycles of the input which occur within a fixed time, a basic distinction may be made between measuring the frequency directly and measuring period. In period measurement, the reciprocal of frequency is measured and converted to frequency in the processor. This is the most common method for relatively low frequency inputs, due to the length of time required to accumulate sufficient counts for an accurate frequency measurement. It is necessary to measure the period of several cycles to average out the effects of gear-train and pole-piece irregularities. The normal use of this circuit is signal conditioning of speed inputs and vibrating cylinder type pressure transducers (if used). It will be necessary to multiplex these circuits and to provide a processor programmable divider to accommodate the various frequency ranges. For very low frequencies, where the signal is well below its operating range, the counter may overflow; to detect this, an overflow signal is incorporated to warn the computer to disregard the measurement.
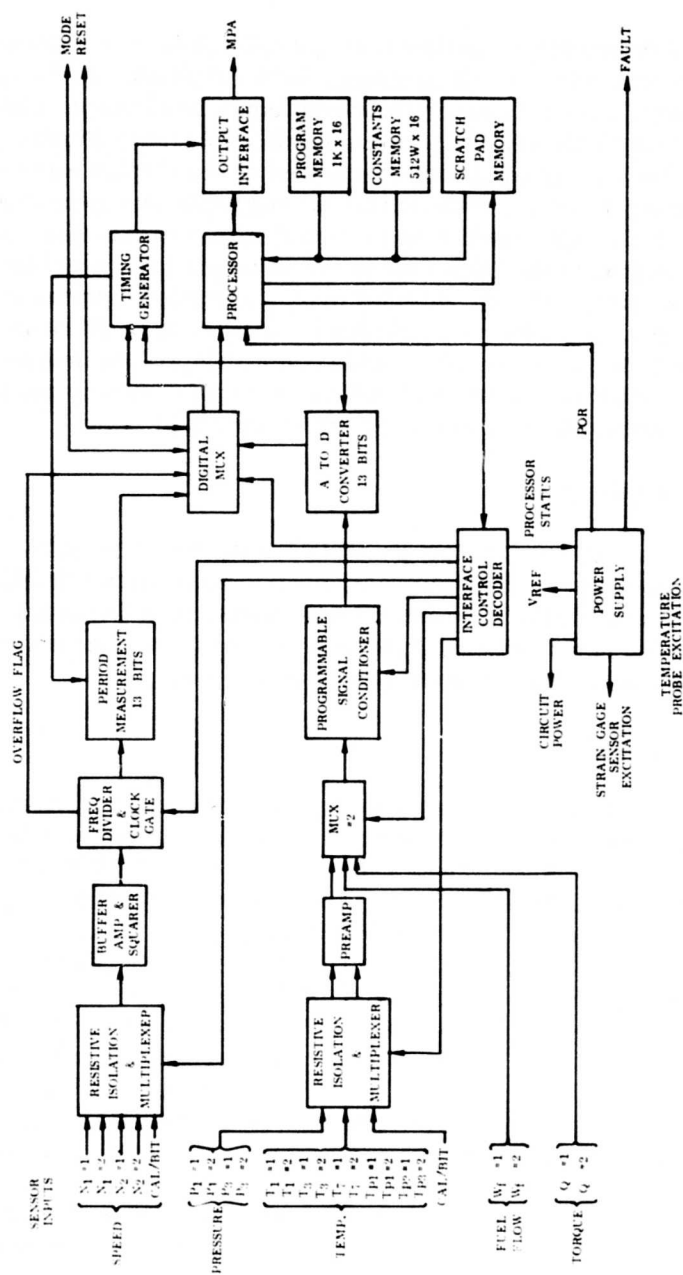
Figure 20. MPA System Block Diagram.

96

Analog Input Interface

The remaining sensor inputs are dc voltages cr voltage ratios. Except for fuel flow and torque, a direct input from the sensor is assumed. The present state of the art permits the input signals to be directly multiplexed without prior individual amplification. Adequate resistive isolation can be provided in each signal lead to prevent overloading or back currents, even under faulty conditions. A preferred form of multiplexing is current multiplexing, in which the computer end of the isolation resistor is grounded when not selected. This eliminates multiplex noise and gives a very accurate, constant input impedance. Additionally, back-to-back diodes may be connected from the computer end of the isolation resistor to ground to give a passive limitation on fault overvoltage.

The pressure sensors used are strain-gage sensors excited by constant voltage. The T_1 temperature sensors are four-wire probes excited by constant current, and the T_3 and T_7 temperature sensors are thermocouples, as are also the correction temperature sensors on the pressure gages. All these signals are less than 1 volt in amplitude and are preamplified before further multiplexing with the 0-5V signals for fuel flow and torque. This second-level multiplexing is followed by a programmable gain amplifier to provide a constant-range signal to the analog to digital converter, thus providing maximum dynamic range and accuracy. A 13-bit converter is required for sensor accuracy considerations.

Input Interface Control

A special characteristic of the MPA computer is that although the programmed algorithm is complex, the required operating speed is slow. It is quite reasonable to allow one or more seconds to complete the computer computation. This factor influences interface design and could lead to a special-purpose, simplified processor requiring neither interrupt or direct memory access (DMA) input-output facilities. It is still possible to input data under direct program control, using a combination of program timing, wait loops, and timing flags. The procedure is that the processor will output a control word defining an input channel and gain condition for either of the input interfaces and then repetitively monitor a timing signal until an adequate time has elapsed for signal conversion. In this way, input frame timing is ultimately controlled by the countdown circuits in the crystal-controlled timing generator.

Processor

A 16-bit processor has been selected which provides less than .05% of power turbine shaft horsepower round-off error under conservative worst-case conditions. A custom-designed processor having the minimum capabilities for the application can be used to minimize size, weight, and cost and to provide high reliability. The suggested unit could be a micro-programmed serial computer, in which the instruction set is contained within a 1024-word by 8-bit read-only memory. The remainder of the processor would comprise three 16-bit serial-in serial-out registers, a bit counter, a 16-bit inverted shift register for input-output and memory, and a minor amount of additional logic. In low-power off-the-shelf TTL implementation, such a computer requires 16 packages and will perform an addition in 32 microseconds and a division in 3 milliseconds. If implemented in custom MOS LSI, it requires two packages and would be 5 or 10 times slower. However, the computation time would still be fast compared with the waiting time for the engine to reach a steady-state condition. The processor has 16 arithmetic and logic instructions and will address directly any memory location or input-output required for the MPA application.

Memory

Memory is required to store the program instructions, the engine base line, and other curves and constants, and for intermediate calculations (scratch pad). The scratch pad is a read-write memory and is not required to retain data when power is off.

A major implementation consideration is the type of memory to be used for storage of the engine base-line curves. The error analysis has determined that stored engine base-line data must be matched to the particular engine(s) installed. The most operationally desirable base-line acquisition and storage method would be to incorporate the necessary program into the MPA computer itself, and to use an electrically alterable memory for the base-line storage. This could be a plated-wire NDRO memory.

The custom base-line data could be automatically acquired by the MPA computer during a test flight with new (or overhauled) engines installed in the helicopter. A nominal base line could also be permanently stored in read-only memory and used for backup. This technique would ensure continued MPA system operation, although at reduced accuracy, if custom

base-line data could not be acquired because, for example, of helicopter operational problems or in the event of NDRO memory malfunction.

Use of electrically-alterable memory for base-line acquisition and storage is also readily adaptable to an advanced MPA system, where the MPA prediction is automatically updated by the results of previous flights which are stored in the MPA computer. Advanced MPA systems of this nature are discussed in the system growth section of this report.

Since the program has not been reduced to airborne machine language for this study, firm figures for required program memory capacity are not available. A list estimate at this time is 1024 words. In MOS ROM, this would require four packages. The requirement for memory constants is estimated at 519 words for up to three engines, and would require eight packages if implemented in presently available programmable read-only memory. For scratch-pad memory, 64 words are sufficient, which may be obtained in four packages. Scratch-pad memory should be designed to retain data even during short power-supply interruptions.

Output Interface

The output interface receives MPA data words from the processor and encodes them is a form suitable for serial transmission to the indicator/ control unit. The transmission is asynchronous and therefore requires a means of indicating the start of each data word. However, no addressing is required as there is only one transmitting unit (the MPA computer), and all required data can be contained in one data word. Error control methods include repetition of transmission, parity, verification of the presence of start and stop bits, and counting of data bits.

The data transmitted is the MPA of each engine or total MPA selected by the mode switch, if available. Otherwise a code is sent, blanking the display. When in standby, the data sent is the result of a self-test calculation, except for one frame which, when changing mode into or out of standby, causes an all-8's lamp test data signal to be transmitted.

Power Supply

The power supply provides all circuit voltages, excitation for strain-gage and temperature probe sensors, and an accurate reference voltage for the analog-to-digital converters. A primary power source of 115 V, 400 Hz,

single phase is recommended. The power supply checks itself for malfunctions and for power resumption following an interruption. The drive transistor for the fault indicator in the I/CU is located here and is activated either by a power supply fault or by a processor fault, which is a signal resulting from a routine check of processor instructing and addressing performed once per frame. The circuit also has a time-out feature so that program "hang-up" is detected.

In a production configuration, the computer unit might be contained in a volume of approximately 200 cubic inches and might weigh less than 10 pounds. Size and weight are functions of the technology used (e.g., MOS, TTL, etc.) to implement the digital sections of the computer.

Indicator/Control Unit Description

The I/CU is not required to perform any independent function by itself, and therefore it can be small, simple, and reliable. The only functions requiring electronic circuits are receiving the MPA digital transmission and displaying the data.

The data should be received with a differential line interface circuit, which rejects common-mode interference on the aircraft structure. This data should be verified to ensure that only correctly received data is displayed. It is anticipated that data transmission will be periodic, so that if the first transmission is not correctly received, the data will appear on the second transmission. Display processing includes serial to parallel conversion and BDC to seven-segment conversion. No provision for display dimming should be necessary, as the display is blanked during flight.

The I/CU should contain its own power supply to provide low voltage for the data receive-and-display circuits and for the fault lamp. It is feasible to use 28 volts dc if this is preferred by the airframe manufacturer.

In a production configuration, the I/CU might be contained in a standard 2-inch-dia. x 6-inch-deep (less connector) instrument case and might weigh approximately 1 pound.

Parametric Sensors

Eleven parametric sensors are required for the MPA system selected as a result of this study. These sensors are listed in Table XXXVI together with their operating range, type and required accuracy. The accuracies presented

TABLE XXXVI. PARAMETRIC SENSOR SUMMARY

Sensor	Sensor Range Min.	Max.	Sensor Type	Sensor Accuracy
N_1	20K rpm	25K rpm	Pulse Pickups	±2.5 rpm
N_2	13K rpm	22K rpm	Pulse Pickups	±2.5 rpm
T_1	400°R	600°R	Platinum Resistance	±.5°R
T_3	670°R	1050°R	Platinum Resistance	±.5°R
T_7	1100°R	1800°R	Thermocouple (Chrom-Alumel)	±6.3°R
T_9	1000°R	1500°R	Thermocouple (Chrom-Alumel)	±6.3°R
P_1	11 psia	16 psia	Vibrating Cylinder	±.01 psi
P_3	50 psia	110 psia	Vibrating Cylinder	±.05 psi
P_7	20 psia	30 psia	Vibrating Cylinder	±.03 psi
W_f	350 PPH	800 PPH	Angular Momentum Mass F/M	±4 pph at 800 pph ±2 pph at 400 pph
SHP	300 hp	1500 hp	Torque Sensor	±10 hp
	300 hp	500 hp		

are achieved via computer compensations to eliminate all systematic errors associated with each sensor type. In addition, the pressure sensors are individually compensated as well as the torque sensors. Further, improvements in accuracy may be achieved if custom-compensation techniques are used with fuel mass flowmeters, thermocouples and platinum resistance probes. The need for this additional compensation depends on the final overall system configuration. Therefore, individual sensor accuracy requirements can be specified only where the final system configuration and accuracy requirements are defined.

Speed Sensing

The sensing of engine speeds will be accomplished with the use of magnetic sensors mounted to detect the frequency of passing teeth on shaft-mounted gears. The errors associated with sensing speed are: the tooth-to-tooth position tolerance and the eccentricity of the gears. These errors are very small and are about ± 2.5 rpm depending on the particular gear diameter.

Temperature Sensing

Platinum Resistance Probes -- Platinum resistance probes were selected for sensing T_1 and T_3 due to excellent repeatability of probe output (resistance) for a given input (temperature). An accuracy of $\pm .5°R$ can be achieved for the platinum probe. This accuracy of $\pm .5°R$ is not the normally quoted probe accuracy but is achievable if a digital computer is the termination of the probes signal. The digital computer allows for compensation of the following probe's sources of error:

- non-linearity

- recovery

- self-heating

- de-icing

The error sources which cannot be compensated are the probe non-repeatability from unit to unit and the deviation from its calibration with time. The probe can be purchased (at extra cost) with a tighter than normal calibration characteristic, resulting in the total statistical error of unit interchangeability and drift of $\pm .5°R$.

Thermocouple Probes -- The sensing of T_7 and T_9 should be implemented via Chromel-Alumel thermocouples. An accuracy of $\pm 6.3^{\circ}R$ is required. The maximum limit for using a platinum resistance probe is approximately $1400^{\circ}R$. The resultant statistical (RSS) error for a chromel-alumel thermocouple is made up of unit-to-unit variation, and long-term drift. All of the other systematic or repeatable errors are compensated out within the digital computer. These compensatable errors are: non-linearity and recovery.

Torque Sensing

Torque sensing to an accuracy of ± 10 hp is required. Such accuracy can be best achieved through the use of a strain-gauge type of sensor. The strain gauge would be mounted on the engine or transmission shaft. The strain gauge output would be a function of shaft torque or horsepower. A temperature sensor would be required to measure the temperature of the shaft, at the strain gauge, for temperature correction of the strain-gauge signal by the digital computer. Also included as compensation by the computer are the gauge nonlinearity and possibly shaft-to-shaft variations. The shaft variations could be compensated on an individual basis by first dead weight calibrating the shaft and including a correction factor in terms of resistors which are part of the shaft-mounted strain-gauge sensor/correction package. Having the compensation resistors as part of the shaft makes the system interchangeable without recalibration.

Pressure Sensing

The sensing of pressures would be implemented using a highly accurate digital type of pressure transducer. The pressure transducers are accurate to $\pm .06\%$ of full scale under all normal aircraft environment of temperature extremes, vibration, acceleration, etc. These sensors are produced at present in 17, 50 and 100 psi ranges accounting for the .01, .03 and .05 psi errors of the sensor accuracy summary.

The pressure transducer which is able to meet the state accuracies is a vibrating-cylinder device. This transducer has an electrical pulse train (frequency) output which is a function of input or measured pressure. The pressure sensor is composed of a thin-walled sensing cylinder with an end cap on one end and is grounded to a base on the other end (Figure 21). Pressure is ported to the inside of the vibrating cylinder exerting an outward force on the end cap due to the differential pressure across the cylinder and end cap. This outward force results in a tensile load in the cylinder wall as a function of pressure. If the cylinder wall was to be induced into vibration, the frequency of vibration would be a function of the load in the
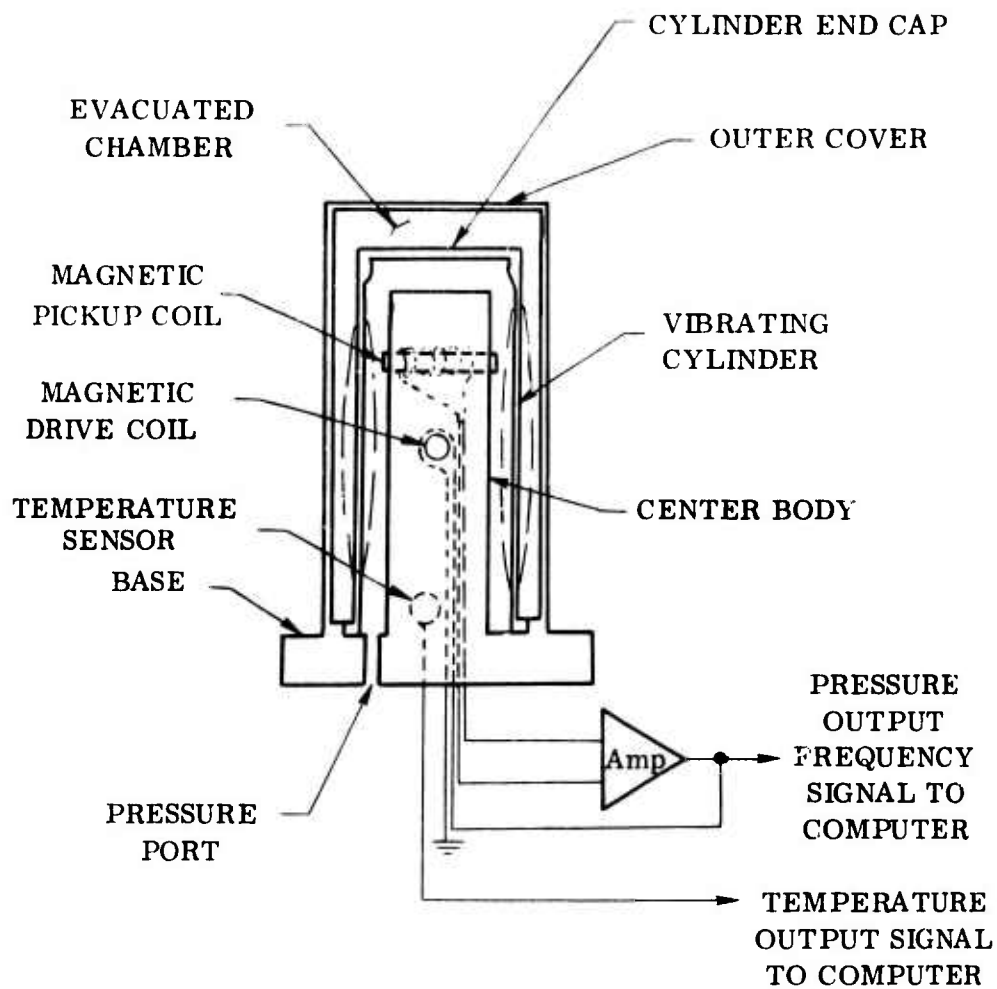
103

Figure 21. Vibrating Cylinder Pressure
Transducer Schematic.

104

walls. Therefore sensed pressure, similar to a plucked violin string. A closed-loop electronic circuit is added to maintain the wall in vibration at its resonant frequency. A temperature-sensing element is imbedded in the base of the pressure sensor which provides an electrical output as a function of the pressure sensor's temperature. The digital computer then uses the temperature sensors indication cf temperature to compensate for the effects of temperature on the pressure sensor's frequency output. Each individual sensor's unique pressure and pressure/temperature characteristics are incorporated on a memory chip mounted with each pressure transducer. This compensation of ambient temperature effects provides for sensor performance which is essentially ambient temperature insensitive.

This vibrating-cylinder pressure sensor is also insensitive to ambient vibration inputs. The range of frequency out of the sensor is 4500 to 5500 Hz which is well above any normal environmental vibration normally specified at a maximum of 2000 Hz.

The remaining sources of error for the pressure sensor are repeatability, long-term drift, and residual temperature effects. The net results of all of these errors are sensors which achieve ± .06% of full scale accuracy under all possible aircraft environments.

Fuel Mass Flow Sensing

Fuel mass flow sensing can be achieved using a linear or angular mass flowmeter. These flowmeters measure mass flow directly and are not volumetric flowmeters with added compensation to do the conversion to mass flow. A temperature probe measuring fuel temperature would still be added to achieve the final state accuracy of ±.5% of the point. The fuel temperature would be utilized by the computer to compensate any residual temperature effects on the flowmeter. The computer will also compensate for any residual nonlinearity of the flowmeters output.

CONCLUSIONS

Conclusions resulting from this study are as follows:

1. The concept of predicting MPA from a helicopter gas turbine engine, while taking into account variations in ambient conditions and engine degradation, is feasible.

2. MPA can be predicted with an accuracy of ±3.5% if the prediction is made, under the study ground rules, at 30% power using only the original engine base-line data. Errors associated primarily with parametric sensors, engine degradation and computations made at nonstandard-day conditions and at low-power levels prevent attainment of the ±1% MPA prediction accuracy goal under these study conditions.

3. Significant improvement in MPA prediction accuracy can be achieved if the prediction is made at higher power levels, on multi-engine helicopters for example, and if engine base-line data stored in the MPA system is continuously updated. MPA prediction accuracy of ±1% may be feasible under these conditions where errors due to power setting, ambient variations and engine and parametric sensor degradation have been virtually eliminated.

4. Parametric sensor requirements have been determined for an MPA prediction system configured under the present study ground rules. Errors associated with power turbine inlet temperature and shaft horsepower sensing are major contributors to MPA prediction error. Sensor accuracy requirements are dependent on system configuration and error compensation techniques. Therefore, final sensor requirements for a continuous updating MPA prediction system with an accuracy of ±1% cannot be determined until such a system is configured.

5. An MPA prediction system can be implemented using present-day state-of-the-art digital electronic technology.

6. MPA prediction techniques are highly compatible with other diagnostic and control functions. Overall hardware utility can be improved by combining these functions on advanced Army helicopters.

RECOMMENDATIONS

Recommendations resulting from this study are as follows:

1. Analytical Studies

   Analytical studies should be conducted to determine the feasibility of predicting MPA to within ±1% accuracy at power levels higher than 30% using a continuous update type of prediction system, and to determine the required accuracies of parametric sensors associated with the system.

2. Hardware Fabrication

   If at the conclusion of these additional feasibility studies, it is concluded that MPA can be predicted with suitable accuracy, then system hardware should be fabricated. A breadboard MPA system could be used in conjunction with a Lycoming T53 engine or engine computer model to verify the analytical findings of the feasibility studies and to optimize system hardware implementation.

   Breadboard hardware can be fabricated economically and within a reasonable length of time. Existing state-of-the-art parametric sensors can be used for initial system development.

   The breadboard hardware could be designed so that only minor modifications are required to allow the use of more accurate sensors, as they become available, and to allow growth from an MPA system to a hover-lift computer system or small diagnostic system.

   At the conclusion of the breadboard evaluation program, a prototype MPA system could be fabricated for hardware development, and finalization under actual flight conditions.

3. Advanced MPA System Studies

   It was concluded that MPA prediction techniques are highly compatible with other helicopter diagnostic and control functions. It is, therefore, recommended that further studies, such as those described briefly in Appendix I of this report, should be undertaken to determine how improvements in overall hardware utility can be made on advanced Army helicopters by combining these diagnostic and control functions with an advanced MPA prediction system.

APPENDIX I

NOTES ASSOCIATED WITH ERROR SUMMARY SHEETS

NOTE 1

Linearization of the nonlinear engine equations introduces an error in both "B" and "C". Accuracy checks of individual elements in "B" and "C" indicate that errors of as much as $\pm 5\%$ may occur. It is assumed that there is a possible $\pm 5\%$ error in "C" and in the computed degradation at low power (efficiencies and geometrics).

NOTE 2

The influence coefficients, "C", were computed at standard day ($P_1 = 14.7$ psia, $T_1 = 59°F$, $P_1/P_{AM} = 1.0$). Nonstandard day was assumed to be any combination of the following:

$$P_1 = 11 \text{ to } 16 \text{ psia}$$

$$T_1 = -60°F \text{ to } 120°F$$

Ambient conditions where each limit can occur are defined in Figure 18.

NOTE 3

Tolerances of new engines are dependent on both quality and size. Similarly, degradation tolerances are not certain. The assumed engine tolerances used in this study are shown in Table XXXVII.

NOTE 4

"C" is computed at standard day when using constant "C". Interpolation of "C" based on ambient-day conditions can reduce the error in "C" to less than $\pm.01$ on N_1 limit and W_f limit and $\pm.02$ error in "C" on the T_7 limit.

NOTE 5

The variation in "C" caused by a "typical degradation" was evaluated at the condition shown below:

TABLE XXXVII. ASSUMED ENGINE TOLERANCES			
Engine Parameter	New Engine Tolerance	Severe Degradation	Maximum Tolerance
η_c	±.5%	-3%	3.5%
η_t	±.5%	-2%	2.5%
η_{pt}	±.5%	-2%	2.5%
A_5	±.2%	+2%	2.2%
A_N	±.2%	+2%	2.2%
W_a	±1%	-1%	2%

Engine Parameter	Typical Degradation
η_c	-1%
η_t	-1%
η_{pt}	-1%
A_5	+1%
A_N	+1%

The variation in "C" caused by a "severe degradation" is assumed to be twice the variation in "C" caused by the above "typical degradation."

NOTE 6

The prediction algorithm assumes that the degradation at high power (in terms of percentage of point η_c, η_t, η_{pt}, A_5, A_N, W_a) is equal to the degradation computed at low power. The estimated errors in this assumption are as follows:

$$\eta_c = \pm.15\%$$

$$\eta_t = \pm.10\%$$

$$\eta_{pt} = \pm.10\%$$

$$A_5 = 0\%$$

$$A_N = 0\%$$

$$W_a = \pm.10\%$$

NOTE 7

Compressor bleed air (W_{BL}) and compressor shaft power extraction (SPE) influence maximum power available. The estimated maximum $W_{BL} = 5\%$ and maximum SPE = 1 hp/PPS; however, the actual values are dependent on accessory requirements. The assumed uncertainty in predicting high power W_{BL} and SPE while at low power is shown below:

$$W_{BL} = \pm 1.5\%$$

$$SPE = \pm.3\% \text{ hp/PPS}$$

NOTE 8

The compressor bleed air (W_{BL}) and compressor shaft power extraction (SPE) are not measured. It is assumed that W_{BL} and SPE can be estimated to $\pm.5\%$ of W_a and $\pm.3\%$ hp/pps of W_a respectively at low power.

NOTE 9

The sensor accuracies are considered the "best available." Detailed sensor characteristics are listed in Table XV.

NOTE 10

The sensor accuracies are typically good sensors, although often not the "best available." In particular, the pressure sensors and shaft horsepower sensor (SHP) are not the "best available." Detailed sensor characteristics are listed in Table XV.

NOTE 11

It is assumed that $\partial A_N/A_N$ differs by 2% from the assumed condition of $\partial A_N/A_N = -\partial \eta_{pt}/\eta_{pt}$.

APPENDIX II

SYSTEM GROWTH

There are three aspects of possible system growth which should be considered in further studies. They are as follows:

- Modification or expansion of the base-line MPA system to improve accuracy.

- Incorporation of other aircraft-related functions to attain a hover lift computer.

- Integration of the MPA function with other aircraft systems.

Growth To Improve Accuracy

The system implemented is that which complies with the requirements as specified by the Army, both in writing and verbally. A major restriction of these requirements is that the MPA calculation be made only on ground prior to flight.

An alternate approach which would provide an improved accuracy at some increase in complexity is to continually update the MPA calculation in flight whenever the engine operating condition enables a better estimate than that currently made. The decision whether or not to update the reading at any time would be an automatic computer function based on evaluation of the relative merit of a new reading compared to the old. This would be a function of engine and flight condition, age of previous MPA computation, etc.

The improved accuracy of this approach results from the ability to make the MPA calculation at high power levels and the expanded operational envelope, which would also allow evaluation to be made of the engine's deviation from the standard base line. The MPA reading presented to the pilot prior to flight would be that obtained from the last update on the previous flight.

The basic hardware required to implement this approach would be the use of a long-term, nonvolatile read/write memory system such as plated wire. An alternative could be regular scratchpad memory with a mechanically latched readout system.

Other means to improve accuracy without significant hardware impact involves operational procedures in multiengine helicopters. It is, for example, possible in these applications to operate individual engines to higher percent powers without approaching lift-off. The on-ground MPA calculation accuracy is then improved by virtue of the higher power setting.

Growth to Hover Lift Computer

The MPA indicator as described in this study provides a useful indication to the pilot as to the engine's capabilities. It falls short, however, in that it does not provide him with information pertinent to the performance capabilities of the helicopter itself. It is still necessary to manually assess whether he could hover at a specific altitude to perform his mission, etc.

The hover lift computer could provide this information automatically. The helicopter-related performance characteristics would be incorporated into the computer logic and other related variables would be provided as additional inputs. The most important (and possibly the only) one of these is weight. This could be obtained as dynamic weight (rotor shaft lift), on-ground weight (strain gage on struts), payload capability, etc., and could include the use of fuel flow measurements for weight update. The output information to the crew could be presented in a variety of ways to the pilot. Possibilities range from a go no-go response to interrogation to a flight envelope display.

It may also be required to provide means to manually input the computer with ambient conditions known to exist at the mission destination to enable advance estimates to be made as to whether it will be possible to successfully complete the mission.

Integration With Other Systems

A side benefit of the MPA system is that the sensor signals which are conditioned and read into the computer could also be provided to other on-board systems. These include crew instrumentation, diagnostics (including TREND analysis), yaw dampers, and automatic stabilization equipment (ASE). The conditioned signals are most readily made available in a digital format, requiring only coding and outward transmission serially on a single pair of wires. Under some circumstances an analog-type buffered signal could be provided. The accuracy requirement for the MPA system will be the pacing item for the sensors, and it may well be possible to tolerate some accuracy degradation in the instrument

drive channel. The MPA system could also be totally integrated with other on-board systems to improve overall hardware utility, since MPA prediction techniques are highly compatible with diagnostic and control functions on advanced Army helicopters.